ANL/OTEC-BCM-026

FIVE OTEC BIOFOULING AND CORROSION EXPERIMENTS AT KEAHOLE POINT, 1976 - 1980

F. C. Munchmeyer, L. R. Berger,
and B. E. Liebert

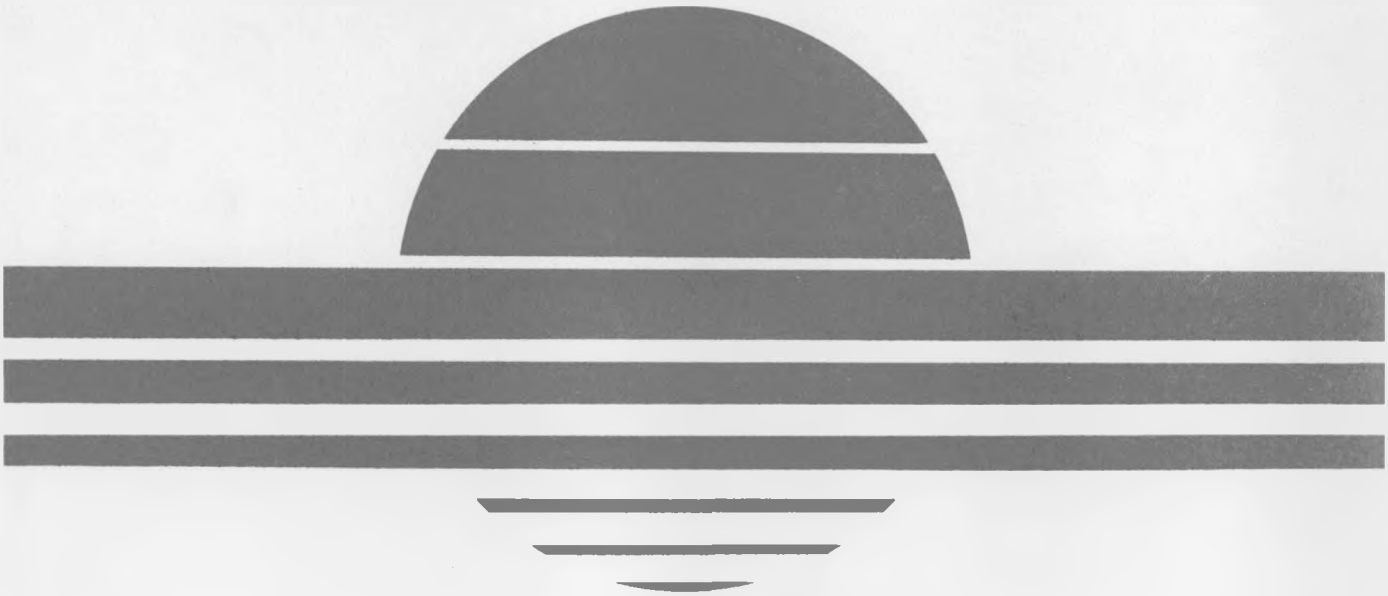

Argonne National Laboratory
9700 South Cass Avenue
Argonne, Illinois 60439

Prepared for the
U. S. Department of Energy
Division of Ocean Energy Systems
under Contract W-31-109-Eng-38

SOLAR ENERGY

The facilities of Argonne National Laboratory are owned by the United States Government. Under the terms of a contract (W-31-109-Eng-38) among the U. S. Department of Energy, Argonne Universities Association and The University of Chicago, the University employs the staff and operates the Laboratory in accordance with policies and programs formulated, approved and reviewed by the Association.

MEMBERS OF ARGONNE UNIVERSITIES ASSOCIATION

The University of Arizona
Carnegie-Mellon University
Case Western Reserve University
The University of Chicago
University of Cincinnati
Illinois Institute of Technology
University of Illinois
Indiana University
The University of Iowa
Iowa State University
The University of Kansas
Kansas State University
Loyola University of Chicago
Marquette University
The University of Michigan
Michigan State University
University of Minnesota
University of Missouri
Northwestern University
University of Notre Dame
The Ohio State University
Ohio University
The Pennsylvania State University
Purdue University
Saint Louis University
Southern Illinois University
The University of Texas at Austin
Washington University
Wayne State University
The University of Wisconsin-Madison

Printed in the United States of America
Available from
National Technical Information Service
U. S. Department of Commerce
5285 Port Royal Road
Springfield, VA 22161

NTIS price codes
Printed copy: A06
Microfiche copy: A01

Distribution Category:
Ocean Energy Systems
(UC-64)

ANL/OTEC-BCM-026

ARGONNE NATIONAL LABORATORY
9700 South Cass Avenue
Argonne, Illinois 60439

FIVE OTEC BIOFOULING AND CORROSION EXPERIMENTS AT KEAHOLE POINT, 1976 - 1980

by

F. C. Munchmeyer, L. R. Berger,
and B. E. Liebert

University of Hawaii
Honolulu, Hawaii 96822

November 1981

Prepared for

Argonne National Laboratory
under Subcontract No. 31-109-38-4487

TABLE OF CONTENTS

FIVE OTEC BIOFOULING AND CORROSION EXPERIMENTS AT KEAHOLE POINT, 1976 - 1980

by

F.C. Munchmeyer, L.R. Berger, and B.E. Liebert

1.0 Introduction and Summary

Five sets of experiments were conducted on simulated OTEC (ocean thermal energy conversion) heat exchangers at Keahole Point, Hawaii during the period 1976 - 1980. The purpose of the experiments was to evaluate the effects of biological fouling and corrosion on the seawater side of a heat exchanger tube.

An OTEC plant extracts thermal energy from warm ocean surface waters using a heat exchanger. It converts a small fraction of that energy to electric power and rejects waste heat to the ocean by means of a second exchanger. These two heat exchangers are the largest internal elements of an OTEC plant; they control overall size and cost. Seawater flows through tubes in one class of heat exchangers. An OTEC plant that would serve a city of 100,000 people would require approximately 10,000 miles of 1 inch diameter heat exchanger tubing; this is an order of magnitude more tubing than is required in the boilers and condensers of an equivalent but conventional power plant.

The design of such an OTEC plant would depend in large measure on the rate of heat transfer between seawater and the inner walls of thousands of tubes; it would also depend on tube life in flowing seawater. A biological film will form on and foul the seawater side of an OTEC heat transfer surface. This fouling film will impede heat exchange; if allowed to grow in thickness, and if the film does not slough, it might reduce the net power of the plant to zero. Tube life is limited by corrosion; the seawater may cause either general corrosion or pitting or both. Corroded tubes imply plant stoppages and maintenance costs. Brushing the tubes should improve heat exchange. These considerations set the objectives of the Keahole experiments which were (1) to determine the character and rates of growth of fouling films and their effects on heat transfer, (2) to observe

corrosion of candidate heat exchanger tube materials and (3) to estimate the effect of brushing on fouling films in a simulated OTEC heat exchanger.

One measure of fouling is labeled R_f, the change in resistance to heat transfer due to fouling. In this report the units of R_f are (Hr Ft^2 °F/BTU). the five experiments gave these preliminary answers to cleaning with a bristle brush:

- over a period of months, the tubes can be cleaned well enough, and
- after 10 months exposure to flowing water the tubes must be brushed approximately twice a week, however,
- a fraction of the fouling film may not be removed by a bristle brush and in 10 months that fraction may account for an R_f value after brushing that approaches $1.x10^{-4}$ units.

Six candidate tube materials were exposed during the experiments and preliminary answers to corrosion questions were found. Two of the most important results are, first, that 5052 aluminum tubes did not pit and second that their rate of general corrosion was slow enough to suggest a 30 year design life when the tubes are cleaned with a bristle brush.

A model for biofouling was developed which relates R_f to thickness of the fouling film and also to total nitrogen and total carbon in the film.

The apparatus used to measure heat transfer in all the experiments was designed and built by J.G. Fetkovich of Carnegie-Mellon University. He proposed the original project and led it through the first years.

The Keahole experiments produced valuable information. However, they should not be considered as broadly definitive, for several reasons. The time period for each experiment was short relative to the design life at an OTEC plant. The ocean attacked the apparatus itself and often wrested control of the experiments from the hands of operators. The first of the series was the first such experiment ever done at sea. The second was a major departure from the first, and the fifth was yet another new approach. Techniques and procedures evolved during the series. These factors: exploratory tactics, relative time, incomplete control, and evolutionary procedures limited the accuracy and precision of the results.

The first and fifth experiments, in which the apparatus was not immersed in the ocean, have been repeated at other locations by other investigators. In the other Keahole experiments the apparatus was mounted on an underwater buoy; those three provided unique *in situ* data on OTEC biofouling and corrosion.

Table I is an outline of the five experiment groups. The next sections of this chapter give brief descriptions of the experiments and their results.

TABLE I

Five OTEC Biofouling and Corrosion Experiments at Keahole Point

Experiment Group No.	1	2	3	4	5
Year:	1976	1977	1977-78	1978-79	1980
Location:	NOI'I	Buoy	Buoy	Buoy	Ashore
Aliases:	NOI'I	Buoy 1, Buoy I	Buoy 2, Buoy II	Buoy 3, Buoy III	3" Pipeline
Number of Experiments:	2	3	4	4	2
Duration, Months:	3	5	8	10	4
Pipe Materials:	6061-T6 Al (2 pipes)	6061-T6 Al (2 pipes) Grade 2 Ti	5052 Al (2 pipes) Grade 2 Ti (2 pipes)	5052 Al Grade 2 Ti AL-6XSS 90.10 CuNi	Grade 2 Ti (2 Ti Pipes plus an AL-CLAD corrosion sample)
Nominal Water flow Velocities ft/sec:	3 and 6	6 (Ti) 3 and 6 (Al)	6	6	6
Lead University:	CMU	CMU	CMU	UH	UH
Contract Monitor:	Battelle	Battelle	Battelle	Argonne	Argonne
Prior References					
•Heat transfer:	[4,7,8]	[6,7,8]	[11]	[11,13,14]	-
•Biofouling:	[5,8]	[5,9]	-	[15]	-
•Corrosion:	[5,8]	[5]	[12]	[14,16]	-
•Water temp:	[5,8]	[5]	[11]	[11,14]	-
•Water quality:	[5]	[5]	-	[14]	-

1.1 Noi'i

Lead University	Carnegie-Mellon
Number of Experiments:	2
Observation Periods:	Exp. #1, July 13 - September 22, 1976 Exp. #2, August 19 - September 26, 1976
Location:	65 foot research vessel Noi'i, anchored 1 mile NNW of Keahole Point lighthouse in 300 feet of water. Instruments mounted on deck. Control and recording on board. Water supply taken from approximately 20 feet below still water surface.
Materials and Nominal Flow Velocities:	1st Exp: 6061-T6 Al at 3'/s 2nd Exp: 6061-T6 Al at 6'/s
Pipe Pre-cleaning Methods:	Exp. #1 - stroked 100 times with bristle brush using a commercial cleaning powder and tap water. Exp. #2 - gently swabbed with acetone to remove oil.
Water Supply Arrangements:	One water supply system for each experiment. Food grade suction hose, with submerged inlet, led to HTM pipe entrance approximately 15' above sea surface. Pump was located downstream of its HTM pipe and coupon holder; it discharged overboard. Suction hose inlet protected by cast iron strainer. Maximum head loss in the hose was approximately 35 feet between hose inlet and pipe entrance.
Water Flow History:	Pumps stopped bi-weekly for 2-hour periods for system maintenance. Rolling and heaving of Noi'i caused ± 3% variation of instantaneous flow velocities. A large number of short-term stoppages occurred in Exp. #1.
Flow Meter History:	Not reported.
Estimated Resolution in R_f:	$\leq 0.3 \times 10^{-4}$ $\left(\frac{Hr\ Ft^2\ °F}{BTU}\right)$.
Pipe Brushing History:	Not brushed.
Biology and Corrosion Samples in Flow:	Coupons of the HTM pipe material were placed end-to-end inside a 1-1/4 inch plastic pipe. The plastic pipe was plumbed into the flow between HTM and pump. Glass slides were included in the flow and in the ocean near the hose intake.

Water Quality Samples:	30 daily water samples taken between August 13 and September 19, from depth of suction hose inlet.
Maximum R_f Growth Rate:	Exp. #1, $2.x10^{-4}$ $\frac{Hr\ Ft2\ °F}{BTU\ week}$, 10th week
	Exp. #2, $1.x10^{-4}$ $\frac{Hr\ Ft2\ °F}{BTU\ week}$, 5th week
Biology Results:	Biofouling film contained living organisms, their products, particulate inorganic material, inert biologically derived materials such as diatom frustules and apparently significant amounts of glass and glass fibers.
Corrosion Results:	A layer of material under the biofouling film had a cracked and checked appearance. Pits formed in the 6061-T6 pipes.
Water Temperatures:	∿ 24°C
Water Quality Results:	Total bacteria in many seawater samples were in the order of 20,000 per milliliter of seawater.

1.2 Buoy 1

Lead University:	Carnegie-Mellon
Number of Experiments:	3
Observation Periods:	Exp. #1, February 12 - July 3, 1977 Exp. #2, February 12 - July 3, 1977 Exp. #3, February 12 - April 27, 1977 (See Note (1)
Location:	Buoy, anchored 400 yd WNW of Keahole Point lighthouse in 200 ft of water. Buoy was submerged. Water inlet end of HTM pipe was approximately 40 feet below still water surface.
Materials and Nominal Flow Velocities:	1st Exp: 6061-T6 Al at 3'/s 2nd Exp: 6061-T6 Al at 6'/s 3rd Exp: B337-Ti (grade 2) at 6'/s
Pipe Pre-cleaning Methods:	100 strokes with bristle brush using a commercial cleaning powder and tap water.
Water Supply Arrangement:	One water supply system for each experiment. Water flowed directly into each pipe entrance. Each pump was downstream of its HTM pipe and of the pipe coupon holder; it discharged to the sea, downward, approximately 12 feet below the pipe entrance. Each pipe entrance was protected by a nylon screen. Head loss through the HTM pipe was approximately 3 feet.
Water Flow History:	Experiment #3 terminated when pump failed at 10.6 weeks. Pumps serving both Exp. #1 and Exp. #2 stopped for unknown period(s) between 11.4 weeks and 12.6 weeks. See note (2).

Flow Meter History: Meter on Exp. #3 stable for entire 10.6 week period. Meters on Exp. #1 and #2 stable until pump stoppage at 11.4/12.6 weeks. Calibration apparently changed after pump stoppage. Velocities estimated for period 12.6/20.2 weeks.

Estimated Resolution in R_f: 0.1×10^{-4} $\frac{Hr\ Ft^2\ °F}{BTU}$

Pipe Brushing History: MAN brush, controlled by diver. Pulled forth by flowing water and pulled back by diver.

	Exp. #1	Exp. #2	Exp. #3
Date	June 5	June 6	
No. of Passes	1	1	
$R_f 10^4$ before/after	8.5/4.5	2.5/-.3	
No. of Passes	11	5	
$R_f 10^4$ before/after	4.5/3.0	-.3/-.8	

See Notes (3) and (4)

Bio-corrosion Samples in Flow: A pipe coupon holder similar to that used in Noi'i was placed in the flow.

Water Quality Samples: Not reported

Maximum R_f Growth Rates:

Exp. #1, $3.\times 10^{-4}$ ($\frac{Hr\ Ft^2\ °F}{BTU\ week}$) after brushing, 16th week

Exp. #2, $1.\times 10^{-4}$ " " " , 16th week

Exp. #3, $1.\times 10^{-4}$ " no brushing, 9th week

See note (5)

Biology Results: Reported together with Noi'i results; see above.

Corrosion Results: Corrosion of Buoy I aluminum reported together with Noi'i results; see above. The Ti pipe sections through which water had flowed for 5.4 weeks were not corroded.

Water Temperatures: 24.2 - 26.7 °C

Water Quality Results: Reported together with Noi'i results; see above.

Notes:

(1) Pipes were exposed to stagnant and flowing seawater water for about 1 week before the first observations were made.

(2) R_f dropped in both Exp. #1 and #2 during the pump stoppage that occurred between 11.4 and 12.6 weeks.

(3) Negative values of R_f after brushing in Exp. #2 believed traceable to loss of flow meter calibration at 12.6 weeks.

(4) Failure to reach R_f value of approximately zero after brushing in Exp. #1 possibly related to pump stoppage. Barnacles were found in this HTM.

(5) A comparison of curves of R_f versus time for Noi'i and Buoy I indicates that no effect of flow velocity has been determined. Further, comparison between Al and Ti indicates that the effect, if any, of initial surface roughness is not seen after the initial fouling layer has formed.

1.3 Buoy 2

Lead University:	Carnegie-Mellon
Number of Experiments:	4
Observation Periods:	Exp. #1, November 6, 1977 - (July 24, 1977) Exp. #2, November 6, 1977 - see note (1) Exp. #3, November 6, 1977 - Exp. #4, November 6, 1977 -
Location:	The submerged buoy that was used for Buoy I experiments.
Materials and Nominal Flow Velocities:	Exp. #1: 5052 Al 6'/s Exp. #2: 5052 Al " Exp. #3: Grade 2 Ti 6'/s Exp. #4: Grade 2 Ti "
Pipe Pre-cleaning Method:	Exp. #1 and #2 - A caustic soda treatment followed by a nitric acid treatment. Exp. #3 and #4 - Treatment with a mixture of nitric and hydrofluoric acids. See note (2).
Water Supply Arrangement:	One system for each experiment with flows directly into the pipe entrances as in Buoy I experiments.
Water Flow History:	One pump failed on February 8. The pipe of the corresponding HTM was connected in series with the pipe of another experiment. No further records are available.
Flow Meter History:	Records indicate that the signal cable failed sometime between February 15 and May 16. Three instruments, bearing field labels "A", "C" and "D" were operating in June-July. Flow rates were measured by divers using TSK flow meters in June-July. See note (3).
Estimated Resolution of R_f:	Not reported.
Pipe Brushing History:	Records indicate "another" brushing of instruments "A" and "C" on June 26 using 20 passes of a MAN brush.
Bio-corrosion Samples in Flow:	See note (4).

Water Quality Samples:	A regular program at collecting samples was initiated in June. Samples were collected by divers at the buoy.
Maximum R_f Growth Rates:	Not reported.
Biology Results	See note (4).
Corrosion Results:	Grade II titanium was essentially inert; 5052 aluminum did not pit and its corrosion rate was low.
Water Temperatures:	June and July, 26 - 27 °C.
Water Quality Results:	June and July -

Salinity	34.5 - 34.7 o/oo
pH	8.24
Alkalinity	2.34 mg/l
Dissolved O_2	5 - 6 ml/l
NO_3^-	0.2 - 0.4 µg•atom/l
PO_4^{-3}	0.3 - 0.5 µg•atom/l

Notes:

(1) Three experiments were terminated July 24, 1977. One experiment was terminated at an unknown earlier date.

(2) The soda and acid treatments affected aluminum pipe surfaces adversely.

(3) Sessile organisms were found in the region just upstream of the flow meter in each HTM.

(4) The approach to biology, corrosion and water quality was changed during Buoy II. New Researchers were added to the team. Goals were set. Sampling and analysis procedures were changed [9,10]. Brief results are available indicating that average dry film thicknesses reached approximately 100µm in 154 days. The ratio of wet to dry film thickness was 6.7:1 for aluminum pipes.

1.4 Buoy 3

Lead University:	Hawaii
Number of Experiments:	4
Observation Periods:	Exp. #1, November 6, 1978 - August 31, 1979 Exp. #2, November 6, 1978 - July 24, 1979 Exp. #3, November 6, 1978 - August 31, 1979 Exp. #4, November 6, 1978 - August 31, 1979
Location:	The submerged buoy that was used in Buoy I and II experiments.
Materials and Nominal Flow Velocities:	Exp. #1: 5052 Aluminum 6'/s Exp. #2: Grade 2 Titanium 6'/s Exp. #3: AL-6X Stainless Steel 6'/s Exp. #4: CA-706 (90-10) Copper Nickel 6'/s

Pipe Pre-cleaning Method: 40 strokes with a MAN brush, using Liqui-Nox, a liquid soap, followed by a rinse with tap water. See note (1).

Water Supply Arrangement: One system for each experiment with flows directly into the pipe entrances as in Buoy I and II experiments.

Water Flow History: Flow stopped in one or more experiments and for periods up to 1 day in November, February, March, April, July and August. Flow to Exp. #4 was interrupted for 4 days in February.

Flow Meter History: Data was obtained from the HTM flow meters for the first 10 days of the experiments. From November 16 to June 11, all flow velocity data was obtained by divers using portable meters. From June 11 to August 31 the HTM flow meters were operational.

Estimated Resolution of R_f: The uncertainty in R_f due to uncertainty in flow velocity was approximately $(+ 0.0, - 0.2 \times 10^{-4})$. The uncertainty in R_f inferred from scatter of the cooling curve data about the mean line was approximately $\pm 0.2 \times 10^{-4}$. The net uncertainty in R_f was $(+ 0.2 \times 10^{-4}, - 0.3 \times 10^{-4})$. The units of R_f are $(\frac{Hr\ Ft^2\ °F}{BTU})$.

Pipe Brushing History: The MAN Brush was modified so that it would spin while being passed back and forth by a diver through the HTM pipes. Two passes were made with the brush at each instance when the pipes were cleaned. The total elapsed weeks at the times of pipe brushings and the values of $R_f 10^4$ before and after each 2-pass brushing were:

Total Elapsed Weeks	Exp. #1 (Al)	Exp. #2 (Ti)	Exp. #3 (SS)	Exp. #4 (CuNi)
8.4				1.8/0.0
8.7	3.0/0.2		3.0/0.2	
13.7	2.9/0.2	4.8/-0.4	4.6/0.2	
35.7	13.2/0.8*		16.1/0.5	11.0/0.8
37.7			3.0/0.8	
38.1				2.6/0.6
39.6			3.2/0.9	
39.7	7.3/1.1**			3.6/0.6

* R_f for Al dropped to 0.4 at 36.1 weeks.
** R_f for Al dropped to 0.4 at 40.1 weeks.
See note (2).

Bio-corrosion Samples in Flow: Sections of pipe of the same material as in the HTM were pre-scored at coupon lengths and placed in pipe holders in the flow path. Short term samples were collected at the end of 3 hours, 6, 9, 12 hours, 1 day, 2 and 3 days, and then 1 week, 2 and 3 weeks. Sampling ceased after an equipment failure at the end of the 13th week. Samples were also taken from the HTM pipes after they were recovered.

The bio-corrosion coupons were brushed during the 8th and 13th weeks when the corresponding pipes were brushed (see "Tube Brushing History"). The coupons were not brushed after the 13th week.

Water Quality Samples: Nine samples were collected by divers at the buoy during the period October 1978 - June 1979.

Maximum R_f Growth Rates (after brushing):

Exp. #1 (Al)	2.7×10^{-4} ($\frac{Hr\ Ft^2\ °F}{BTU\ week}$)	40th	week
Exp. #2 (Ti)	$.9 \times .0^{-4}$	13th	"
Exp. #3 (SS)	2.7×10^{-4}	40th	"
Exp. #4 (CuNi)	1.7×10^{-4}	40th	"

Biology Results: Increases in R_f were related to organic film dry weight and also to total nitrogen and total organic carbon in the films for Exp. #2 and #3 (Ti & SS). Similar relationships were found in Exp. #1 (Al) but only after the 1st 3 weeks.

CuNi was colonized by microorganisms but their contribution to dry film weight was small.

Neither Ti nor SS was toxic to microorganisms.

Carbon to nitrogen ratios were essentially constant over time. They were:

Exp. #1 (Al)	4.0 ± 0.8
Exp. #2 (Ti)	4.2 ± 0.9
Exp. #3 (SS)	4.8 ± 0.7
Exp. #4 (CuNi)	7.9 ± 0.8

A comparison of SS and Ti indicates that initial surface roughness does not affect fouling rates after a primary fouling film has formed.

See note (3) re stray currents in the Al and CuNi pipes.

Corrosion Results: Grade 2 titanium and AL-6X stainless steel (Exp. #2 and #3) were essentially inert under the conditions of the experiment.

5052 aluminum did not pit. MAN brushing did not remove the corrosion product film. The uniform corrosion loss in 30 years is predicted to the 114μn (4,5 mils). However, a cleaning method that would remove the corrosion film would result in a loss of about 2,160μm (8.5 mils) in 30 years.

90-10 CuNi showed a complex pattern of film formation which is not yet understood. The corrosion film was a major factor in R_f.

Iron was present in high concentrations in the corrosion products of both Al and CuNi.

See note (3) re stray currents in the Al and CuNi pipes.

Water Temperature Range at Buoy: 25.5 - 27.8 °C (October 79 - January 80)

Water Quality Ranges:

Location - Buoy	Oct.	to	Jan.
Salinity	34.43	-	34.62
pH	8.21	-	8.27
Alkalinity	2.23	-	2.38
O_2	4.6	-	5.1
NO_3^-	.15	-	.42
PO_4^{-3}	.2	-	.38

Notes:

(1) After cleaning, pipes were filled with tap water and capped. Pipe caps were removed after the HTMs were installed on the buoy and minutes before the pumps were started.

(2) Experiment #2 (Ti) was terminated after 206 days due to an equipment failure. No heat transfer data were acquired from Experiments 1, 3 and 4 between the 116th and 198th days due to another failure, however, flows through the HTM pipes was maintained throughout that period.

(3) Evidence was found of stray electric currents in Experiments 1 and 4.

1.5 3-Inch Pipeline

Lead University: Hawaii

Number of Experiments: 2 See note (1).

Observation Period: March 17 1980 - August 29, 1980

Location: Instruments and all electronics were located on shore near the Keahole Point lighthouse. Water was supplied through a 3-inch pipe. The inlet end of the pipe was at the buoy used in Buoy I, II and III.

Materials and Nominal Flow Velocities:
Exp. #1 ("Unit X") Grade 2 Ti 6'/s
Exp. #2 ("Unit Y") Grade 2 Ti 6'/s

Pipe Pre-cleaning Method: 40 strokes with a MAN brush using Liqui-Nox as was done in Buoy III.

One system served both experiments.

Water Supply Arrangement: Water taken from the ocean at the buoy was pumped ashore. The conduit was a 3-inch ID food-grade flexible plastic pipe. Total length of the conduit was 1500 feet. The pump was located on the ocean floor approximately half-way between inlet and discharge of pipe. A header ashore distributed seawater to the two HTM pipes. The pipes discharged to a sandy beach. Flow velocity was 2.2 ft/s. Residence time in the plastic pipe was 11 - 14 minutes.

Water Flow History: Water flow interruptions

Date	Duration
March 17 - April 2	2 minor interruptions
April 3	48 hours
August 11	2.5 hours
August 14	20 hours
August 25	5 hours

Flow Meter History: Meters on both instruments calibrated after 112 days.

Estimated Resolution of R_f: $\pm 0.3 \times 10^{-4}$ $\left(\frac{\text{Hr Ft}^2\ ^\circ\text{F}}{\text{BTU}}\right)$, estimated from graph of R_f vs time.

Pipe Brushing History: Two different techniques were employed. The HTM pipe of Exp. #1 was cleaned with a MAN brush as in Buoy III. The pipe of Exp. #2 was soaked in nitric acid, brushed and rinsed with fresh water. The total elapsed weeks at the times of pipe brushings and the values of $R_f \times 10^4$ before and after cleaning were:

Total Elapsed Weeks	Exp. #1	Exp. #2
15.8	7.6/0.2	7.4/0.3

Bio-corrosion Samples in Flow: Initially, biology coupons were placed downstream of Unit X only. After unit Y was cleaned with acid, pipe coupons were placed in its discharge, also. Al-clad corrosion samples were placed in the discharge.

Water Quality Samples: Five samples were collected by divers at the buoy during the period September 7, 1979 to February 8, 1980, and 4 samples were collected during the period April 18 to May 29, 1980.

In July, comparative tests for dissolved oxygen were made in the ocean at the buoy and ashore at the HTM discharge. Additional tests were made after stopping the pump for a 15 minute interval.

Maximum R_f Growth Rates (after cleaning):

Exp. #1, $1.4 \times 10^{-4} \left(\frac{\text{Hr Ft}^2\ ^\circ\text{F}}{\text{BTU week}}\right)$ 23rd week

Exp. #2, 0.7×10^{-4} " 20th week

See note (1)

Biology Results: A major purpose of the 3-inch pipeline was to compare the results of experiments on the buoy with experiments in water that had been pumped through such a pipe.

Increases in R_f were related to organic film dry weight and to total nitrogen and total organic carbon in the film as was seen in the Buoy III experiment. The total iron and protein in the pipeline experiment were also assayed and found to correlate with R_f.

The limited data suggest that the films contained more carbon per unit of R_f in the Buoy III experiment before cleaning than in the pipeline experiment.

After Unit X was brushed and Unit Y was acid cleaned the value of the ratio of dry film weight to a unit change in R_f for X was found to be larger than the corresponding value for Y.

Corrosion Results: Measurements made of the corrosion film on AL-CLAD coupons in the HTM flow were compared with similar measurements made on 5052 aluminum in Buoy II and Buoy III. A strong correlation was found between the graphs of the film thickness vs platelet diameter for AL-CLAD and 5052.

The graphs of film thickness vs time were also compared for the two metals. The AL-CLAD graph had the same shape as the 5052 graph but the film on AL-CLAD was thicker than the film on 5052 after 3 weeks. Similarly, diameters of platelets in the AL-CLAD film were larger than those in the 5052 film.

Water Temperature Range at Buoy: 25.1 - 25.6 °C (April 18 - May 29)

Water Quality Ranges:

Dates	9/7/79-11/9/79	4/18/80-5/29/80	July
Location	Buoy	Buoy	
Salinity o/oo	34.148- 34.674	34.67 - 34.77	
O_2 ml/l	4.81 - 5.41	4.78 - 5.20	6.0±0.5 (buoy)
pH	8.15 - 8.27	8.14 - 8.18	
Carbonate Alkalinity meg/l	2.00 - 2.49	1.98 - 2.18	
NO_2+NO_3 µm/l	0.14 - 1.98	0.09 - 0.13	
PO_4 µm/l	0.13 - 0.19	0.22 - 0.24	
O_2 ml/l			6.0±0.5 (on shore)

Notes:

(1) A corrosion experiment was conducted simultaneously on AL-CLAD which was not a coupon from the HTM pipe.

(2) Exp. #1 (Unit X) was brushed; #2 (Unit Y) was cleaned with acid.

1.6 Remarks

This report summarizes five groups of experiments that evolved from concept which originated at CMU in 1973. The experiments put OTEC hardware into the ocean for the first time. The hardware met what George Claude called "...that terrible adversary, the sea." It survived long enough to produce results that will aid OTEC designers.

Several teams and several organizations participated in the Keahole experiments. John Fetkovich of Carnegie-Mellon University wrote the first proposal and led the effort through the first, second and third groups of experiments. The University

of Hawaii led the fourth and fifth efforts. H.J. White and F.C. Munchmeyer were co-principals for the Hawaii team during the entire series. L.R. Berger and B.E. Liebert of the University of Hawaii joined the project for the last two experiments; they led the biology and corrosion studies, respectively, and also reviewed earlier data. Glenn Granneman of CMU heads a long list of others who were major contributors.

Succeeding chapters discuss sites and field apparatus, heat transfer, water quality, biology and corrosion aspects of the OTEC experiments at Keahole Point.

1. J.G. Fetkovich, G.N. Granneman, D.L. Meier and C.W. Fette, "A Novel Method of Measuring Heat Transfer Coefficients with High Precision," in Proceedings, 12th Southeastern Seminar on Thermal Sciences, June 6-8, 1976, University of Virginia, Charlottesville.

2. John G. Fetkovich, "A System for Measuring the Effect of Fouling and Corrosion on Heat Transfer under Simulated OTEC Conditions," Report No. COO-4041-10, Carnegie-Mellon University, Pittsburg, December 1976.

3. J.G. Fetkovich, G.N. Granneman, D.L. Meier and F.C. Munchmeyer, "Studies of Biofouling in Ocean Thermal Energy Conversion Systems," in Sharing the Sun: Solar Technology in the Seventies, Winnepeg, Canada, 1976.

4. J.G. Fetkovich, G.N. Granneman, L.M. Mahalingam, D.L. Meier and F.C. Munchmeyer, "Studies of Biofouling in OTEC Plants," in Proceedings, Second STAR Symposium, San Francisco, May 25-27, 1977, The Society of Naval Architects and Marine Engineers.

5. George W. Harvey, "Biofouling Experiments at Keahole Point, Hawaii, 1976; Biological Studies Program Report," unpublished, Pan Pacific Laboratories, Honolulu, 1976.

6. John G. Fetkovich, Glenn N. Granneman, L.M. Mahalingam and Daniel L. Meier, "Progress Report: A Study of Fouling and Corrosion Problems Related to a Solar Sea Power Plant," Report No. COO-4041-9, Carnegie-Mellon University, Pittsburg, September 1, 1977.

7. J.G. Fetkovich, G.N. Granneman, L.M. Mahalingam, D.L. Meier and F.C. Munchmeyer, "Degradation of Heat Transfer Rates due to Biofouling and Corrosion at Keahole Point, Hawaii," in Proceedings of the OTEC Biofouling and Corrosion Symposium, Robert H. Gray, ed., Seattle, October 10-12, 1977, Pacific Northwest Laboratory, August 1978.

8. J.G. Fetkovich, G.N. Granneman, L.M. Mahalingam and D.L. Meier, "Measurements of Biofouling in OTEC Heat Exchangers," in Proceedings of the Fifth OTEC Conference, V. 4, Miami Beach, February 20-22, 1978, University of Miami, 1978.

9. L.R. Berger and F.C. Munchmeyer, "Summary Report of OTEC Biology, October 1, 1977 to January 15, 1978," unpublished report, College of Engineering, University of Hawaii, 1978.

10. L.R. Berger, W.F. McCoy and I.A. Berger, "Biofouling Assays for OTEC Pipes," in Proceedings of the OTEC Biofouling, Corrosion and Materials Workshop, Rosslyn, Virginia, January 8-10, 1979, Argonne National Laboratory, 1979.

11. Hank White and Cullen Tendick, "Preliminary Results from Ke-ahole Buoy Deployment #3," in Proceedings of the OTEC Biofouling, Corrosion and Materials Workshop, Rosslyn, Virginia, January 8-10, 1979, Argonne National Laboratory, 1979.

12. Bruce E. Liebert, "Corrosion of Aluminum and Titanium at Keahole Point over an Eight Month Period," Proceedings of the OTEC Biofouling, Corrosion and Materials Workshop, Rosslyn, Virginia, January 8-10, 1979, Argonne National Laboratory, 1979

13. Jeffrey A. Moore, untitled report on heat transfer results of Buoy III, The Energy Laboratory of Hawaii, November 30, 1979.

14. B.E. Liebert, L.R. Berger, H.J. White, I. Moore, Wm. McCoy, J.A. Berger and J. Larsen-Basse, "The Effects of Biofouling and Corrosion on Heat Transfer Measurements," in Ocean Thermal Energy for the 80's, V. 2, Gordon L. Dugger, ed., U.S. Department of Energy, 1979.

15. Leslie Ralph Berger and Brenda Little, "Effect of Microfouling on Heat Transfer Efficiency," in Proceedings 5th International Congress on Marine Corrosion and Fouling, Barcelona, May 19-23, 1980, Editorial Garsi, Madrid, 1980.

16. Bruce E. Liebert, K. Sethuramalingam and Jorn Larsen-Basse, "Corrosion Effects in OTEC Heat Exchanger Materials," in Proceedings 5th International Congress on Marine Corrosion and Fouling," Barcelona, May 19-23, 1980, Editorial Garsi, Madrid, 1980.

2.0 Sites and Field Apparatus

Keahole Point is the western tip of the Island of Hawaii, at 19° 44' North Latitude and 156° 04' West Longitude. It is exposed to winds and waves from the western half of the compass. The Island of Maui offers some protection from North Pacific storm swells. The high mountains of Hawaii block all weather from the east.

The shoreline at the Point is a low cliff. Water depth is approximately 15 feet at the bottom of the cliff; it increases to 200 feet at 400 yards offshore. There is no reef. Beyond the 200 foot contour the bottom slopes rapidly to mid-ocean depths; out to that contour, the bottom is lava with some coral outcrop.

The first four experiments were sited near the 200 foot contour. Thus the apparatus was open to attack from the north, west and south.

Local storms rarely strike the Point. Normal surface winds and light and variable. However, waves from distant storms attack often in winter and pose the greatest hazard to personnel and apparatus. A storm in January, 1980, generated waves whose breaking heights reached 20 feet above the cliff. That storm destroyed an unarmored signal cable, sections of a 3-inch water pipe and a pump that had been secured to the bottom near shore.

Ocean currents also created design and operational problems. Large gyres are often present in the ocean west of the island. They sweep the Point with currents which are intermittent and which attain speeds up to 3 knots.

The ocean surface is warm; temperatures at the experiments ranged from 23 to 28°C. Air temperatures under the tropic sun are also warm; scattered clouds cover 10% - 50% of the sky for 99% of the time.

Water quality in the region of the experiments is influenced by the shore. That influence is limited; the shoreline is generally lava with little vegetation and the nearest development lies more than 10 miles from the Point.

The fifth group of experiments was conducted on shore with water drawn from the ocean at the site of three previous experiments.

The Carnegie-Mellon heat transfer module (HTM) was the primary field apparatus at all sites. Fetkovich designed it primarily for the *in situ* experiments. In essence it is a 1-inch ID pipe, 8-1/2 feet long, a pump that induces water flow through the pipe, a system for measuring heat transfer between pipe and flowing water, and finally an outer shell; see Fig. 2.1

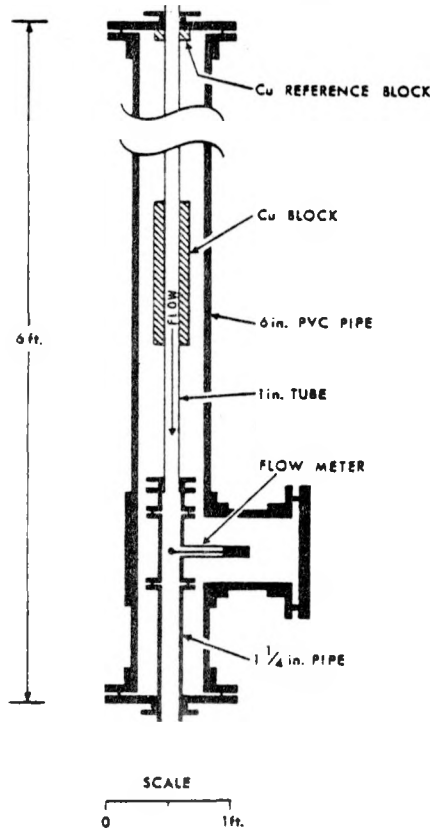

Fig. 1a Schematic of test unit

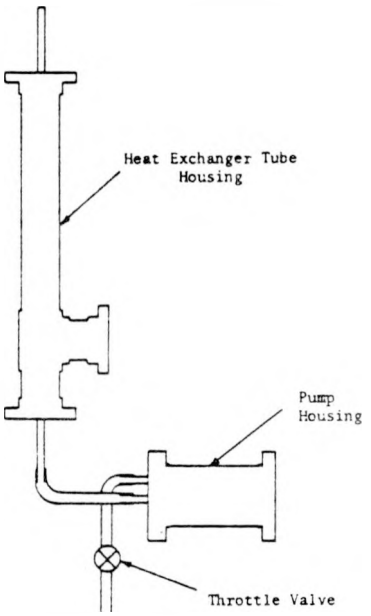

Fig. 1b Test unit showing pump attached

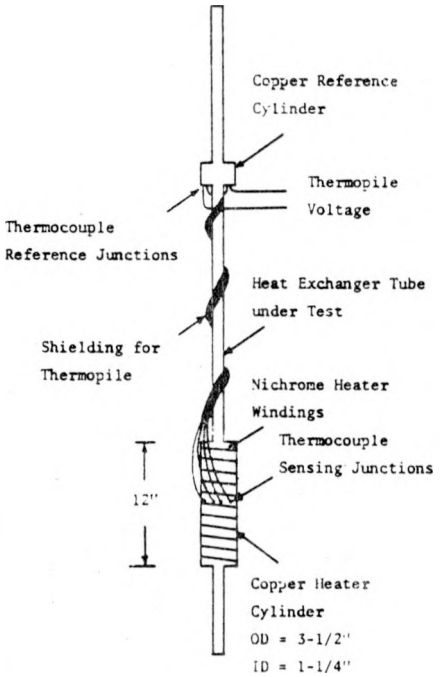

Fig. 1c Tube with instrumentation

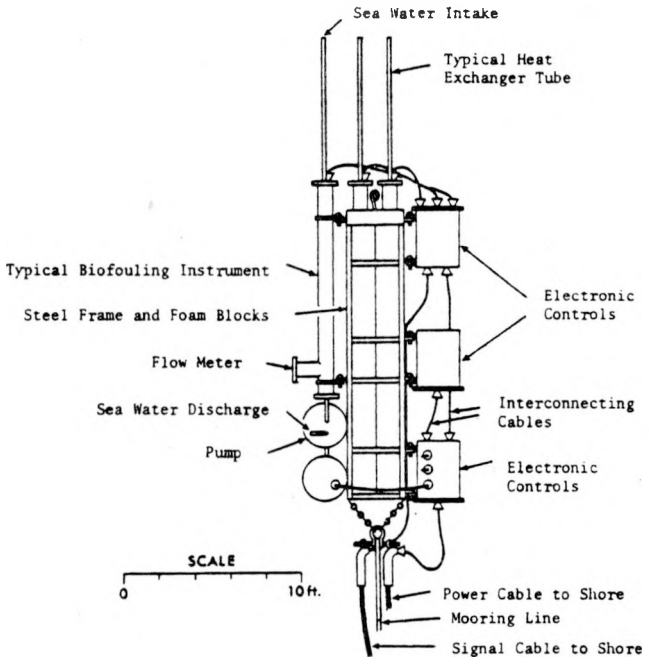

Fig. 1d Test units and electronics attached to submarine buoy

The increase of heat transfer resistance due to fouling on the seawater side of the pipe, R_f, must be inferred from small differences between relatively large numbers. To provide useful data for OTEC plant design the HTM should measure changes as small as 1% in the total resistance. Further, the instrument must measure total resistance accurately without calibration of its internal thermometer and power source. Fetkovich designed his HTM to satisfy these constraints.

The following sections describe details of site and apparatus for the five groups of experiments.

2.1 Noi'i

The first group of experiments was conducted on the research vessel Noi'i. She is a wooden hull boat, 65 feet long, 12 foot beam and 4 foot draft. She was anchored in 300 feet of water approximately 1 mile north northwest of the Keahole Point lighthouse. A 2-man crew maintained the boat and the primary electrical power supply to the experimental apparatus.

Two heat transfer modules were mounted on Noi'i's small afterdeck; each was positioned vertically. A separate pump served each HTM and was located downstream of the module. Water was drawn from the ocean through a food-grade hose which led to the HTM pipe at a point approximately 15 feet above the sea surface. The water was drawn down through the pipe and then overboard at deck level. A cast iron strainer was placed at the inlet of each suction hose. A primary pump was used to start the flow through each experiment.

Each HTM was covered with 2-inch thick fiberglass insulation plus an outer shield of aluminum foil.

The nominal intake depth at the inlet of the suction hose was 20 feet below sea level. The seawater flow rate through each apparatus was regulated by a manual throttling valve located downstream of the pump.

Controls for the HTM were located in Noi'i's main cabin approximately 10 feet from the afterdeck. One circuit controlled power to the heater on the main copperblock. A second circuit returned the thermopile voltage from the block. A third supported the flow meter and a fourth circuit connected the control apparatus to a thermistor that indicated seawater temperature at the HTM inlet.

Seawater flow was interrupted bi-weekly for maintenance of the generator that supplied power to the experiments.

Data for estimating heat transfer rate from the heater block to the flowing seawater were obtained at planned intervals. The procedure, in brief, was:

- record flow meter zero;
- energize heater circuits;
- monitor temperature difference between heater block and thermocouple reference junction at short intervals (< 10 seconds);
- allow heater block to attain a steady temperature (which was approximately 2°C higher than the reference);
- de-energize the heater;
- begin recording four items:
  - time,
  - heater-block thermopile voltage (the "cooling curve"),
  - sea-water-temperature thermistor resistance, and
  - flow meter voltage;
- continue recording these items for a period in excess of four heater-block time constants.

The data were recorded on a punched paper tape. The paper tapes were mailed to CMU for analysis. That analysis is discussed in Chapter 3, "Heat Transfer."

2.2 Buoy 1

In the second group of experiments, three HTMs were mounted on a submerged buoy. The buoy was anchored 400 yards west-northwest of the Keahole Point lighthouse in 200 feet of water. See Fig. 2.2.

The nominal water depth at the inlet to each HTM pipe was 40 feet. Each HTM had its own water pump which was located downstream of the pipe and flow meter. Flow rates were controlled individually by an orifice which was plumbed into the pump discharge line.

Each pipe inlet was protected by a nylon screen. A section of plastic pipe was plumbed into the flow between each HTM and its pump; this pipe served as a coupon holder for biofouling and corrosion samples. Pump discharge was directed downward at a point approximately 12 feet below the HTM inlet.

Power to operate pumps, heaters and instruments was supplied from the shore; the source was a pair of diesel generators. A double-armored cable transmitted power from generators to an "electronics box" which was mounted on one side of the submerged buoy. Power was distributed from the box to the three HTMs and their pumps through flexible, watertight cables fitted with special terminals.

The experiment was monitored and operated from a shore station. Signals were carried between buoy and shore station by shielded signal pairs which had

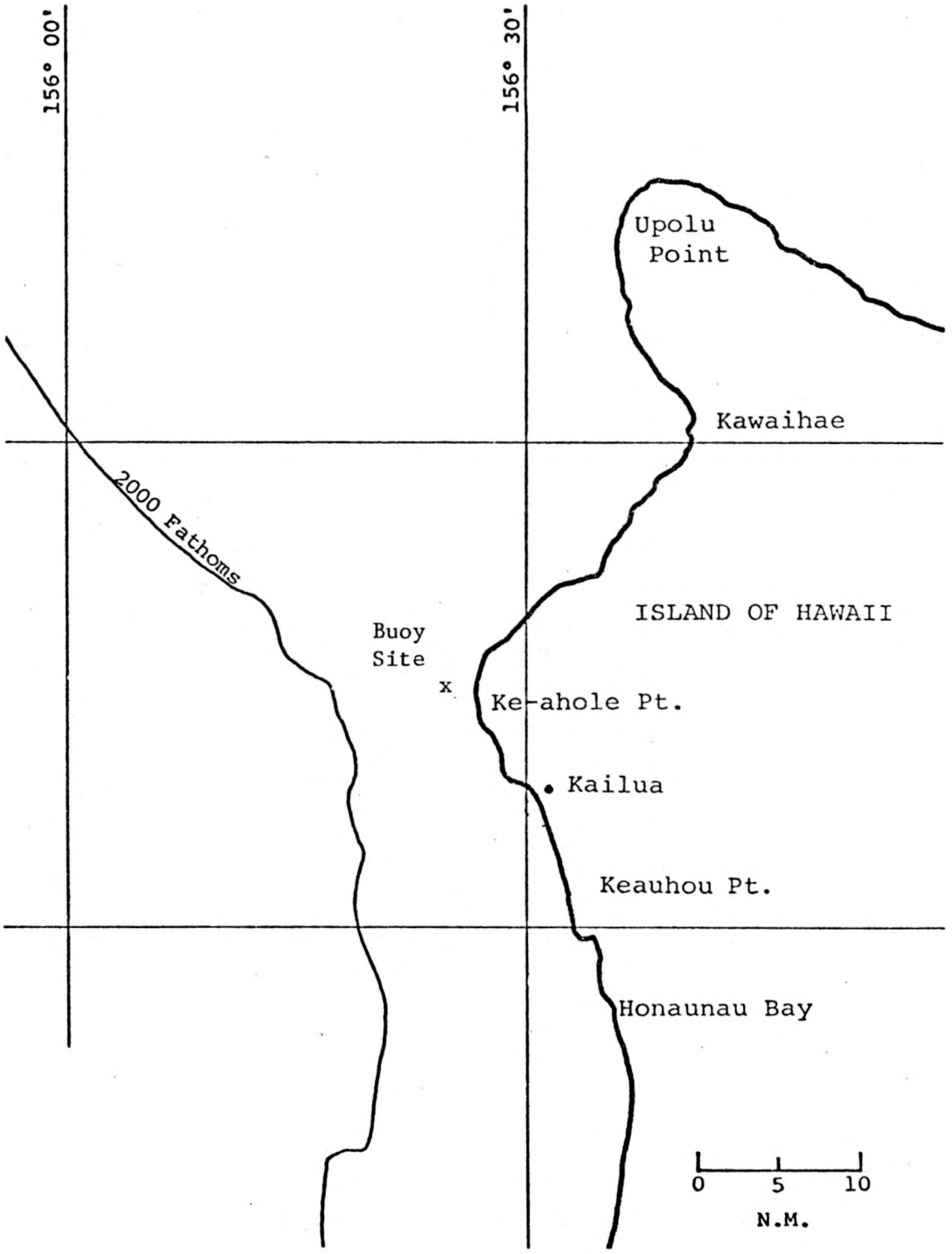

Fig. 2.2 Experiment site

been laid with the power wires in the armored cable. Signal connections between electronics box and the HTMs were made through watertight coaxial cables fitted with special terminals.

The buoy was composite; a rectangular steel frame provided structure and covered foam blocks provided buoyancy. The double-armored signal-power cable served as the buoy's tether to an anchor.

Prior to installation, the armored cable was given extra protection over the length that would lie in the surf zone. During installation, the cable was fastened to the bottom through the surf zone.

The buoy, its anchor and the cable were installed in one operation. They remained in place throughout this entire series of Keahole experiments.

The electronics box, HTMs and pumps were assembled and tested on shore and then taken to the buoy site on a workboat. Divers swam these seven units down, fastened each one to the buoy and then made the plumbing and electrical connections. The special fittings on the cables permitted divers to make signal and power connections underwater.

At intervals of time, divers serviced the buoy. On routine service calls they cleaned the inlet strainer on each HTM, brushed marine growth from the buoy and apparatus and inspected the external plumbing and wiring.

HTM preparations on shore consisted of electrical and watertightness checks, pipe cleaning, flow rate calibration and thermal calibration. For Buoy I, each of the three pipes was cleaned with a bristle brush, a commercial cleansing powder and tap water.

The flow meters were calibrated using tap water, a weigh tank and a stopwatch. A plot of heat transfer coefficient versus flow velocity (a Wilson plot) was made for each instrument.

After installation of the apparatus on the buoy, tests were made to prove each signal and power circuit. The operator on shore then initiated the same series of measurements that were taken previously on Noi'i, including a cooling curve, water temperatures and flow rates and elapsed time. The experiment controller and paper tape recorder were located in an instrument house which was adjacent to the generators at the shore end of the signal-power cable. The tapes were sent to CMU for analysis.

Divers also collected coupons that had been in the water flow path. These were sent to a laboratory in Honolulu for analysis of the fouling film.

On two occasions, divers brushed the HTM pipes. A MAN brush was attached to a fish line and inserted into the inlet of a pipe. Flowing water dragged the brush down the pipe, beyond the heater block; the diver pulled the brush out to complete one pass.

2.3 Buoy 2

The site for the third group of experiments was the same buoy that was used previously. The apparatus was similar to that used in Buoy I.

Four HTMs were available. Their pipes were cleaned by new methods which were adapted from ASTM standards. Two aluminum pipes were treated with caustic soda, followed by a nitric acid neutralizer then a rinse with deionized water. Two titanium pipes were pickled in a solution of nitric and hydrofluoric acids and rinsed with deionized water.

Flow meter calibrations and Wilson plots were made on each HTM prior to deployment. Field operations were essentially the same as in Buoy I for the first three months.

One pump failed during the third month of operation. The corresponding HTM was restored to service by plumbing it in series with a neighboring instrument.

Signals were lost after three months due to a failure of the signal portion of the armored signal-power cable. The power circuits continued to function and water flow was maintained through the HTM pipes.

A new, plastic-jacked signal cable was laid between the electronics box and the operator's station ashore and the system was restored to full operation 7 months after deployment. The experiments were concluded during the 9th month.

2.4 Buoy 3

Four instruments were available for the third and last group of buoy experiments.

The buoy itself had not changed significantly since the launching, nearly 3 years earlier. It appeared to have adequate reserve buoyancy. The frame was corroded but was structually adequate. The armored cable continued to function both as a tether to the anchor and as a conductor for power. The plastic jacketed cable that had been laid during Buoy II carried signals.

The two diesel generators continued to supply primary power.

A new pipe pre-cleaning method was adopted. Each HTM pipe, regardless of material, was cleaned by brushing with a liquid soap called Liqui-Nox. Each

pipe was given 40 strokes of a MAN brush followed by a freshwater rinse. The clean tubes were then filled with tap water and capped. The caps were not removed until the instruments were in place and shore control was ready to start the pumps.

The HTMs were modified to minimize the influence of temperature changes in the flowing water. Each instrument was calibrated for flow rate and thermal properties, continuing the prior practices.

New pumps and modifications to old pumps were introduced. The bio-corrosion samples were redesigned for better handling.

The deployment was standard. Pump outages occurred occasionally during the course of Buoy III. The flow meters failed early; portable flow meters operated by divers provided substitute data.

The *in situ* pipe brushing scheme was modified; the MAN brush was allowed to spin during each pass through a HTM pipe. The pipe coupons that were plumbed into the flow downstream of each HTM were brushed, also.

The signal cable failed during the 3rd month. The electronics box flooded, partially, during the 4th month. Power to the pumps was supplied through a substitute distribution box during repairs to the electronics box. A new plastic-jacketed signal cable was laid, the electronics box was redeployed and the system was restored to operation during the 7th month.

A device was installed which would maintain the primary power supply in the event of a temporary generator failure.

The heat transfer data collected during Buoy III were analyzed at Keahole Point. Biofouling and corrosion samples were analyzed at the University of Hawaii. Seawater samples collected at the buoy were analyzed at the Oceanic Institute in Hawaii. Buoy III was terminated in its 10th month.

2.5 3-Inch Pipeline

The fifth and final group of Keahole experiments was conducted on shore with water that was drawn from the ocean at the buoy. A 3-inch food-grade flexible suction pipe was laid from the shore station 1500 feet seaward. It was supported on a bridge over the land, to the edge of the cliff, and then it followed the armored cable to the buoy. The pump was sited on the bottom 150 feet seaward of the cliff in 35 feet of water.

The pipe was shaded from the sun over the land portion of its route.

Simultaneous experiments on shore and at the buoy had been planned. However, the buoy phase was cancelled after its signal cable was destroyed by severe waves.

In operation, the seawater flowed through the pipe at 2.2 lineal feet per second. Its residence time there was approximately 11 minutes.

The water was supplied to two HTMs and to corrosion and biofouling coupons downstream. Its flow rate through each HTM was controlled by downstream throttle valves.

The two HTMs were prepared as in the Buoy III experiments. They were installed in an air conditioned house. Heat transfer experiments were conducted in the manner that was developed for Noi'i and followed, essentially, through Buoy I, II and III.

Three water flow stoppages occurred during the first 5 months of the 3-inch pipeline experiments. The flow meters functioned normally.

One HTM pipe was brushed to reduce the fouling film using the Buoy III brushing technique. The fouling film in the other instrument was removed completely by soaking in nitric acid and brushing. The acid-treated HTM pipe was rinsed in freshwater before return to service.

Dissolved oxygen was measured at the inlet of the 3-inch pipe and then at its outlet, on one occasion.

Heat transfer data and samples of biofouling, corrosion and water were analyzed as in Buoy III. The 3-inch pipeline experiment was terminated in its 5th month.

2.6 Remarks

The Keahole Point site was selected initially for its topography and environment; experience supported that rationale. The buoy was anchored close to shore in water that was deep enough to afford protection from wave attack. The buoy itself survived well beyond its expected life as did the power cable. Operations at sea on the buoy experiments were rarely hampered by weather, waves or currents.

Water quality samples over the years indicated a mild island effect.

The Fetkovich HTM performed as designed in all five experiment groups.

Pumps, connectors, signal cables and primary power were weak points. Corrosion of cooling coils took pumps out of service often. The sea claimed several underwater connectors and three signal cables. The reliability of the primary power supply was limited by the availability of resources.

3.0 Heat Transfer

Confident measurements of the degradation in heat transfer were central to all five groups of experiments at Keahole. In the earliest days of the revival of OTEC, Zener at CMU recognized the biofouling and corrosion would degrade heat transfer. Fetkovich responded to Zener's problem with an instrument that would yield confident measurements over long periods of time without repeated calibrations.

The instrument was first reported in [1]. It does not require calibrations of either power or temperature, which are two basic measurements in heat transfer. It avoids calibration by measuring differences rather than absolute values of temperature. A massive copper cylinder is in close thermal contact with the sea water that flows through a one-inch pipe. The block is heated until the temperature difference between it and a reference becomes steady. In practice, that difference is approximately 2°C. Power is shut off and the copper block is cooled by the flowing sea water. The cooling rate and the physical properties of the block supply the principal data needed to determine heat transfer rates.

Fetkovich refined his basic idea and achieved high precision in laboratory measurements at CMU, as reported in [1]. The primary result of such an experiment is a value for the heat transfer coefficient, h, in the equation:

$$Q = h\ A\ \Delta t$$

Q is the heat transfer rate across a suface of area A in response to a temperature difference Δt. A typical value of h in a HTM experiment is $1000\ \frac{BTU}{hr\ ft^2\ °F}$. Fetkovich reported that the overall precision to which h can be measured and corrected is estimated to be better than 1%, in his laboratory.

The degradation of heat transfer in a simulated OTEC heat exchanger tube can be estimated with this instrument by observing changes in the heat transfer coefficient h over time. The custom in heat transfer is to report these changes in the form of heat transfer resistance due to fouling. The symbol is R_f:

$$R = \frac{1}{h}$$

$$R_f = \frac{1}{h} - \frac{1}{h_o}$$

where h_o refers to a clean surface, before fouling.

The coefficient h depends on instantaneous values of both temperature and velocity of the flowing waters. Thus those two properties of the flow are measured during an experiment. If they remain constant over the period in which copper block temperatures are measured then the corresponding value of h is assumed to be constant also. That value of h is normalized to a standard temperature and flow rate. The value of h_o is normalized also and the corrected resistance due to fouling is:

$$R_f = \frac{1}{h_{normalized}} - \frac{1}{h_{o_{normalized}}}$$

The precision required in measurements of R_f of Keahole was influenced by estimates of the value of R_f that would be practical in OTEC heat exchanger design. The order of magnitude of a design R_f is 0.0003 $\frac{hr\ ft^2\ °F}{BTU}$. This implies that the uncertainty in h should not exceed approximately 1%.

In the field the uncertainty of a single measurement of h lacked the precision that could be achieved in the laboratory. Several factors intervened. Both the temperature and the flow rate of ocean water passing through a HTM varied with time. Biofouling attacked the flow meter and the ocean attacked signal circuitry. Precision was improved by running as many as 16 experiments on the same HTM in succession. (The rate of increase of R_f was slow when compared with the time required for one experiment.)

In normal operation, each of the experiments in a particular sequence was evaluated for acceptance. A cooling curve was rejected if either the water temperature or the flow rate deviated from the mean value by more than a set amount. The reported value of h for that sequence was the average of values of h for experiments that were accepted.

When flow meter signals failed then best estimates of water velocity were used, with corresponding losses of certainty.

Heat transfer degradation was reported in the form of a graph of R_f versus time. The fifteen experiments produced eleven graphs.

All graphs showed a slow growth of R_f for a new surface. The rate of growth increased with time. In general, R_f could be reduced to zero by brushing. The MAN brush was used consistently. The rate of growth immediately after brushing was not constant but also increased with time.

Heat transfer details for four of the five groups of experiments are given in the following sections.

3.1 Noi'i

Initial values of the heat transfer coefficient h_o were obtained in a series of experiments on July 13 and 14, 1976. The one-inch by 8½ foot tube was made of 6061-T6 aluminum. The range of water velocities for this series was approximately 2 to 13 feet per second. The graph of $1/h$ vs. $1/v^{0.8}$, Fig. 3.1, was the expected straightline but the scatter was greater than had been experienced in the laboratory. That scatter was attributed to motions of Noi'i, which caused changes in water flow rates, and to variations in sea water temperatures. Figure 3.2 indicates that a small change in sea water temperature (<0.1°C) can cause the cooling rates to depart sharply from its expected linear behavior.

The first experiment was maintained for 10 weeks; the nominal water velocity was 3 feet/second throughout the period. The second experiment, at a nominal velocity of 6 feet/second, ran for 5 weeks. The resulting graphs of $R_f=(\frac{1}{h} - \frac{1}{h_o})$ versus time are shown in Fig. 3.3. The uncertainty in R_f was approximately 3×10^{-5} (hr ft^2 °F/BTU). An R_f value of 3×10^{-4} units was reached in approximately 5 weeks.

3.2 Buoy 1

Three instruments were deployed for the first buoy experiments. Two were intended to repeat the Noi'i experiments, using 6061-T6 aluminum at 3 feet/second and 6 feet/second. The third used a titanium tube at 6 feet/second.

Figure 3.4 shows the primary heat transfer results. There are no significant differences between the R_f growth rates due to flow velocity (3 vs. 6 feet/second) or due to material (Al vs. Ti). The growth rate of R_f was slower for the buoy experiments than for the Noi'i, reaching 3×10^{-4} units in approximately 8 weeks.

The Noi'i tubes were not brushed. The growth rate comparisons are made only for the initial periods of the experiments when the method of tube preparation should have its greatest relative effect; different methods were used in the two groups of experiments.

The titanium experiment was concluded during the 10th week when its pump failed. The aluminum experiments continued through 20 weeks. At 16 weeks the aluminum tubes were brushed in place. R_f for the 6 feet/second tube dropped to an indicated zero.

The aluminum pumps were stopped during the 11th and 12th weeks. R_f data degraded after that stoppage. However, it was evident that brushing had a major effect and may in fact have reduced R_f to near zero.

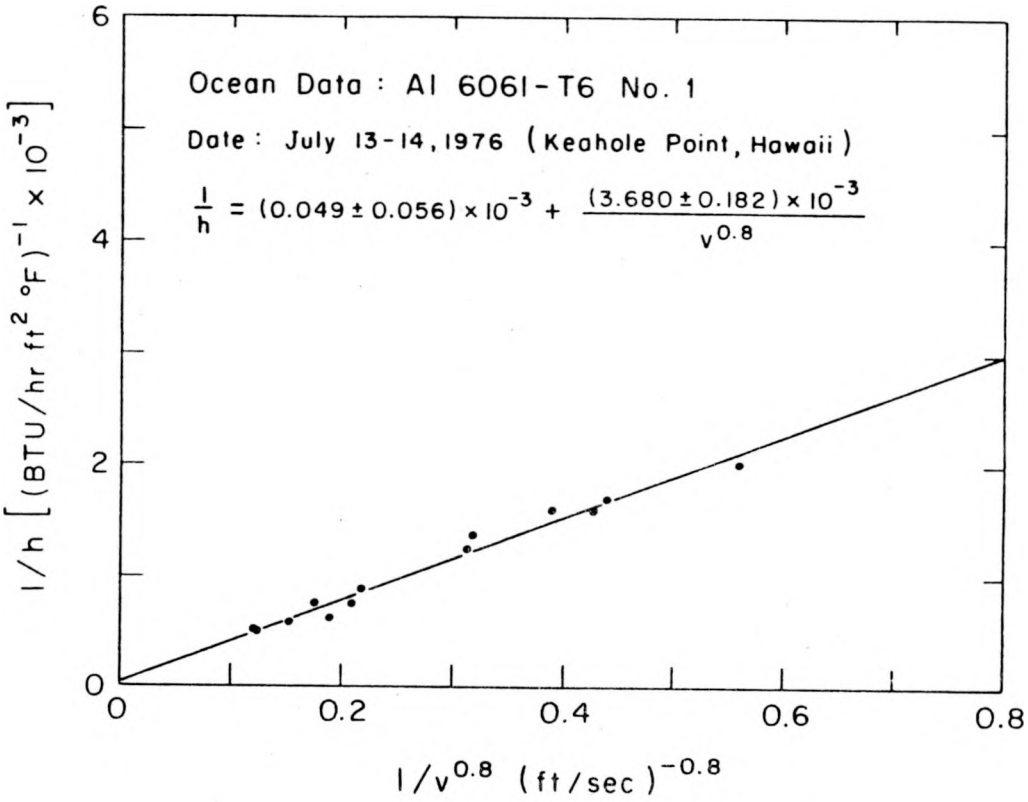

Fig. 3.1 Baseline ocean data for an aluminum tube.

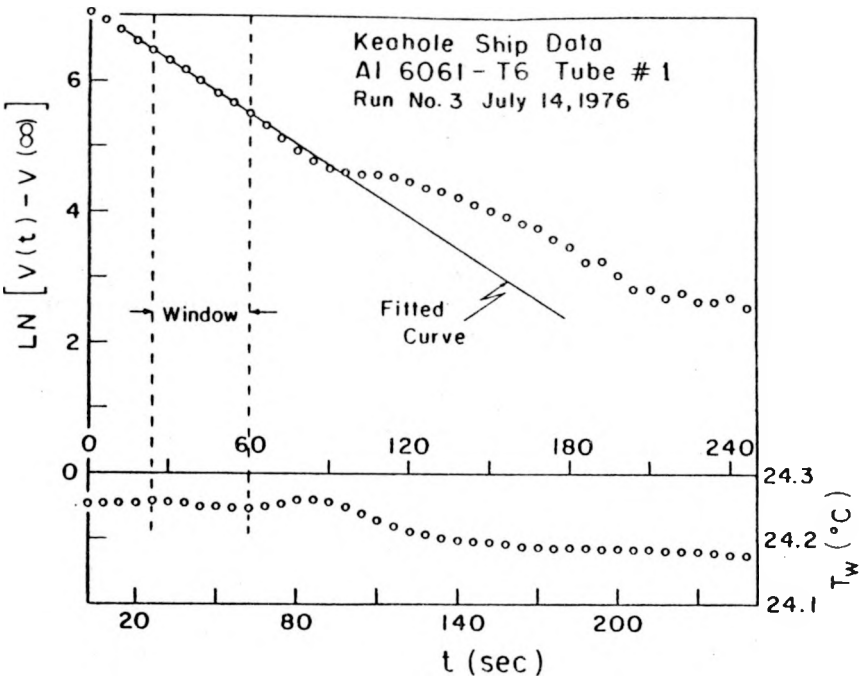

Fig. 3.2 Correlation between water temperature fluctuations and deviations of the thermopile decay data from the fitted curve.

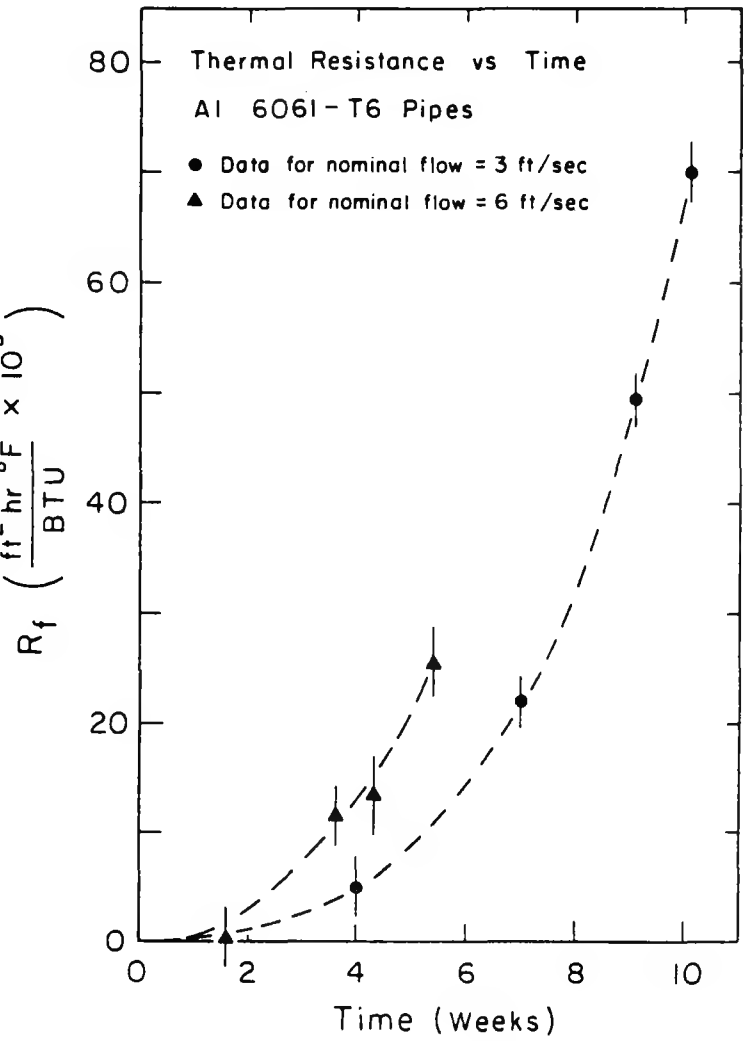

Fig. 3.3 Thermal resistance due to biofouling layer as a function of time.

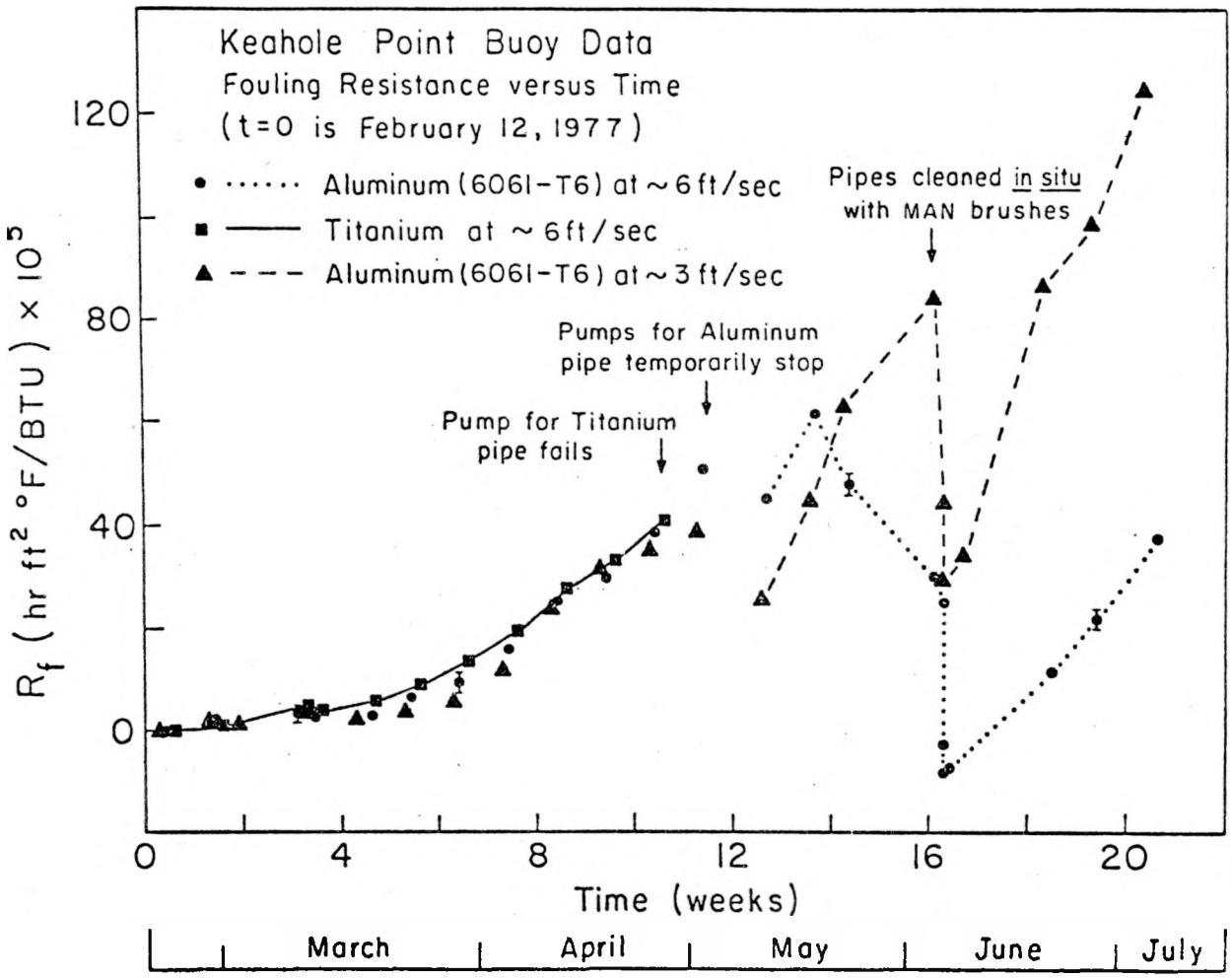

Fig. 3.4 R_f vs time for Buoy I.

3.3 Buoy 2

Two aluminum pipes, alloy 5052, plus two titanium pipes were deployed for the third group of experiments. The signal cable failed during this experiment which limited the collection of heat transfer data. The available data were transmitted to Carnegie Mellon. Insofar as we know, R_f analyses have not been published by CMU.

3.4 Buoy 3

Four HTMs were deployed for Buoy III. All were operated at 6 feet/second but four different pipes were used: aluminum, titanium, stainless steel and copper nickel. The Ti experiment was terminated during the 26th week; the other three experiments continued for 41 weeks.

The heat transfer data is affected strongly by the fact that the flow velocities used in most calculations were coarse. After the 2nd week, flow velocities were obtained by divers using a portable flow meter. In general, flow velocities were not measured at the time that cooling curves were recorded. Thus both accuracy and the precision of R_f were poor compared with R_f measurements made previously.

This group of experiments did produce useful cleaning data as is shown in Fig. 3.5 [4]. Each tube was brushed at least once. One was brushed five times. A 3-element pattern is seen in the plots of R_f versus time after brushing. First, R_f does drop to zero, or nearly so, whenever a tube is brushed. Second, the rate of increase of R_f increases after each brushing. Third, the value of R_f that is measured just after brushing may increase over time.

After 40 weeks the value of R_f measured just after brushing appeared to approach 1×10^{-5} in units of hr-ft^2-°F/BTU. Also after 40 weeks, the R_f growth rate appeared to approach 0.5×10^{-5} units per day.

3.5 3-Inch Pipeline

Two titanium HTMs were used in the 3-inch pipeline experiments. Flow velocities were 6 feet/second in both. R_f increased, initially, at approximately the same rates that were observed in the buoy experiments; Fig. 3.6.

Both tubes were cleaned and the experiments were continued. Tube "X" was brushed once, in the same manner that was employed in Buoy III. Its fouling rate after cleaning was faster than the rate at time zero and was comparable to Buoy III after-brushing rates.

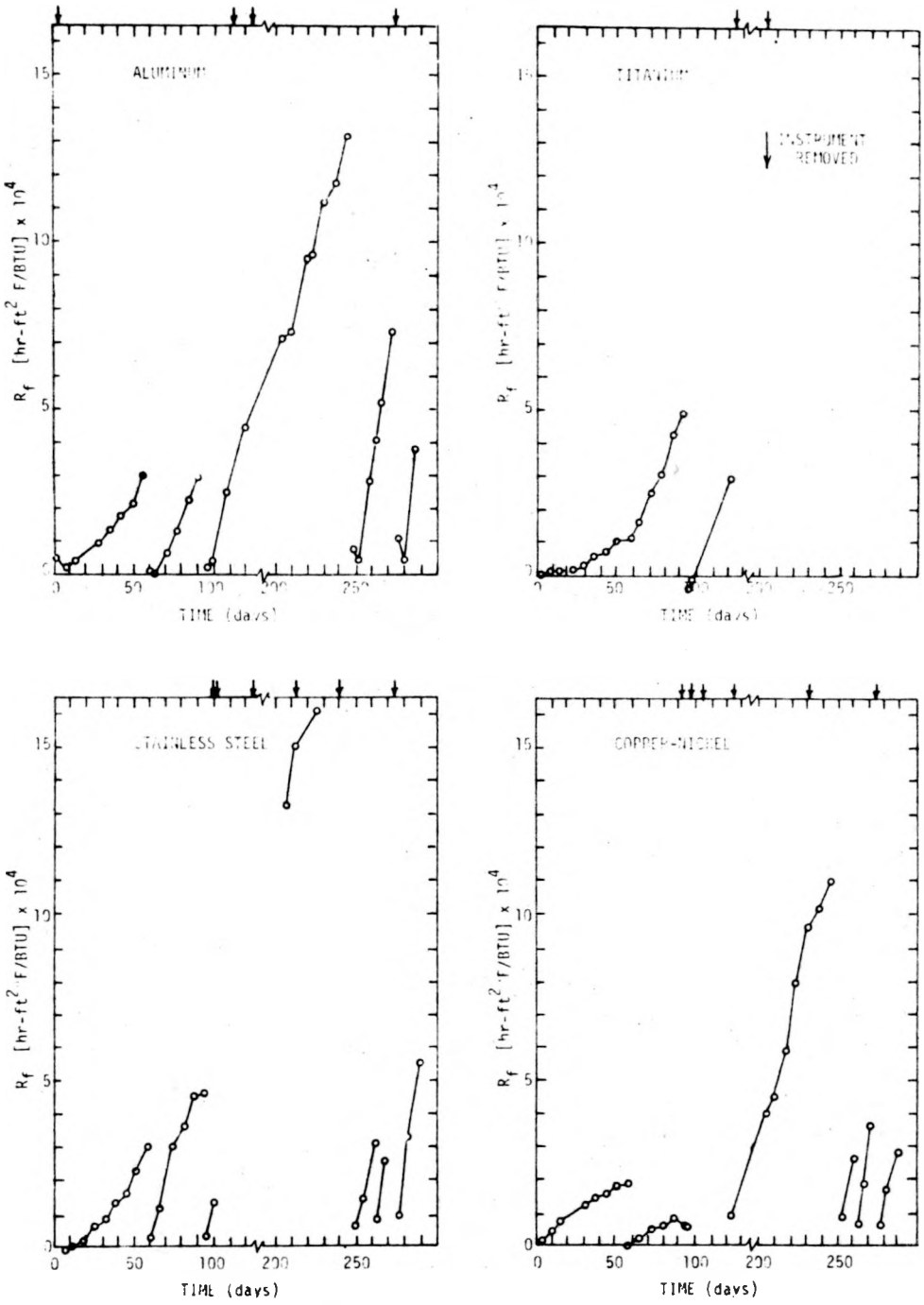

Fig. 3.5 Heat transfer resistance due to fouling (R_f) vs time of exposure to flowing seawater for the four metals studied in the flow of water. Drops in R_f were due to cleaning.

Tube "Y" was cleaned with acid in an attempt to replicate the time-zero surface condition. On resumption of the experiment, the fouling rate was slower than the tube "X" rate and was similar to its own time-zero rate.

3.6 Remarks

Confident measures of fouling rates were achieved in four of the five groups of experiments. The four groups produced eleven curves of R_f versus time. Eight of these curves displayed effects of tube brushing.

The level of confidence varied among curves depending on velocity changes, the method of measuring velocity and on pump failures. The data to not show differences in fouling rates due to materials or to flow velocities. They do indicate that tubes can be cleaned by an MAN brush, at least during the first eight months of operation. They also indicate that the fouling rate increases after successive brushings.

3.7 References

1. Fetkovich, J.G., et al., "A Novel Method of Measuring Heat Transfer Coefficients with High Precision," in Proceedings of the 12th Southeastern Seminar on Thermal Sciences, June 6-8, 1976, U. of Virginia, Charlottesville.

2. Fetkovich, J.G., et al., "Studies of Biofouling in OTEC Plants," in Proceedings, Second STAR Symposium, San Francisco, May 25-27, 1977, The Society of Naval Architects and Marine Engineers.

3. Fetkovich, J.G., et al., "Degradation of Heat Transfer Rates Due to Biofouling and Corrosion at Keahole Point, Hawaii," in Proceedings of the OTEC Biofouling and Corrosion Symposium, Seattle, October 10-12, 1977, Pacific Northwest Laboratory.

4. Liebert, B.E., et al., "Corrosion Effects in OTEC Heat Exchanger Materials," in Proceedings, 5th International Congress on Marine Corrosion and Fouling, Barcelona, May 19-23, 1980.

4.0 Water Quality

A program for evaluating water quality was initiated in June 1978, during the last few weeks of the Buoy II experiments. A few measurements of water quality were made prior to that time. The following indicators of quality were selected for measurement: pH, salinity, dissolved oxygen, carbonate alkalinity, nitrate and phosphate. The program called for bimonthly sampling and analyses. The primary sampling site was the buoy and the primary results are shown in Ch. 5, Fig. 5.5.

5.0 Biofouling

Biofouling as a factor in the efficiency of heat exchangers was not seriously recognized in the early OTEC engineering. Indeed studies on biofouling were added to the work description after the initial UH contract was written. For this reason the early biofouling work was assigned to a subcontractor.

It was during the early experiments in Hawaii and elsewhere that it became apparent what types of biofouling measurements were required. The results of the first three experiments (Sec. 5.1,5.2,5.3) therefore, should be considered part of the evolution of OTEC biofouling technology. Subsequently a more rigorous program was established leading to more successful experiments. It is the results of the later experiments which should be critically scrutinized.

5.1 Noi'i

5.2 Buoy 1

The Noi'i and Buoy 1 experiments are combined together in this biofouling report because of limited amount of useful data obtained from the standpoint of heat exchanger operation and the unavailability of some reports written for CMU/ Battelle at the time this summary was written. The general approach taken in both experiments was similar. Pipes were examined microscopically and macroscopically after removal from the test system. Microscope slides were inserted in the water in and near the flow and later examined by a variety of methods outlined below. The work was done by subcontract by Pan Pacific Laboratories, Honolulu.

5.2.1 Methods and Materials

Sections of 1-inch aluminum pipe, 33.58 mm O.D. X 26.24 I.D., removed from the flow experiments units at the end of the tests at Keahole Point were sawed into convenient pieces for examination. The interior surfaces were examined without further preparation, after biological staining, after mounting in glycerine jelly, and after removal of surface deposits by film stripping and by scraping. The surface deposits, after removal, were mounted for microscopy on coverglasses.

Sections of the same kind of aluminum pipe, 37 mm long, with the O.D. reduced for clearance, were placed in a PVC 1 1/4-inch pipe which was inserted into the experiment flow system. These sections were removed at different times, and preserved in 2.5% glutaraldehyde-seawater solution except for one that was air-dried immediately upon removal. These were treated and observed in the same way as were the other pipe sections.

A section of titanium pipe, 26.4 mm I.D., 32 mm long, with the O.D. reduced for clearance was inserted in the 1 1/4-inch PVC pipe along with the 37 mm long aluminum pipe sections, at the end of the string, so that it could be left in place until the end of the experiment. This section was preserved in 2.5% glutaraldehyde-seawater solution, and treated in the same way as the aluminum sections except that deposits were not scraped off because there were practically none left after film stripping.

Eight microscope slides, 25 mm X 75 mm X 1 mm (Corning No. 2948), were placed in the flow within a 1 1/4-inch PVC pipe. These were cemented with narrow strips of silicone rubber cement at each end, four slides on either side, to a stainless steel strip running down the center of the PVC pipe. The slides were removed after different lengths of time in the flow, and immediately preserved in 2.5% glutaraldehyde-seawater solution. They were then stained and mounted for microscopy using Corning No. 1 coverglasses.

Paired microscope slides, 25 mm X 75 mm X 1 mm (Corning No. 2948), were placed in Wheaton glass staining trays, which were in turn held in groups in a polymethylmethylmethacrylate frame that was submerged at approximately the depth of the experiment intake. Slides were removed at various times and immediately preserved in 2.5% glutaraldehyde-seawater solution. These were subsequently stained and mounted for microscopy using No. 1 Corning coverglasses.

The pipe inner surfaces, glass slides, membrane filters, preserved seawater samples, and surface deposits on the pipe surfaces were examined microscopically. To simplify enumeration, bacteria with dimensions below 1 micrometer were grouped under "small bacteria"; those above 1 micrometer were classed as "large bacteria". For each visually observed microscopic field, many image planes were utilized so that the smallest bacteria could be detected.

5.2.2 Results

Examination of glass surfaces immersed near experiment intake

The particulate material found on the glass slides with the shortest immersion time (1 day) was composed mostly of small bacteria. There were no large particles, although a very few glass flakes and mineral grains approaching 5 micrometers in size were present. No organisms larger than bacteria were found.

Slides with a 4-day immersion time had increased numbers of small rod bacteria, a few large rod bacteria, fewer inorganic particles than the 1-day slides, and considerable numbers of large diatoms.

Slides with an eight-day immersion time were still more heavily populated by small rod bacteria. The species composition of the diatom population was different from that of the 4-day slides, being made up mostly of Nitzschia, many of which were dividing. Flagellates smaller than 6 or 7 micrometers were also present, but in smaller numbers than the diatoms. Inorganic particles were fewer than on the earlier slides.

Examination of glass surfaces exposed to flow in pipes

Slide exposed to flow for 6 days: there were very few particles or organisms on the slide, but widely scattered groups of bacteria were present. There were also significant numbers of flattened nucleated cells 15 micrometers across. These very thin cells were not encountered on the other slides.

Slides exposed to the flow for 32 days presented a very different appearance from the earlier slides. At low magnifications, the most striking feature was a strongly developed pattern aligned with the pipe axis. This pattern was due to strings of bacteria, various filamentous organisms, and a variety of particulate material that included glass flakes and fibers. Several kinds of diatoms were present.

The surface of the glass was covered, entirely, by a well developed film containing much fine and ultrafine granular material. This film was very dense, and contained various kinds of bacteria including filamentous types.

One of the 32-day slides was extensively covered by a colonial hydrozoan. This colony grew on the surface of the primary fouling film.

Examination of seawater samples

The seawater samples collected near the experiment intake, and at "New Site" and "Buoy Site" after completion of the flow experiment were examined qualitatively. By far the most numerous organisms were bacteria, with small rod and coccus forms predominating. Small diatoms (Nitzschia), small heterotrophic flagellates, and dinoflagellates of several species were common, but all combined made up only 1/100th of the number of total bacteria. In some seawater samples there were relatively large quantities of plant fibers that probably originated in runoff from land, or from sewage.

Numbers of bacteria in many of the samples were on the order of 20,000 per ml of seawater, with small rods making up about 43%, small cocci making up about 39%, and large rods and large cocci contributing equally to the remainder.

Examination of the pipes

Aluminum 6061 T6 pipes were removed at the end of the experiment. One set was immediately air dried, the other was preserved in 2.5% glutaraldehyde-seawater. The inner surface of the dried section was covered with an orange-yellow colored deposit that had a fibrous, ropy appearance under the microscope. The major features of the deposit paralleled the axis of the pipe, but others ran at an angle to the axis. The surface of the fouling layer was very irregular, with many ridges and mounds. The inner surfaces of the preserved portions of the aluminum pipes were very similar in appearance to those of the dried ones, but more detail could be observed. In order to facilitate measurement of deposit thickness and observation of particulate materials within the deposit, the entire deposit was removed by means of collodion films and mounted for observation with high resolution optics. The average height of the deposits, from 10 measurements at random, was 22.9 micrometers. The thickest of these was in a "ridge" area, and measured 34.8 micrometers. There were occasional portions of the deposits that were much thicker--up to 87 micrometers.

Portions of the preserved pipes were washed and dried, and the deposits removed from it by careful scraping. Microscopic examination of this deposit showed the thickness to be from 6.5 micrometers to 24 micrometers within the small area observed. This material contained pennate diatoms, glass fibers, and other filamentous material. A portion of the deposit was orange colored and contained filaments, but individual bacteria could not be resolved because of the density of the material. A colorless portion appeared to be full of bacteria, but many of these particles could be other than bacteria since they were not tested by characteristic staining properties.

5.3 Buoy 2

This section is also part of the "old biology" program.

5.3.1 Materials and Methods

Cleaning of Pipes and Coupons

The following acid/base treatment was used to prepare the pipes for the various experiments in 1977:

1. Aluminum pipes were immersed in 10% NaOH for 5 minutes. The specimens were then rinsed and allowed to dry to observe degree of cleaning.

2. The caustic treatment was repeated for 3 to 5 minutes, and the tubes rerinsed. Before drying, the inside of the pipes were scrubbed using a ramrod and cloth. The pipes were then rerinsed with water.
3. Tubes were immersed in 10% nitric acid for 2 or 3 minutes. The tubes were then rinsed with water and scrubbed with cloth as above.
4. After final rinsing, the pipes were allowed to air dry.

Titanium pipes were cleaned as follows:

1. A mixture of 5% nitric and 1% hydrofluoric acids was used to preclean the pipes. The reagent was made up by diluting a 20% nitric acid solution + 4% HF solution to volume with deionized water.
2. After rinsing with water the pipes were dried as above.

All pipes were checked for cleanliness and all superficial inhomogeneities were recorded. The corrosive cleaning agents had an adverse effect on the aluminum surface which became evident in some of the scanning-electron micrographs. Cracks or fissures developed across the surfaces when they were exposed to seawater. These cracks were initially interpreted to have resulted solely from the shrinking of layers of aluminum hydroxide on desiccation during their preparation for SEM examination. In subsequent deployments coupons were degreased with a commercial detergent and rinsed in water. There was no acid or alkali pretreatment.

Biofouling

Biofouling was studied both inside and outside the flow system. In early experiments both aluminum and titanium pipe sections were cut from the apparatus, filled with 2.5% glutaraldehyde-seawater solution, plugged, and transported for laboratory study. In late 1977, tube samples were standardized. Sections of aluminum, titanium, and glass approximately 26 mm I.D. were cut into 25.4 mm lengths, split axially, and held together with black plastic shrink tubing which incidentally also served as an insulator. Immediately upon removal from the test assembly these samples, designated "coupons", were placed in short sealed plastic tubes containing 2.5% glutaraldehyde in seawater. Aluminum and titanium pipe samples that were not precut as above were sawed into pieces 20mm x 20 mm or larger. Most samples were transferred from the glutaraldehyde solution to fresh water and photographed immersed.

Portions of some deposits were removed by casting a collodion film on the surface and then removing the whole film. In the case of aluminum, it was noticed

that an inorganic layer about 10 micrometers thick was removed along with the biofouling material so that both layers could be measured. This material was observed by bright field microscopy before and after staining with Azure B or acridine orange. Other portions of pipe still in the original fixative solution were prepared for SEM by gentle washing with three changes of distilled water to dissolve salts which otherwise would crystallize on the specimens. Samples were then dried at 25°C to between 85 and 65% relative humidity after which they were transferred to a desiccator and further dried over silica gel.

Glass microscope slides (detergent-cleaned and rinsed in membrane-filtered (0.2 um) deionized water were placed in Wheaton slide staining racks (as used by Corpe [1], and supported near the intake area of the flow experiments. After various exposure times ranging from 2 hours to 90 days groups of 5 slides were removed from the rack and placed in Coplin jars containing glutaraldehyde fixative. The schedule of sample removal corresponded to that for the collection of coupons. After fixation for 24 to 72 hours these slides and fixed coupons were examined by optical microscopy. Slides were stained with Azure B (1:10,000, pH4.1) for 30 minutes or in acridine orange (1:10,000, pH6.7) for 3 minutes. They were then mounted in semi-solid fluids with refractive index equal to that of seawater.

Fouling layer thicknesses were measure on both water-immersed and dried samples. In some samples, small cuts were made at 45° angles to the surface, through the biological and inorganic layer exposing metal so that the total thickness could be measured both by optical microscopy and SEM. Weights of fouling layers were measured by first weighing an intact portion of a coupon after careful washing 4 times with filtered deionized water and drying for 12 hours at 70°. The deposits were then carefully removed from a measured area using degreased razor blades or a finely honed triangular blade. Both substrate and fouling layers were weighed separately.

5.3.2 Results

Film thickness measurements

On Buoy 2, two series of measurements of film thickness were done: (1) on samples retrieved from the experimental run begun in December 1977 and (2) on samples taken from earlier runs.

Some of the data are summarized in Table 5.1. Two sets of data are reported. One shows the increase in biofouling, measured wet by optical microscopy of glass slides outside the flow of water but near the experimental water inlet. The other set is taken from metal coupons removed from the flow. Each value is an

TABLE 5.1

Thickness of biofouling layers on glass slides outside of flow system and on aluminum, titanium, and glass coupons in the flow of the experimental heat exchanger in the underwater buoy at Keahole Point, Hawaii. Exposures during period Dec. 21, 1977 to Jan. 18, 1978. Biofouling layers on the slides were undried; those on the coupons dried after washing with distilled water. Temperature of water ranged from 26.2° to 24.8°. Each value, average of 30 measurements

Exposure Time	Wet Glass Slides	Thickness (μm) Dried Coupons Aluminum	Titanium	Glass
48 hours	25	15	---	---
72 hours	115	27	---	---
1 week	277	43	20	22
2 weeks	416	59	49	29
3 weeks	422	---	---	31
4 weeks	646*	47	41	43

* when dried this sample had a measured thickness of 96 μm.

average of 30 measurements. The experiment began on December 21, 1977 when the water temperature was 26.2°. The lowest water temperature during the course of experiment was 24.8°. Water was pumped through the system at 2.1 m sec.

Except for the glass slides, thickness measurements were made on dried films. The method of measuring wet thickness is described in the section above. Coupons exposed for 0, 3, 6, 12, and 24 hours have not been examined by these methods. Film thicknesses were measured by SEM and optical microscopy.

On one occasion, the glutaraldehyde-fixed fouling layer detached from its support, in its apparent entirety, leaving the aluminum base free. The sample had accumulated over 3 weeks in a pipe through which water flowed at 2.1 m sec^{-1}. The film's wet thickness was 230 μm.

The samples with the longest biofouling development in flowing water were aluminum and titanium tubes exposed as long as 154 days to 0.9 and 2.1 m sec^{-1} flow. These samples were obtained in mid-1977. In the experiments, however, some of the pumps failed on one or more occasions with down times from a few hours to as much as 5 days. Careful measurements of film thickness were done, nevertheless, recognizing that the resulting data cannot be strictly attributed to fouling under continuous flow conditions.

Figures 5.1 through 5.4 summarize the thickness measurements which are presented without additional discussion

5.4 Buoy 3

The immediate goal of the third deployment of the buoy was to find ways to quantitatively measure the nature and amount of early biofouling under the simulated OTEC conditions operative on the buoy.

5.4.1 Experimental Methods

Four alloys were used; 5052 aluminum (Al), grade 2 titanium (Ti), AL-6X stainless steel (SS), and CA706 copper-nickel (Cu-Ni).

Details of some of the methods employed in this work were discussed at the January 1979 OTEC Workshop on Biofouling and Corrosion and are summarized in Sec 5.4.3.

Sample coupons were placed downstream of the CMU heat transfer instrument but upstream of the pump. The coupons were cleaned at the same time, and in the same manner, as the heat transfer section using a M.A.N. brush modified to spin while being lowered into the tubing sections. This modification reduced the number of cleaning passes required to achieve an acceptable reduction in R_f from

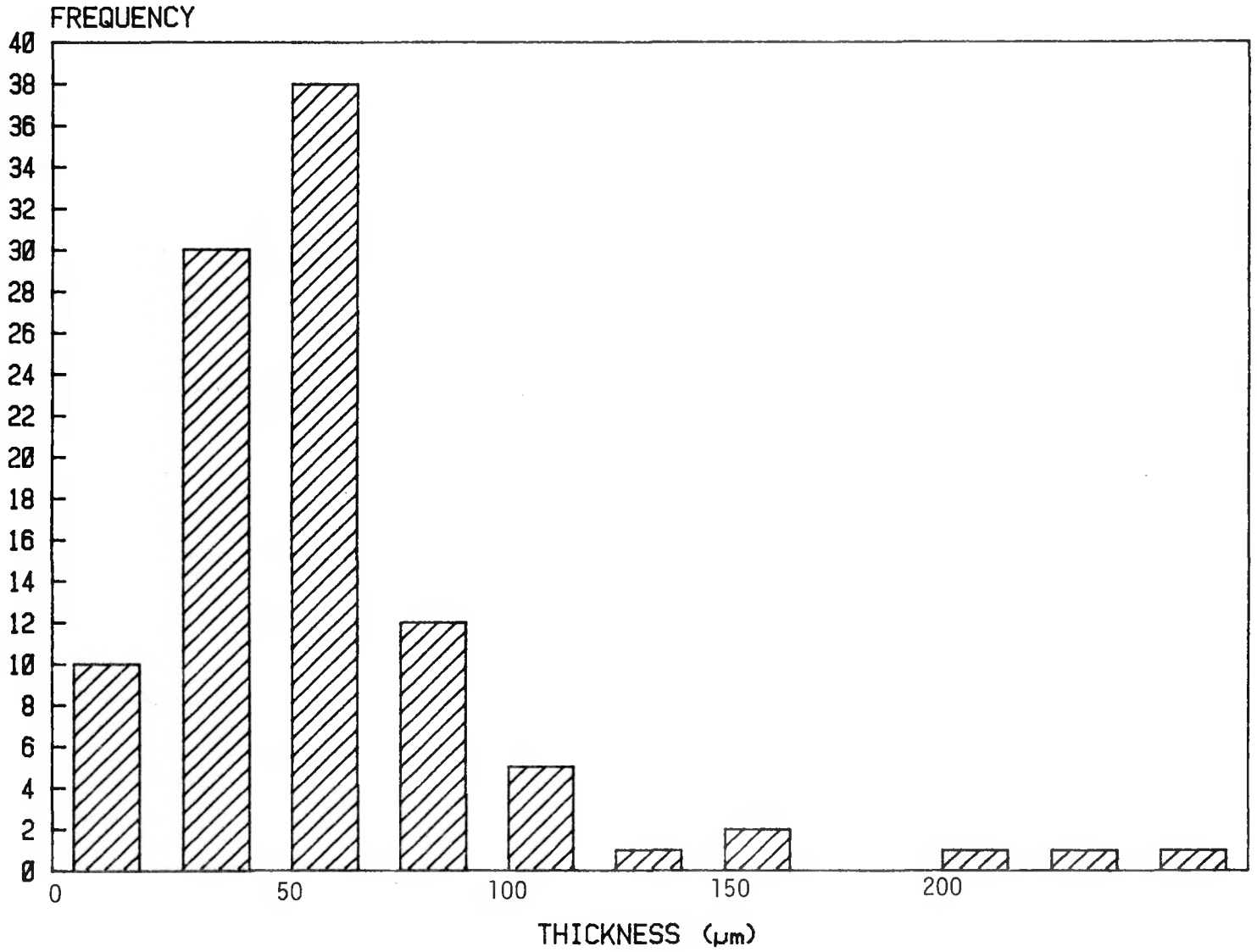

Fig. 5.1 Distribution of biofouling thickness on aluminum pipe (No. 98-3) after 154 days in flow at 2.1 m/sec. Sample was washed in distilled water and air dried.

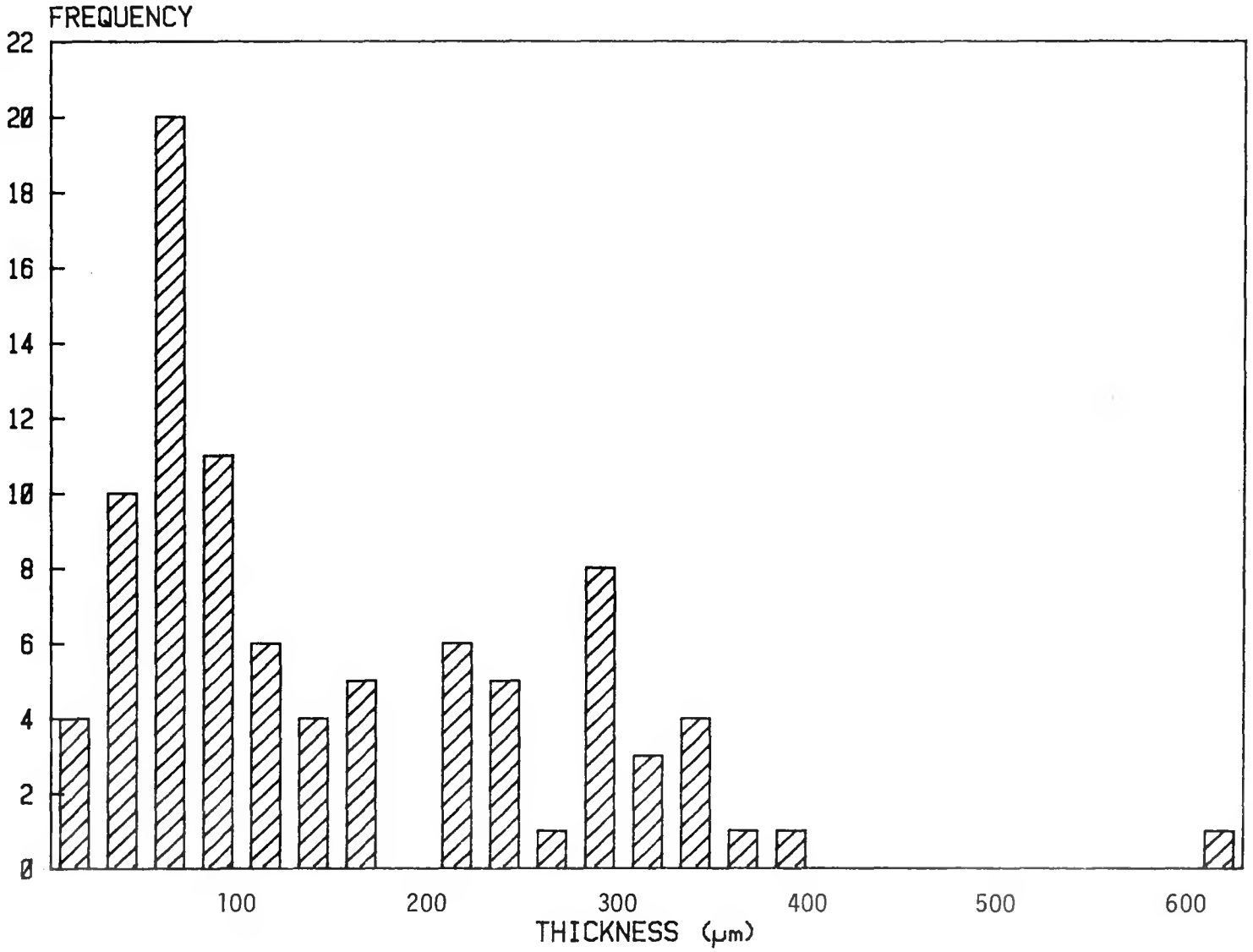

Fig. 5.2 Distribution of biofouling thicknesses on aluminum pipe (No. 98-2) after 154 days' in flow at 0.9 m/sec. The sample was washed in distilled water and air dried.

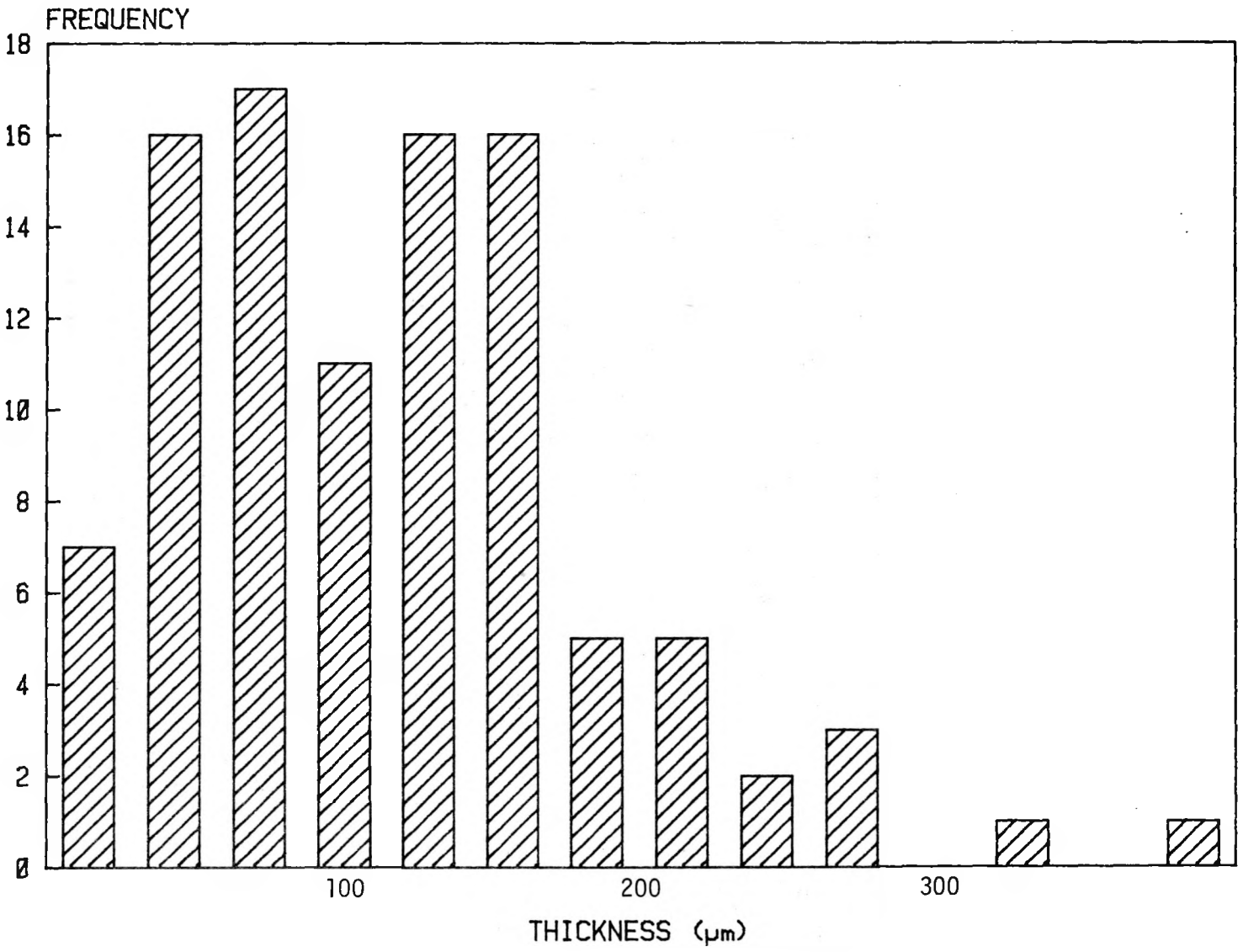

Fig. 5.3 Distribution of biofouling thicknesses on titanium pipe (No. 98-1) after 115 days' in flow at 2.1 m/sec. The sample was washed in distilled water and air dried.

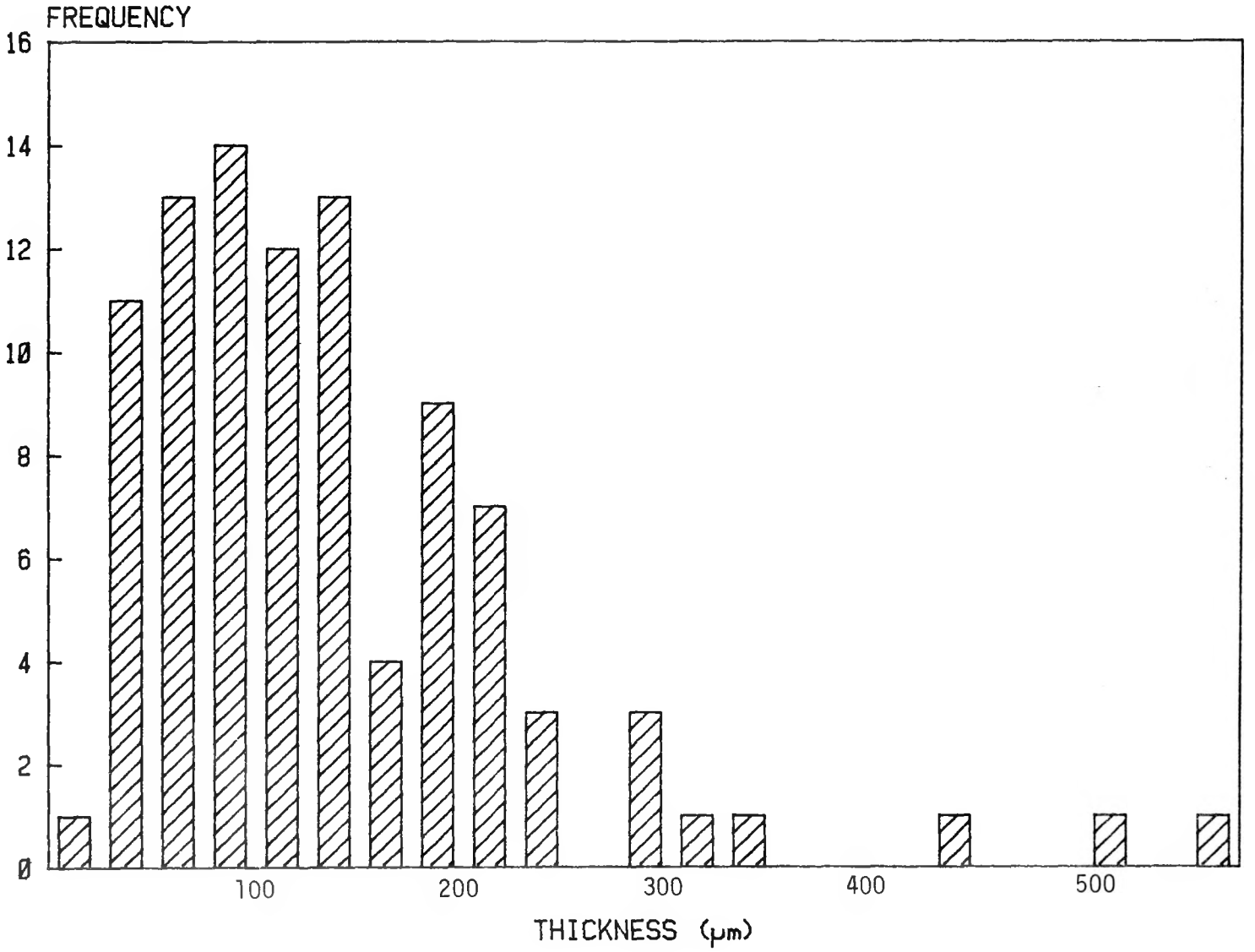

Fig. 5.4 Distribution of biofouling thicknesses on glass slide surface submerged near experimental water intake after 33 days' exposure. The slide was washed in distilled water and air dried.

twenty to two. After removal for biological and corrosion analyses, the coupons were either drained and frozen or filled with a 2.5% glutaraldehyde-seawater mixture, depending on the type of analysis desired.

Except for SEM and x-ray fluorescence studies, the fouling film was removed from the tubing as follows. One-inch sections of tubing were sealed with silicone rubber caps after the addition of 0.5 ml ballitini-type micro-glass beads (Scotch-Lite, MMM Co.) and 3 ml filtered double distilled water. The sample was then placed in a type Vi2 vibrating ballistic disintegrator (RHO Scientific Co., Commack, NY) and processed at approximately 100 Hz for 5 minutes. After allowing the glass beads to settle, 2.5 ml of the turbid liquid was removed from the sample. Two ml filtered dH_2O was then added to the sample and the film removal procedure was repeated. The sequence was repeated a third time and the aqueous suspensions were pooled.

One ml aliquots of the film extract were hydrolyzed in 4N HCl at 121°C for 1 hour. The hydrolysate was then dried over P_2O_5 and NaOH in vacuo, then taken up in 0.15 ml water. The dry weight of the film (less carbonates) was computed from a portion of the hydrolysate and is reported in mg/cm^2 of inner surface of the tube.

Organic carbon and total nigrogen assays were done on aliquots of the same hydrolysate in an automatic carbon-nitrogen-hydrogen analyzer (Hewlett-Packard Co.). Values obtained were converted to $\mu g/cm^2$ of inner surface of the tubes.

Aliquots of the film extract were analyzed fluorometrically for protein by the method of Robrish, et al. [2].

Coupons from sections of tubes were coated with carbon for EDAX analysis. Background and overlapping non-K_a-band quanta were subtracted by computer.

A portion of the loose corrosion film on the Cu-Ni coupons was lifted off the interior surface, mounted perpendicular to the SEM holder, and coated with carbon for film thickness measurements.

5.4.2 Experimental Results

The water temperature at the buoy varied between 23 and 28°C during this portion of the deployment. This is shown in Fig. 5.5 along with the salinity, pH, alkalinity, dissolved oxygen, nitrate, and phosphate levels over the same time period.

Flow velocity measurements are given in Table 5.2 for the four different instruments. The jump in velocity for the Cu-Ni and SS instruments was due to a change in a flow restrictor valve on the pump.

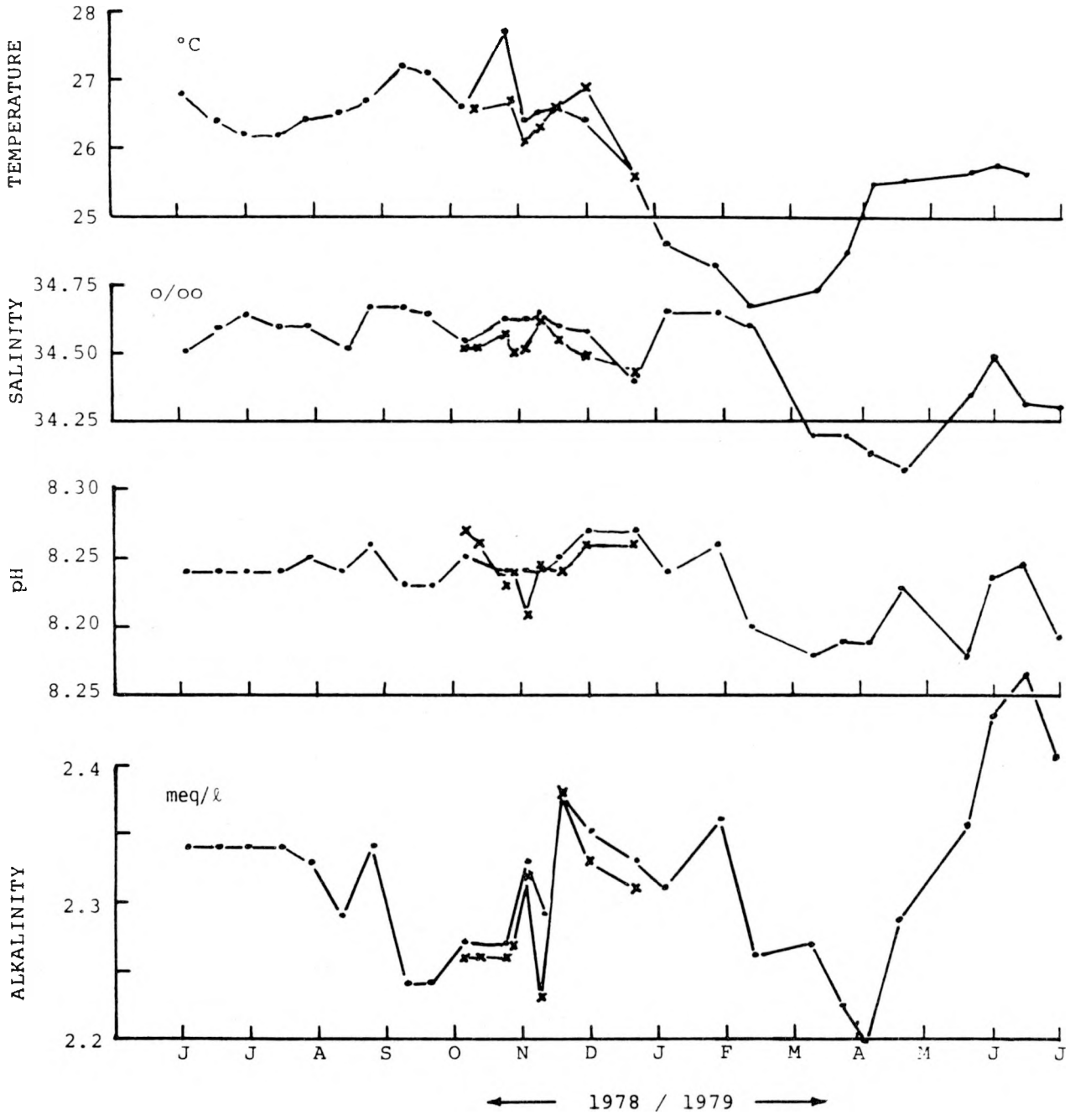

Fig. 5.5a Variation of the temperature, salinity, pH, and alkalinity levels at Keahole Point, Hawaii. x = measurement taken at the underwater buoy and • = measurement taken at a site near shore

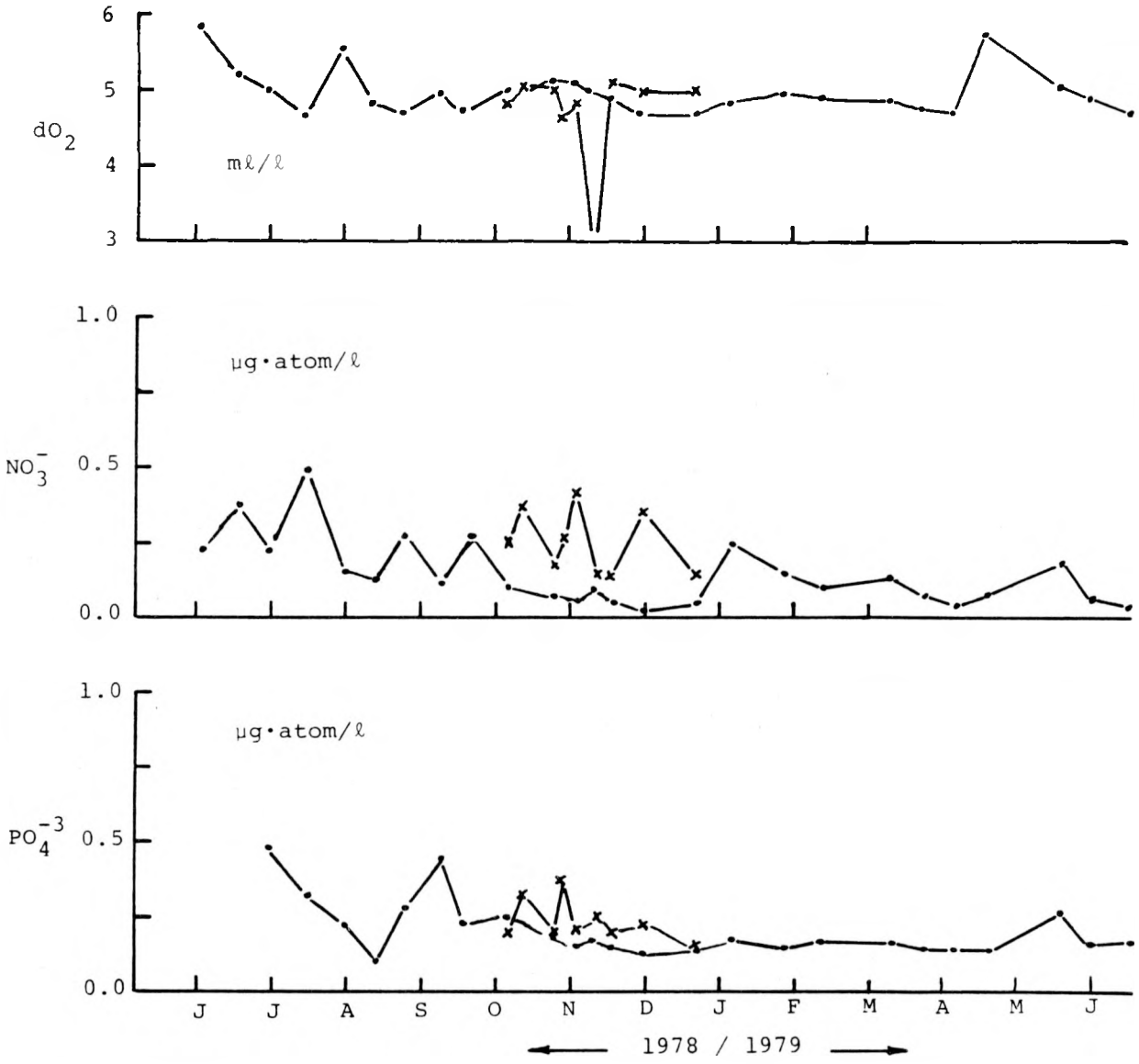

Fig. 5.5b Variation of the dissolved oxygen, nitrate, and phosphate levels at Keahole Point, Hawaii. x = measurement taken at the underwater buoy and • = measurement taken at a site near shore

TABLE 5.2

Velocity Measurements, ft./sec.

Days in Flow	Al	Ti	CuNi	SS
2	5.89	--	--	--
3	R.P.*	7.58	7.15	--
7	--	--	--	7.25
8	5.65	--	--	--
9	--	7.64	--	--
93	--	--	R.P.	--
95	5.97	6.86	7.59	7.03
100	--	--	R.P.	R.P.
102	6.34	6.75	7.04	7.04
102	--	--	R.P.	R.P.
102	6.24	6.82	7.49	7.08
106	--	--	R.V.**	--
107	--	--	--	R.V.
109	6.15	6.98	8.97	8.97
115	R.P.	--	--	--
119	--	--	R.P.	R.P.
124	5.73	6.91	9.01	9.01

* indicates replacement of the pump
**indicates replacement of the pump and flow restrictor valve

The change in thermal resistance from its initial deployment value, the fouling factor R_f, is shown in Fig. 5.6 for the four metals studied, along with the total film weight. The R_f data have been normalized to 21°C and 6 ft/sec[9].

As shown in Fig. 5.6, except for Al, the changes in the total mass of the film closely follow those in R_f. In the case of Al most of the hydrated aluminum oxide layer is probably not removed by the brushing procedure in the field. Therefore this layer does not contribute significantly to the changes in R_f.

The increase with time in the amount of protein correlates with R_f for all metals except Cu-Ni, as shown in Fig. 5.7. However, the amounts of protein detected in the Cu-Ni tubes are at the lower limits detectable by the analytical

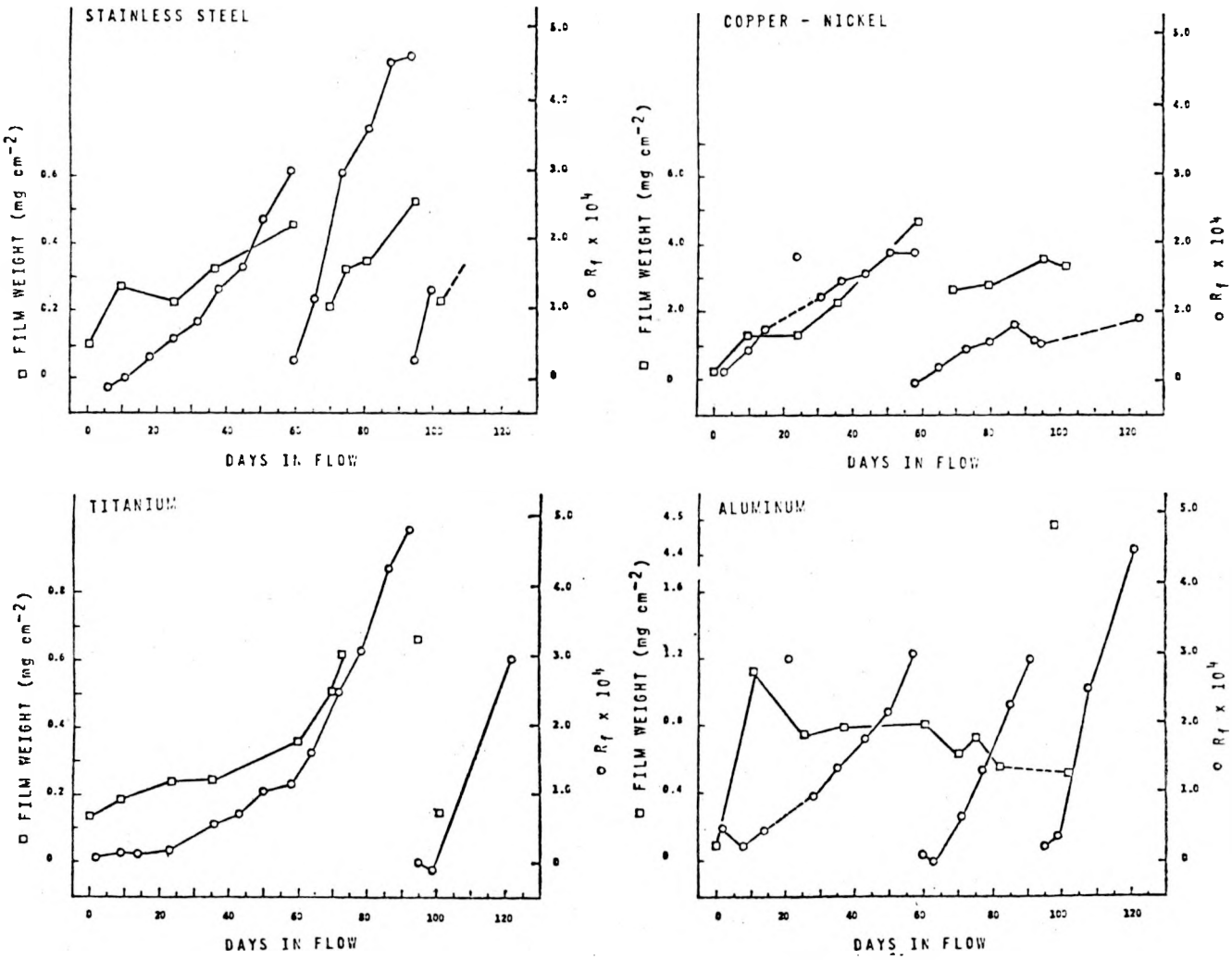

Fig. 5.6 Film weight and resistance to heat flow (R_f) vs time of immersion in flowing seawater.

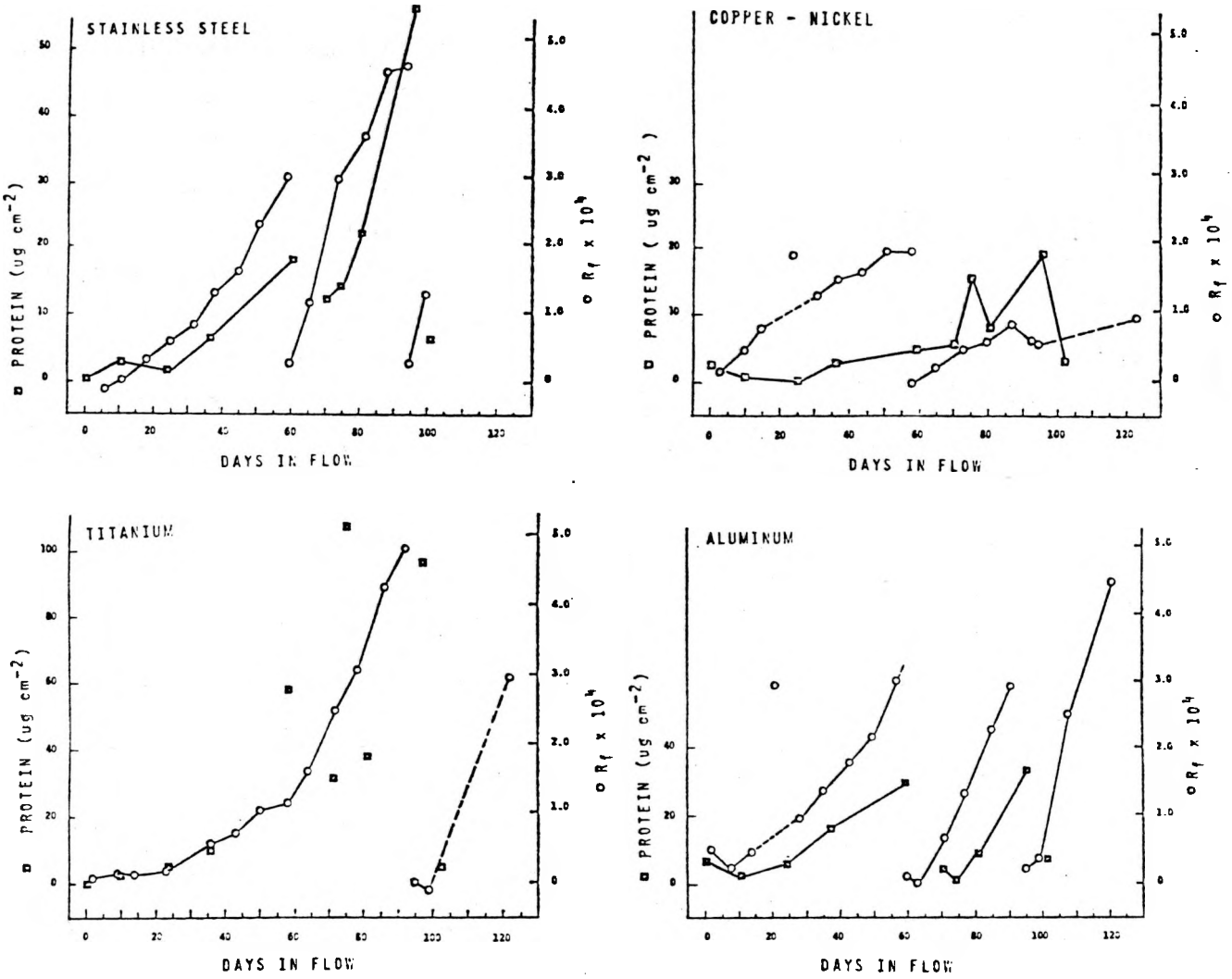

Fig. 5.7 Film protein and resistance to heat flow (R_f) vs time in flowing seawater.

procedure. Nevertheless, SEM micrographs clearly show the presence of biological fouling on the Cu-Ni tubes after 94 days' immersion.

The change in the thickness of the Cu-Ni corrosion product with time in flow is shown in Fig. 5.8. The linear increase in thickness parallels the linear increase in R_f for time earlier than the first cleaning. After brushing, which restored R_f to its original value, the measured film thickness did not decrease back to its original value; rather, it decreased only slightly.

It is possible that the cleaning of the heat transfer instrument resulted in a more complete removal of the film compared to the sample coupon test section and that the film which was removed for thickness measurements was not representative of the entire inside surface. These results are in general agreement with the dry film weight measurements of Cu-Ni shown in Fig. 5.6. Some of the data is compared to that obtained in analogous experiments in the Gulf of Mexico, in Table 5.3.

TABLE 5.3

Ratios of Total Organic Carbon to R_f and Dry Film Weight
from Stainless Steel and Titanium Tubes
From: (Berger & Little, 1980) [2B]

	Hawaii		Gulf of Mexico	
Site	Ti	SS	Ti	SS
Organic C ($\mu g\ cm^{-2}$)	25.2	13.1	4.6	4.7
Film Dry Weight ($mg\ cm^{-2}$)	3.1	1.8	--	--
$R_f \times 10^4$ ($°F\ ft^2\ min\ BTU^{-1}$)	1.6	2.3	0.5	0.93
Ratio (C/R_f)	15.8	5.7	9.2	5.1
Ratio (C/Dry Weight	8.1	7.3	--	--

Data for Gulf of Mexico are taken at 48 days; those for Hawaii are the arithmetic mean taken before the first cleaning.

Microorganisms do chelate substantial amounts of inorganic salts in seawater [3]. Thus, the formation of a significant fraction of the inorganic layer could depend upon the biofilm itself.

One explanation for the differing heat transfer responses observed for the two metals is related to the surface roughness of the stainless steel. Water may become entrapped in the grooves of the SS surface as the overlying biofilm

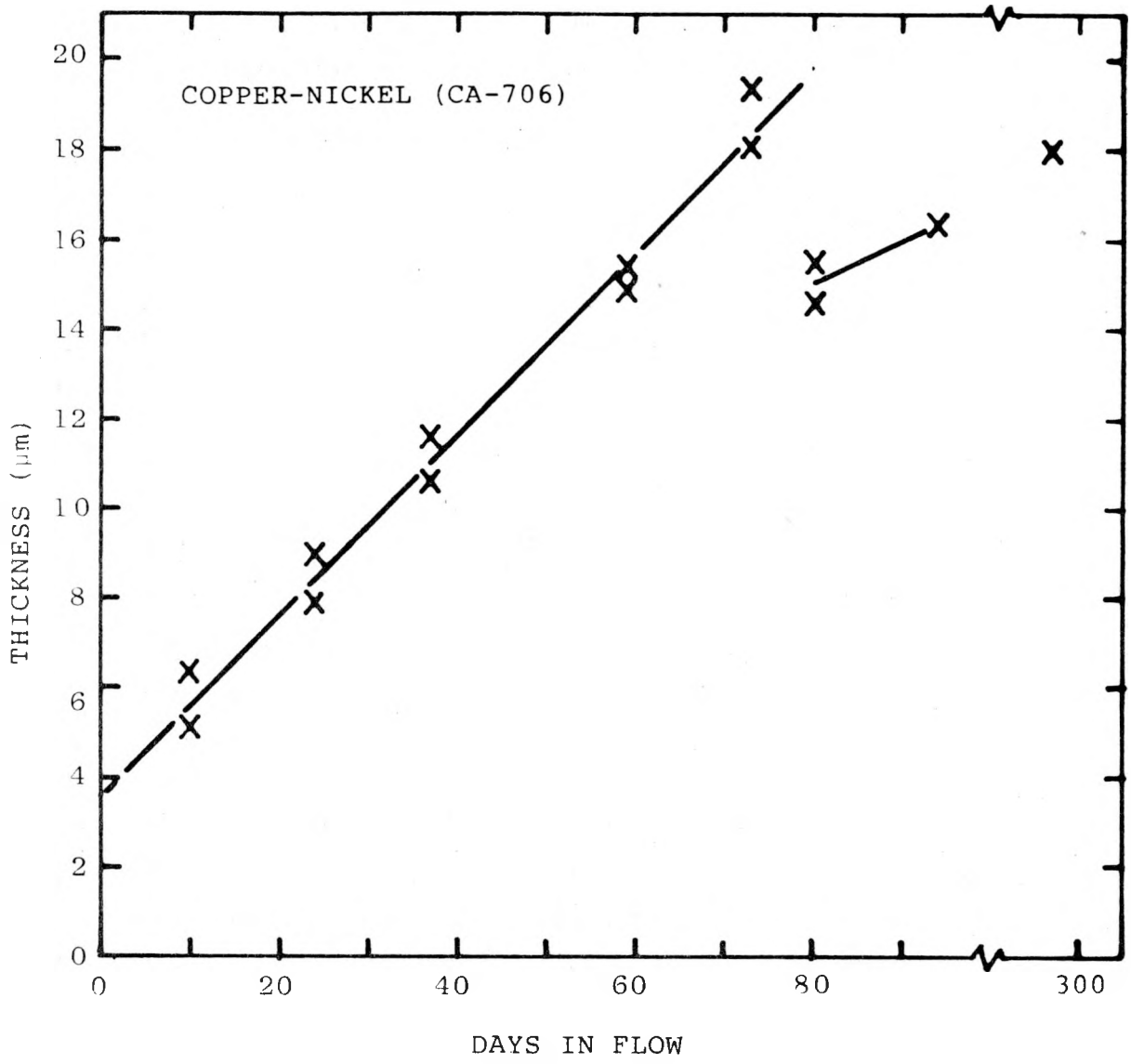

Fig. 5.8 Thickness of Cu-Ni corrosion film thickness measured in the SEM vs time in flowing seawater.

develops, providing greater insulating effects. Such films with identical TOC and TN content and wet film thickness as found on a smooth metal surface would exhibit different heat transfer responses.

Heat transfer resistance, total organic carbon (TOC) and total nitrogen (TN) are plotted against exposure time for all alloys in Fig. 5.9 (a-d). The scales of the ordinate were chosen such that the TOC and TN data for the titanium tube would superimpose on that of R_f. Ti and SS have similar chemical properties; neither corrodes vigorously in seawater (Laque, 1979), [3B] nor is either toxic to microorganisms [4]. One would therefore expect the two materials to exhibit nearly identical fouling and loss of heat transfer efficiency. The results shown in Fig. 5.9 indicate that differences did exist.

One macroscopic difference was the topography of the two surfaces as received from the manufacturer. The inner surface of the SS tubes was marked with deep extrusion lines; these were absent in the titanium tubes. It is unlikely that the nature of the microflora on the two metal surfaces is responsible for the differences observed in the R_f data. Differences were not detected in SEM micrographs of the two fouled surfaces. The biofilm on the stainless steel surface did obscure the surface roughness after 78 days.

Wet film thickness measurements were comparable for the period of investigation [5]. TN:TOC ratios (Fig. 5.10) and dry film weight:TOC ratios (Fig. 5.11) in the fouling layers from the Ti and SS surfaces are very similar. The ratio of TOC to dry film weight was approximately 1:8 for both Ti and SS (Table 5.4) indicating that substantial amounts of inorganic materials are present in the fouling films. As stated previously, neither of those materials corrodes appreciably in seawater.

No correlations can be made between R_f and TOC or TN (Fig. 5.9). The TOC:TN ratio for the Cu-Ni is substantially greater than that for the other materials (Table 5.4). This is consistent with the hypothesis that microorganisms colonizing copper and other toxic metals secrete polymeric materials which chelate metal salts [4]. Compounds, such as polyuronic acid found in such secretions in the primary layer, will raise the TOC:TN ratio for the entire film.

5.4.3 Comparison of Buoy 3 experiment with that done in the Gulf of Mexico

Total film weight was largest in the Cu-Ni and Al tubes and was composed of both biological and corrosion products. After cleaning by brushing, most of the biological material was removed from the aluminum tube but not from the Cu-Ni tube. The corrosion layer in the Al tube was relatively undisturbed by cleaning

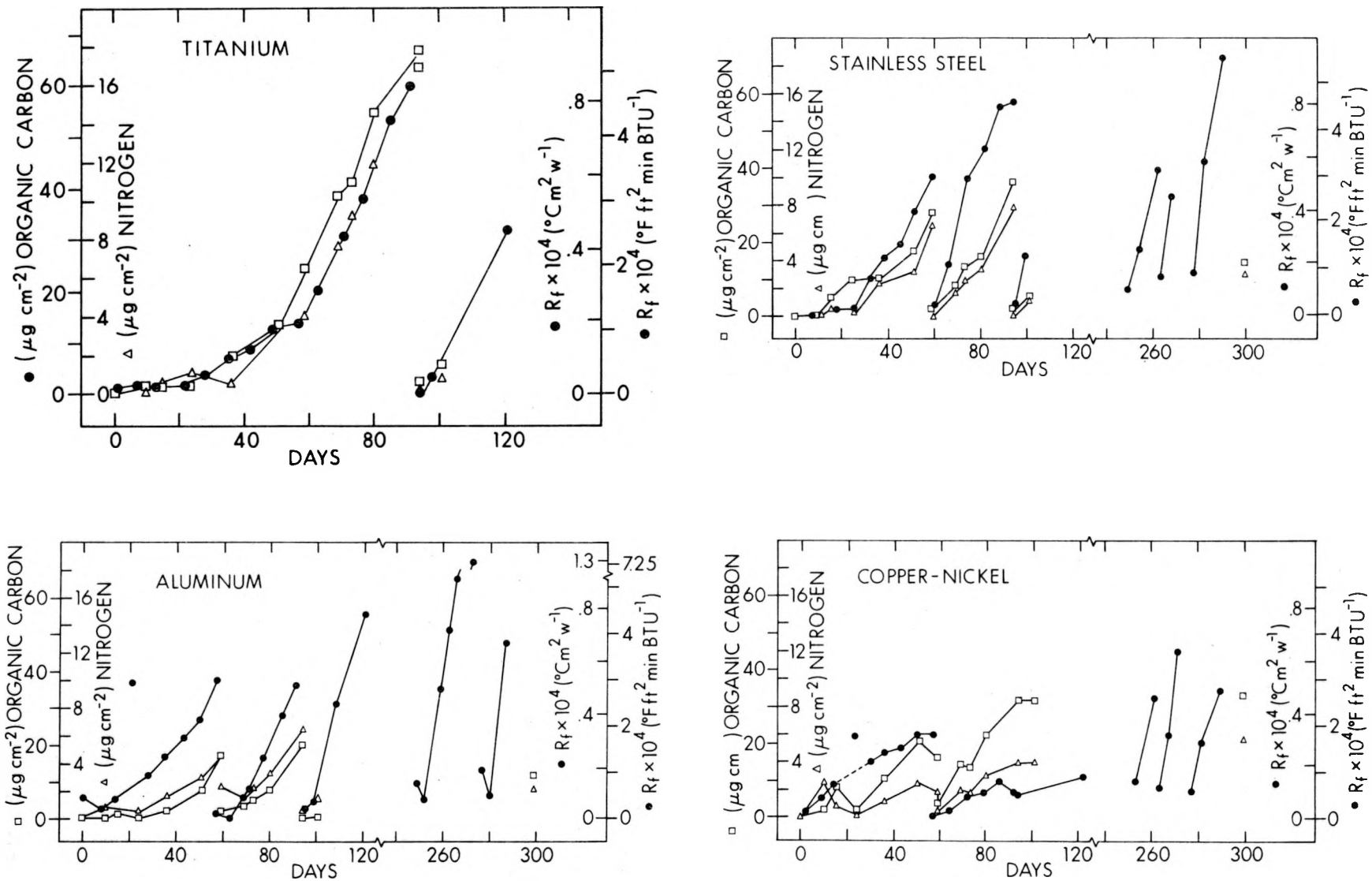

Fig. 5.9 Total organic carbon, total nitrogen, and R_f vs time

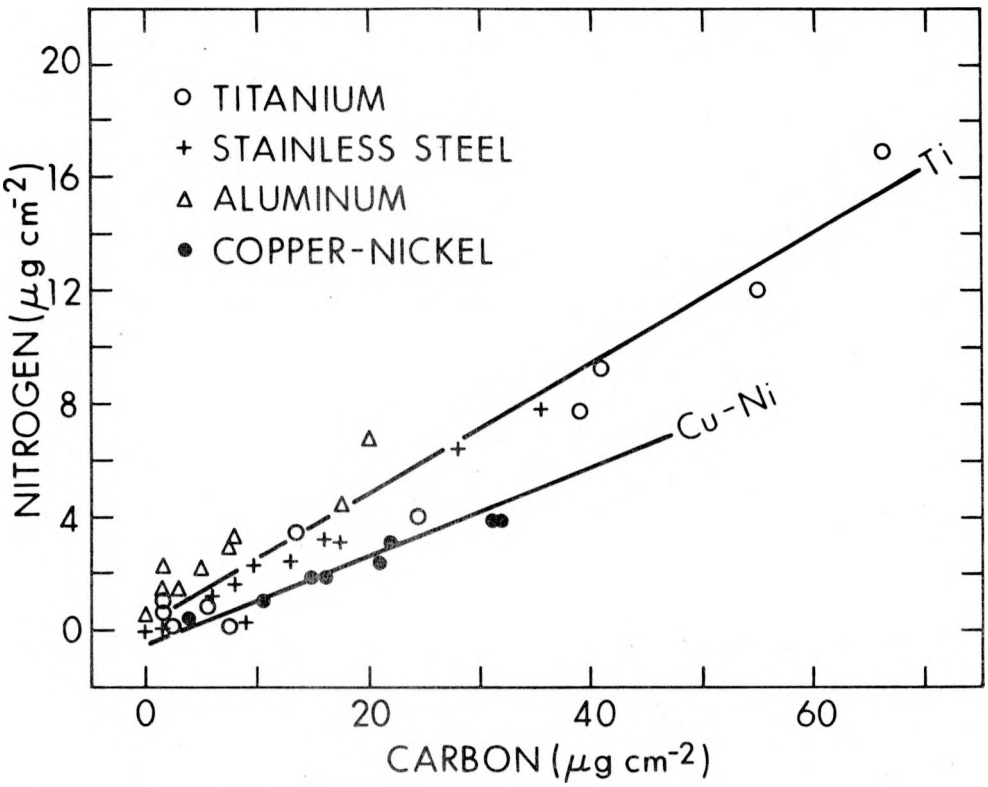

Fig. 5.10 Total nitrogen vs total organic carbon in the fouling films.

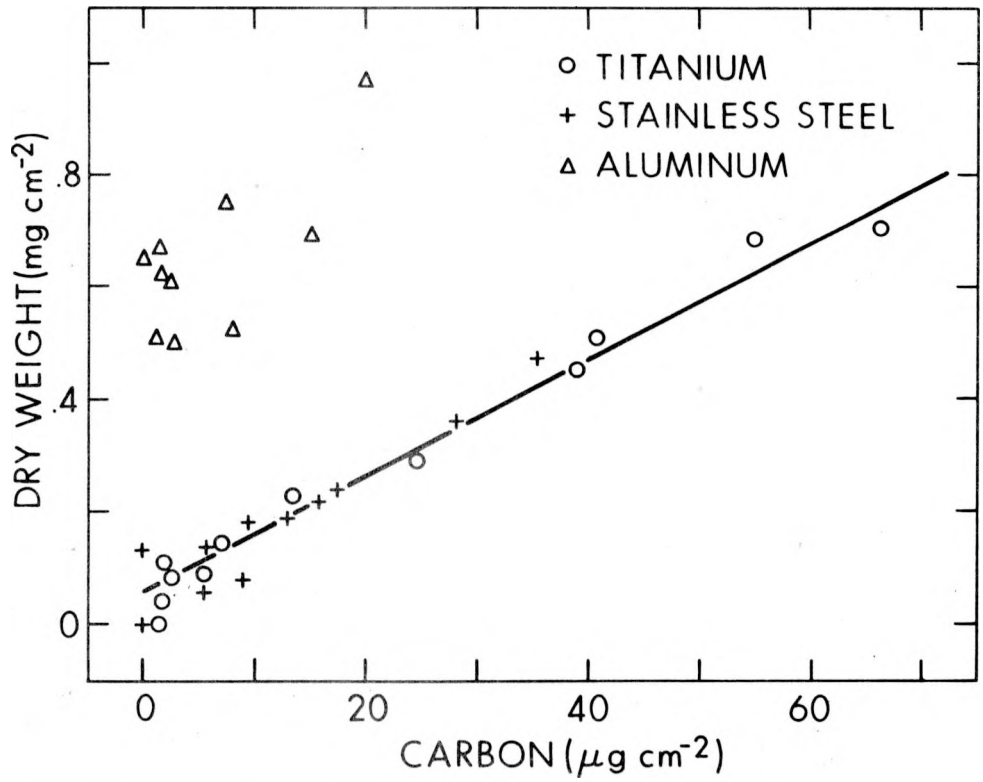

Fig. 5.11 Dry film weight vs total organic carbon in the fouling films

TABLE 5.4

Total Organic Carbon to Total Nitrogen Ratios
in Films on Various Tube Types

(HI Data)

Tube Type	TOC/TN Ratio*	
Ti	4.2	0.9
SS	4.8	0.7
Al	4.0	0.8
Cu-Ni	7.9	0.8

*
1. Zero-values subtracted for all but Al.
2. Average of 2 values for most times.
3. Values taken 1 day after cleaning or removal.
4. Wildly aberrant values deleted.
5. Each ratio based on 12 or more values.

in the Al tube; a significant fraction was removed from the Cu-Ni. The degradation of heat transfer efficiency across the tubes of SS and Ti was directly proportional to the mass (dry wt.) of the film. For these materials the proportion of C and N to total film mass remained nearly constant. The C:N ratios on the fouling films for Ti, Al, and SS were between 3:1 and approximately 5:1 but in excess of 8:1 in Cu-Ni tubes. X-ray fluorescence analyses of fouled tubes indicate that little inorganic material accretes onto the bare Ti and SS surfaces; large amounts of S, Fe, Ca were found on fouled Cu-Ni and Al tubes. From a limited number of measurements it appears that the thickness of the film on Cu-Ni tubing parallels directly the loss in heat flow. Scanning electron microscopy showed that all types of surfaces were colonized by microorganisms in the period reported although the rate of microbial colonization is initially retarded on Cu-Ni surfaces. Except for a slower initial rate of fouling observed in the Gulf of Mexico experiments, the results at the two sites are comparable (Fig. 5.12).

5.5 3-Inch Pipeline

5.5.1 Experiment

The three-inch pipeline experiment was designed to compare the effect of a long intake line on microfouling of heat-exchanger tubes with that of the buoy in which water passed directly from the environment in the fouling test sections.

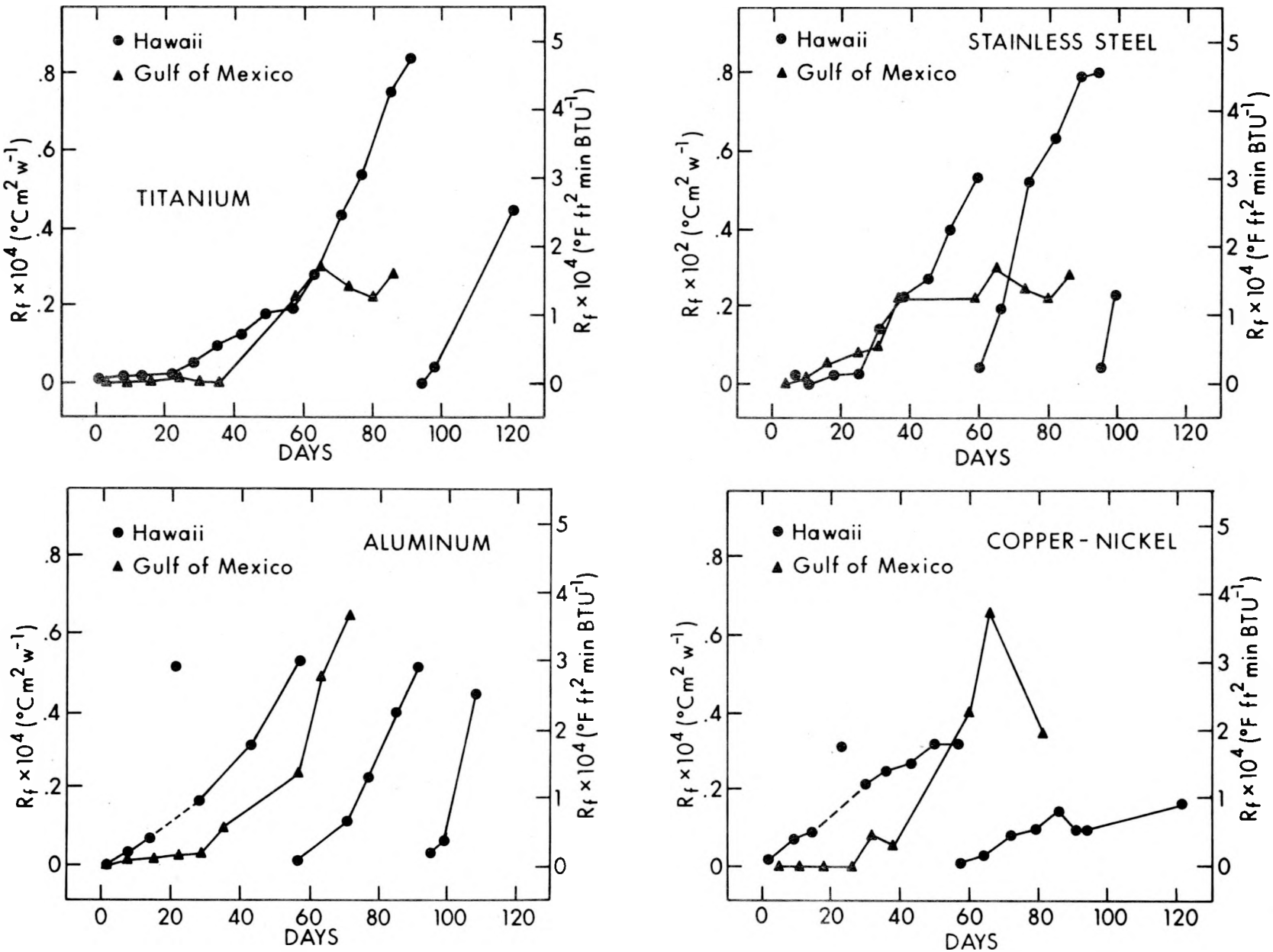

Fig. 5.12 R_f vs time for data from Hawaii and Gulf of Mexico.

The intakes to both systems were located on the submerged buoy. The details of the construction of the 3-inch pipeline experiment are given in Sec. 2. Two HTMs X, and Y, were used throughout the experiment. Initially, biofouling coupons were only mounted in unit X. After 110 days, unit X was cleaned by brushing in the usual manner. Unit Y was dismantled and cleaned by brushing and with nitric acid. After rinsing, the system was reassembled with a series of biofouling test tubing. The purpose of these operations was to test the effect of a fouled, long intake line on "new" HTM and test coupons and to compare the rate of fouling with the fouling rate at the start of the 3-inch pipeline experiment when the long intake line was also "new" and unfouled. The experimental system in the Buoy was never deployed largely because of a ten-year storm which destroyed the submarine control cable and OSHA safety restrictions which prevented its reinstallation within the contract period and budget.

5.5.2 Results

Results are summarized in Figs. 5.13 through 5.18. The results are also tabulated in Sec. 5.9. The various parameters are scaled in the figures such that they approximately superimpose over the R_f data in the X-unit before the dismantling of the apparatus at 111 days for cleaning. It is evident that even after cleaning R_f increase is proportional to the various biofouling parameters. Not so for unit Y. It took less carbon, nitrogen, protein, and film weight to bring about the observed changes in R_f than in unit X. These differences are readily explained. The fouling layer which forms initially on a new surface is looser than that which results following a primary fouling which is brushed off and then permitted to reform. The primary fouling layer probably contains more water and thus increases the effective thickness of the static layer.

Figure 5.19 shows plots of organic carbon vs R_f for the Buoy 3 experiment and these from the 3-inch pipeline experiment. The data suggest that the films contained more carbon per unit of R_f in the buoy experiment before cleaning than in the pipeline experiment. This probably reflects the additional nutrients in the water which reaches the experimental surfaces; in the 3-inch pipeline the 1400 feet of tubing exposes the water to additional surface on which organisms can utilize some of these nutrients. The result may be a more dilute nutrient source for the organisms growing on the test surfaces. Figure 5.20 shows the loss of heat transfer in both buoy and 3-inch pipeline experiments.

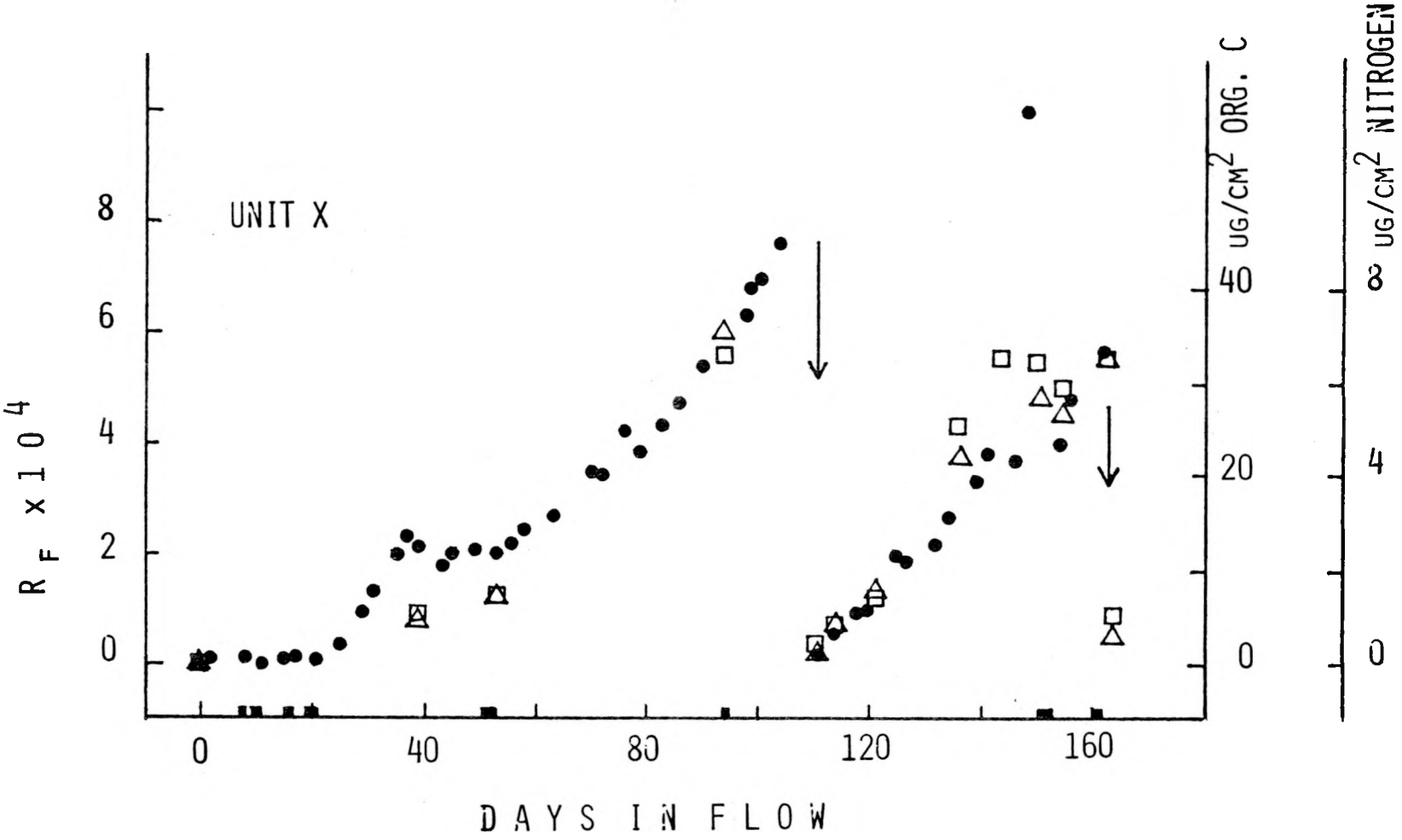

Fig. 5.13 Three-inch pipeline experiment. Plot of R_f, organic carbon, and total nitrogen vs days in flow. Unit X.

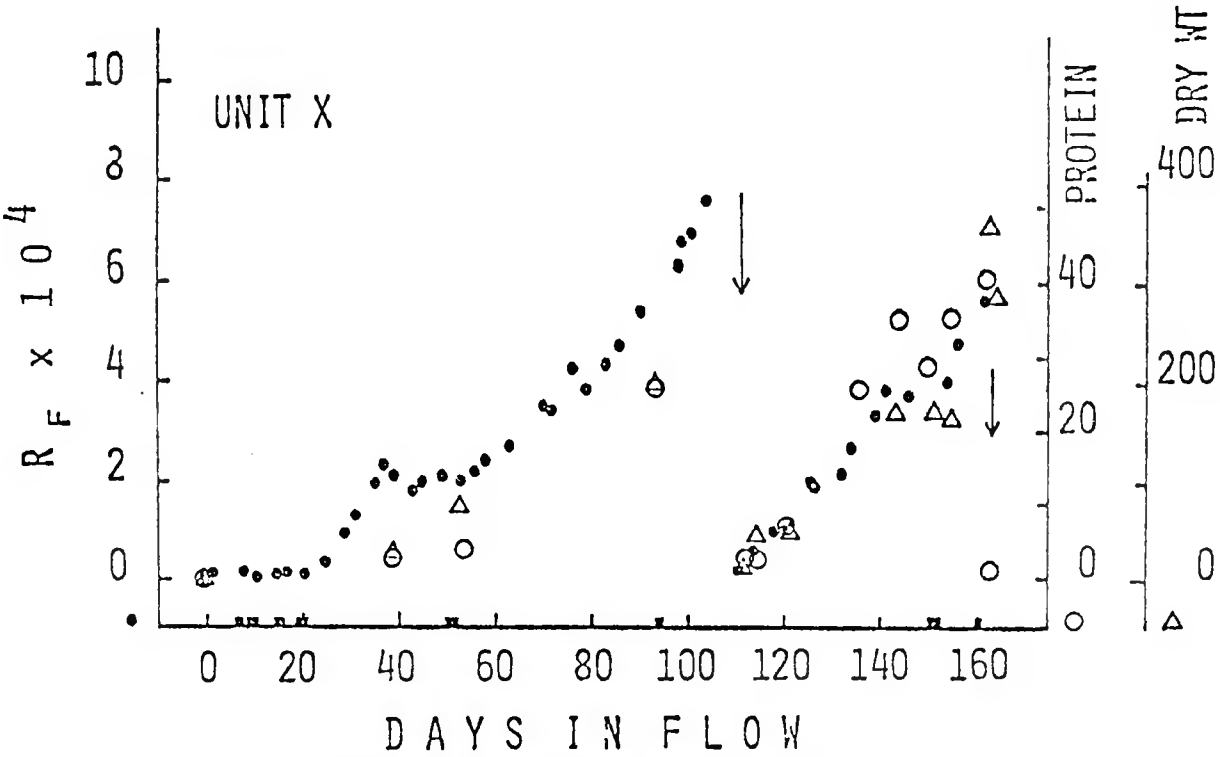

Fig. 5.14 Three-inch pipeline experiment at Keahole Point, Hawaii. Plot of R_f, protein and film dry weight vs days in flow. Unit X.

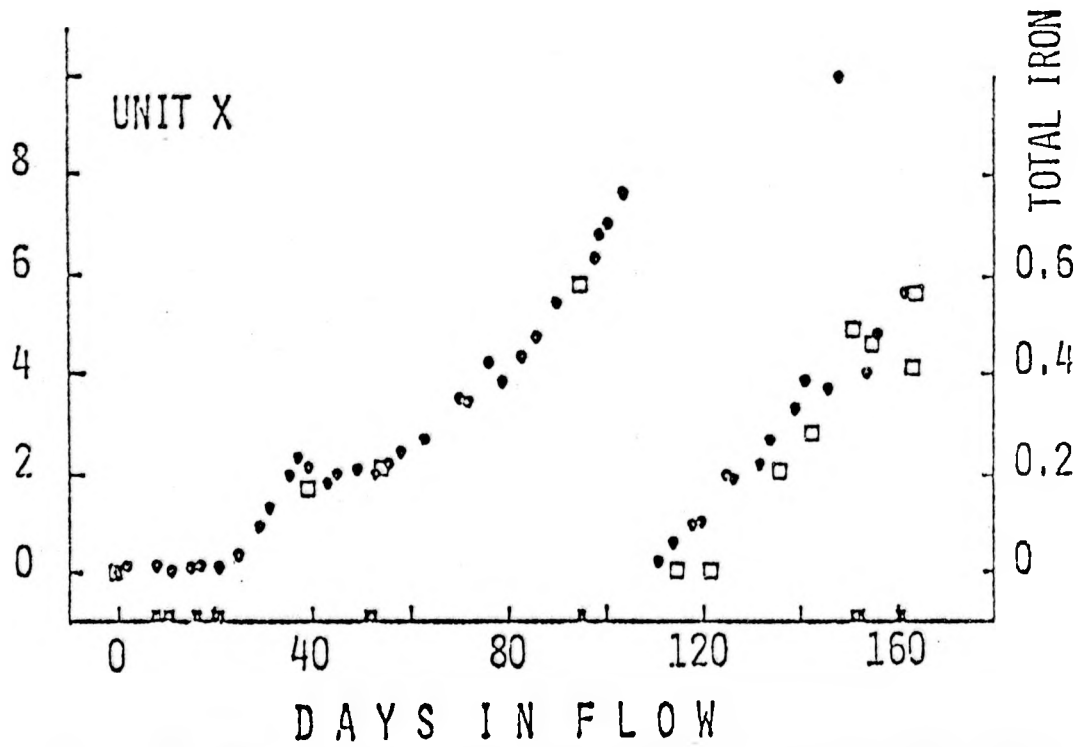

Fig. 5.15 Three-inch pipeline experiment at Keahole Point Hawaii. Plot of R_f and total iron vs days in flow. Unit X.

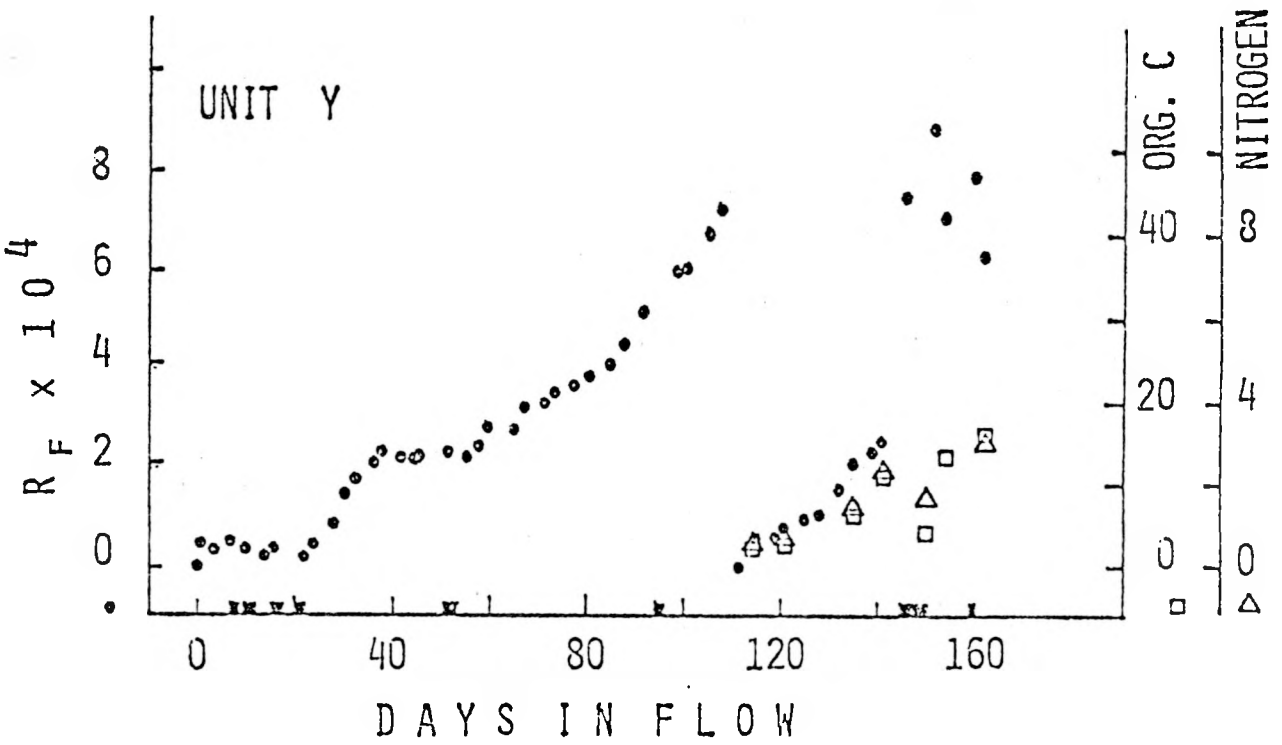

Fig. 5.16 Three-inch pipeline experiment at Keahole Point, Hawaii. Plot of R_f, total organic carbon, and nitrogen vs days in flow. Unit Y. Note: biofouling module was added after the cleaning.

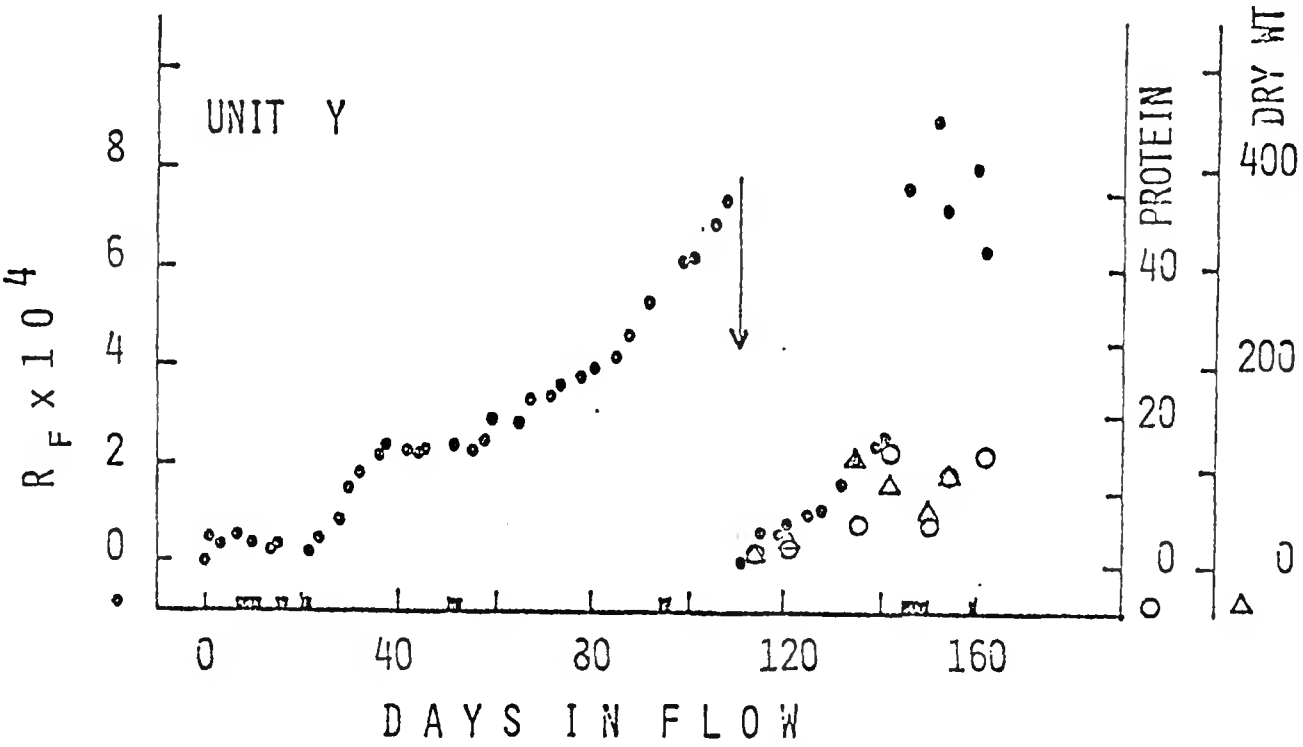

Fig. 5.17 Three-inch pipeline experiment at Keahole Point, Hawaii. Plot of R_f, protein, and film dry weight vs days in flow. Unit Y. Note: biofouling module added after cleaning.

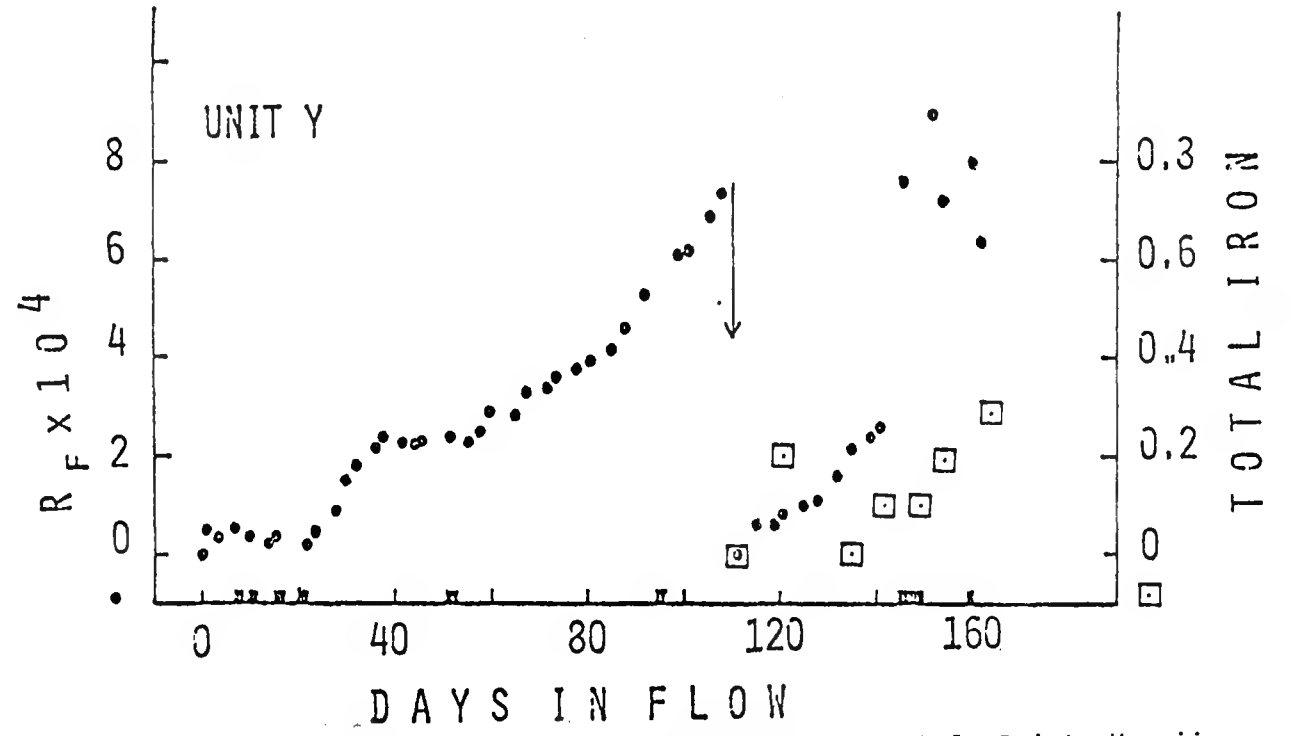

Fig. 5.18 Three-inch pipeline experiment at Keahole Point, Hawaii Plot of R_f and total iron vs days in flow. Unit Y. Note: biofouling module added after cleaning.

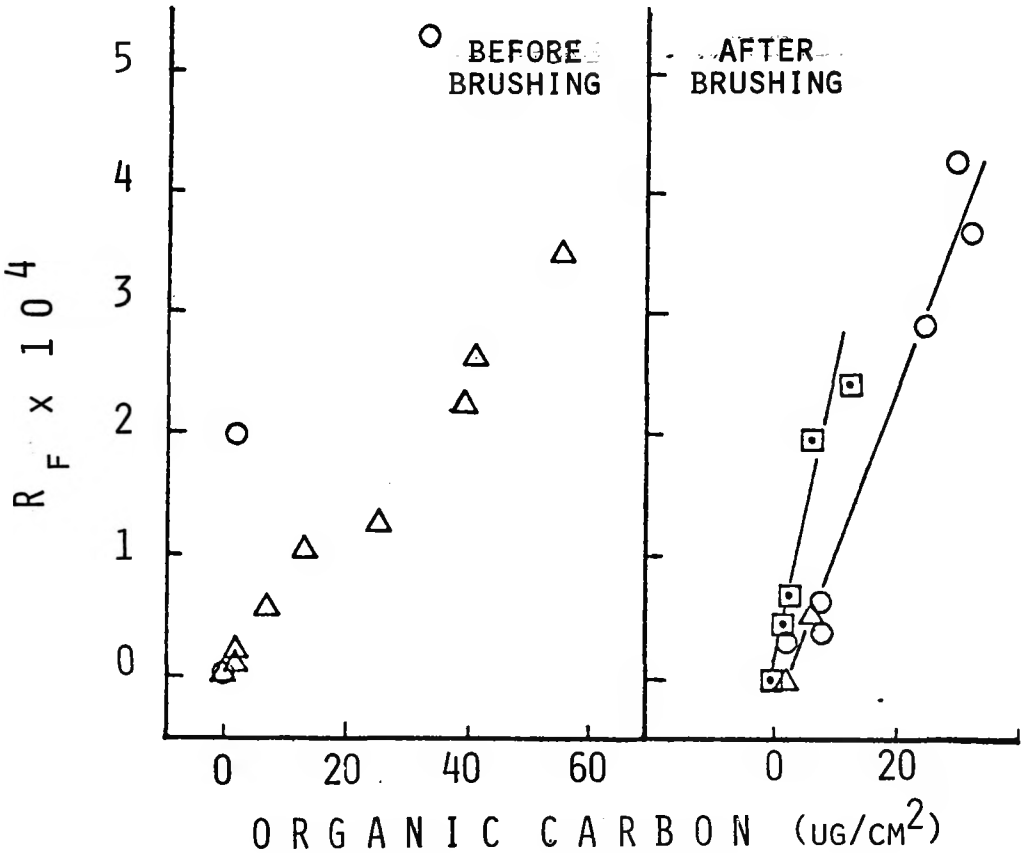

Fig. 5.19 △ 1979 BUOY DATA; ○ 1980 UNIT X FROM 3" PIPE; ⊡ 1980 UNIT Y FROM 3" PIPE STARTED AFTER 113 DAYS OF FLOW.

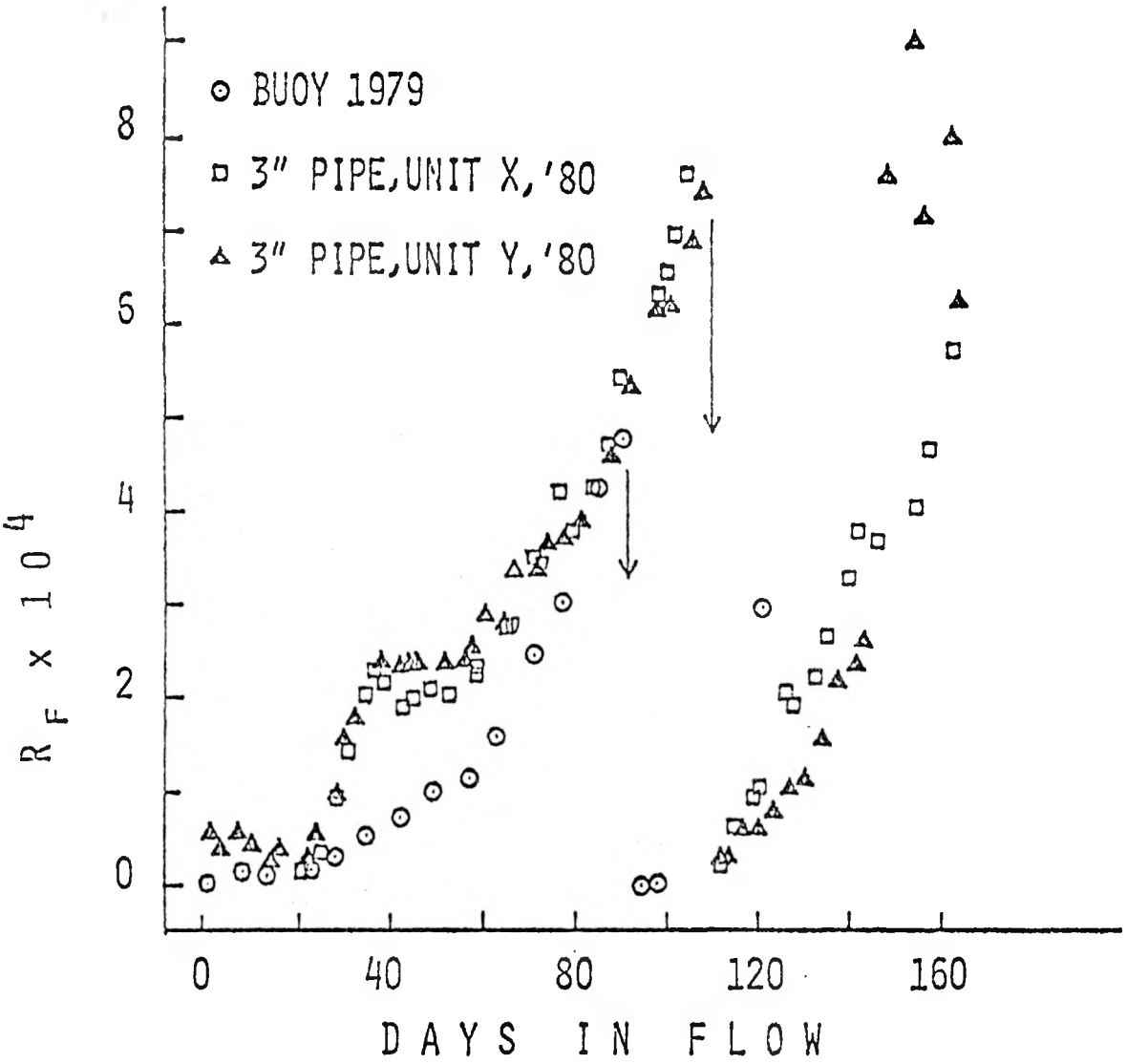

Fig. 5.20 Plots of R_f vs days in flow: composite of data for the Titanium module in the buoy experiment and those in the 3-inch pipeline. Keahole Point Hawaii.

5.6 Biofouling Model

A model is proposed for the kinetics of biofouling on corrosion-resistant tubes, such as Ti and SS, maintained under the OTEC conditions described. Biofouling is assumed to be the cause of the increase in R_f for the corrosion-resistant metals. The rate of refouling after cleaning on such tubes is also considered in the model. The model is limited to early fouling in open ocean waters in which flow rates and water quality are assumed to remain constant during the experiment.

Derivation of the Biofouling Model

1. The rate of primary colonization, dC/dt depends on available uncolonized space, A', and the density of colonization per unit of space, a'. Since experimental data for A' and a' are lacking in the current studies only their product, A, (A = A' · a') is considered. The rate is also dependent on a variety of physical and chemical factors characteristic of the particular system. These factors are lumped together in a constant, K

$$dC/dt = (A - C)\,K \qquad (1a)$$

rearranging: $$dC/(A-C) = K\,dt \qquad (1b)$$

Integrating (1b) between t=0 and ∞, [equation form: dy = dx/(a + bx)]

gives: $$C = A\,(1\text{-exp} - Kt) \qquad (2a)$$

or $$C = A - A\,(\exp - Kt) \qquad (2b)$$

2. The growth of the primary colonizers (and/or production of metabolic products), S, is proportional to their number, the time, and a growth (and/or slime-production) constant, K_1. In the simplest form,

$$S = C \cdot K_1 \cdot t \qquad (3)$$

3. Secondary microbial colonization, i.e., biofouling by other organisms, N, depends upon time, S, and an adhesion constant, K_2 : K_2 also includes a concentration factor, i.e., number of cells/volume of water.

$$N = S \cdot K_2 \cdot t \qquad (4)$$

4. Finally, total biomass, B, of the biofouled layer is

$$B = C + S + N \qquad (5)$$

5. Substitution of equations 1, 2, 3, 4, into 5 gives

$$B = A[(1 - e^{-Kt})\,(1 + K_1 t + K_1 K_2 t^2)] \qquad (6)$$

It becomes evident that A is also a "scaling factor" dependent on the units used. When $K_2 >>> K_1$, the equation becomes largely dependent on the final term, expecially when t is not small and when K is small compared to K_1 and K_2.

Description of the Model

1. The model ignores the various reactions which occur during the first minutes or hours following initiation of the flow of water. The first event considered in the model is the attachment (colonization) of those bacteria which have very high adhesive affinity for the tube surface. Colonization is random as the organisms come into contact with the surface from the seawater. Their rate of adhesion on the tube, however, depends on many factors:
   a. their numbers per unit volume of water
   b. their kind (i.e., their degree of "stickiness")
   c. the flow rate of the water and the hydrodynamic properties of flow
   d. the smoothness of the tube surface
   e. other factors, such as temperature, organic content of the water, etc.
   f. the limited area for colonization
2. The initial colonizers are responsible for making the tube "sticky" for other groups of fouling bacteria. Growth of the primary colonizers, if it occurs, and slime production are assumed to be in direct proportion to cell number and time; nutrient concentration in the flowing water limits both growth and metabolic product formation.
3. Other bacteria, secondary colonizers, adhere randomly to the surface at a rate proportional to their numbers and affinities as well as to the amount of growth or slime already adhering to the tube surface. In the time frame considered no limitation to colonizing space is assumed for the secondary colonizers.
4. During the cleaning of the tubes it is assumed that the primary colonizers, their progeny and/or their macromolecular products are not removed. In contrast, most or all of the secondary colonizers are assumed removed. Re-colonization then occurs at a rate dependent on the amounts of adhering materials still on the pipe.

Analysis of Biofouling Model

Figure 21a shows two superimposed theoretical curves drawn over the R_f, total organic carbon and total nitrogen data from Ti in the HI experiment. The constants used in the model equation are given in Table 5.5. Since the magnitude and units

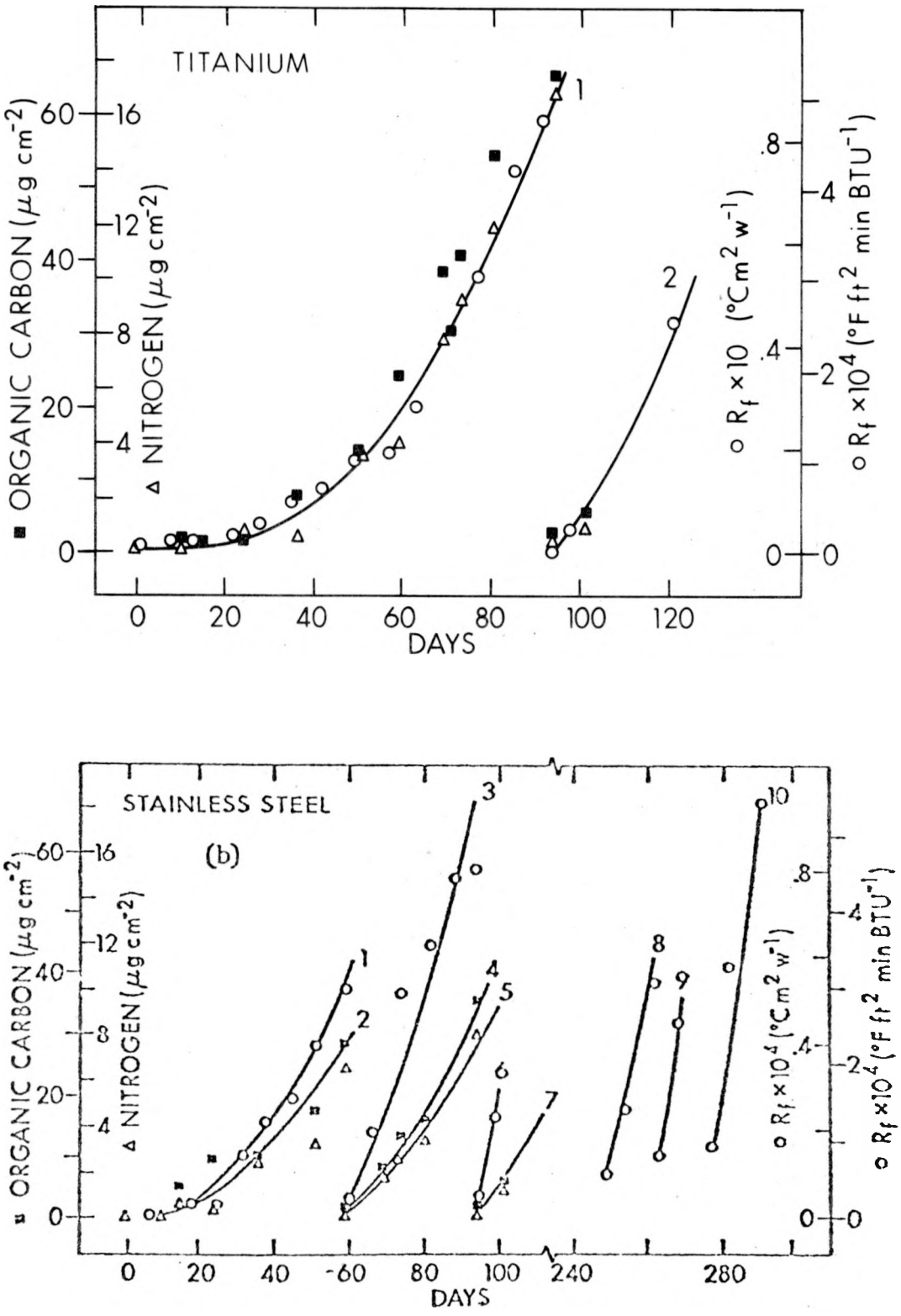

Fig. 5.21 Total organic carbon, total nitrogen and R_f vs exposure time, Hawaii data. The curves were generated from equations of the model.

TABLE 5.5

Biofouling Model:
Constants Giving Good Fitting Curves Through Plots of the Experimental Data for Fouling Before and Refouling of Tubes After Cleaning

Site	Tube Type	Measured Parameter	Following Cleaning #	Model Constants* A	K	K1	K2	Day Series Begun	K2 Pushed Back to ____ Day	See Fig. #	Curve #
Gulf Mexico	Ti	R_f	0	.00505	.01	.03	5.0	0	--	10	
Hawaii	Ti	R_f	0	.00505	.01	.03	6.5	0	--	9	1
Hawaii	Ti	R_f	1	.00505	.01	.03	6.5	94	0	9	2
Hawaii	Ti	Org. C	0	.06313	.01	.03	7.5	0	--	9	1
Hawaii	Ti	Org. C	1	.06313	.01	.03	6.5	94	0	9	2
Hawaii	Ti	N	0	.01683	.01	.03	6.5	0	--	9	1
Hawaii	Ti	N	1	.01683	.01	.03	6.0	94	0	9	2
Gulf Mexico	SS	R_f	0	.00505	.06	.03	5.5	0	--	10	
Hawaii	SS	R_f	0	.00505	.06	.03	6.0	0		9	1
Hawaii	SS	R_f	1	.00505	.06	.03	11.0	59	1	9	3
Hawaii	SS	R_f	2	.00505	.06	.03	17.0	94	0	9	6
Hawaii	SS	R_f	3	.00505	.06	.03	6.0	249	2	9	8
Hawaii	SS	R_f	4	.00505	.06	.03	7.5	263	3	9	9
Hawaii	SS	R_f	5	.00505	.06	.03	7.0	277	3.5	9	10
Hawaii	SS	Org. C	0	.06313	.06	.03	4.5	0	--	9	2
Hawaii	SS	Org. C	1	.06313	.06	.03	5.5	59	1	9	4
Hawaii	SS	Org. C	2	.06313	.06	.03	4.5	94	0	9	7
Hawaii	SS	N	0	.01683	.06	.03	4.0	0	--	9	2
Hawaii	SS	N	1	.01683	.06	.03	4.5	59	1	9	5
Hawaii	SS	N	2	.01683	.06	.03	4.0	94	0	9	7

*See text for explanation of symbols

of the two data sets are different, the constant A is scaled to give comparable numerical values for the Ti data. These same values of A are used for the SS data (Fig. 21b). The same values K and K_1 are used to generate all of the Ti curves. K_2 is chosen to make each curve fit the experimental data. For all Ti curves, K_2 varies little. Figure 22 shows curves constructed through the data obtained in the Gulf of Mexico. Note from Table 5.5 that K_2 is only slightly lower than in the HI curves.

A larger value of K for SS (0.06) is required compared to that for Ti (0.01). This may result from the rougher surface of the SS or other factors which permitted the SS surface to be colonized more rapidly than that of Ti. Curves 3 through 10 in Figure 5.21B for SS mimic the increase in the fouling parameters--after cleaning of the tube. Except for curves 1, 3 and 6 (Fig. 5.21b), values of K_2 are relatively constant for each parameter (Table 5.5). No explanation is offered for the apparent temporary increase in "secondary colonization" in curves 1, 3 and 6. Similar anomalies were not observed on any other tube or parameter measured.

Following cleaning of Ti and SS, the "secondary colonization" term is set back to a time value equivalent to the start of the experiment (zero to 3.5 days). This supports the premise made in deriving the model. It further indicates that the model may be used to predict fouling rates after repeated cleaning of metal surfaces. The gradual rise in the starting value of R_f following repeated cleaning can be attributed to the combined C and S terms of the model: these are small numerically and unaffected by cleaning. They continue to increase with time.

The model curves generated for Ti and SS for COM data, Fig. 5.22, only fit in the early part of the experiment. It appears that the next stage of fouling, that which limits further rapid increase in R_f, was reached earlier than in the HI experiment. The model does not apply to this stage.

A single value of K_1 was used to generate all curves presented in Figures 5.21 and 5.22. This value, 0.03, is arbitrary. The magnitude of K_2 is inversely related to K_1. An independent measurement of either "primary colonizers", C, and their products, S, or of "secondary colonizers", N, would permit assigning absolute values to K_1 and K_2.

The lower values given for K_2 in the organic carbon and nitrogen curves on SS compared to the R_f curves may not be due to differences in the rates of secondary colonization, but to different colonizing densities on Ti and SS surfaces. These should be distinguished in the constant A rather than in K_2.

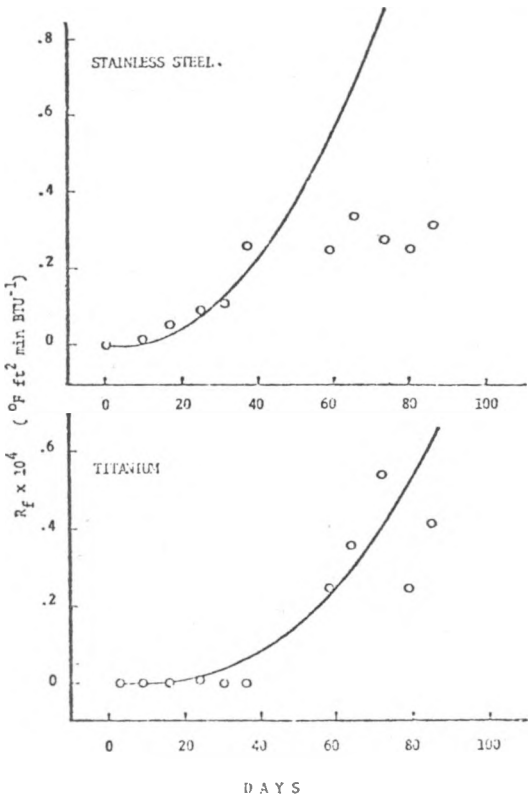

Fig. 5.22 R_f vs time. Smooth curves generated from model for the Gulf of Mexico experiment. (From Berger & Little, 1980)

The precision of the field data makes a more detailed analysis of the model impractical. It is evident that the fouling layer does not form in an exponential manner. This could occur under conditions in which nutrient levels are higher than those found in the present experiments. The model proposed by Bryers, et al. [6], for biofouling was derived for a system exposed to light and in which nutrients were added. The present model does not include a term to limit the increase in the fouling rate.

5.7 Summary of Biofouling Results

Biofouling occurs on all surfaces tested. The primary fouling rate on new pipe surfaces depends in part on the surface smoothness: smoother surfaces foul slower than rough surfaces.

The chemical interactions of the pipe alloy and seawater greatly affect the initial biofouling rate. Toxic compounds leaching from Cu-Ni surfaces retard the establishment of a primary fouling layer. Formation of an unstable oxide film also retards the permanent establishment of a fouling layer because the layer breaks off. With aluminum, gentle brushing removes most of the biofouling material without destroying much of the hydrated oxide layer. This layer does not greatly affect heat transfer. For all surfaces tested, each cleaning removed a progressively smaller fraction of the total fouling layer. Reestablishment of the fouling layer became progressively faster.

The fouling layer seems to be biologically initiated. However the bulk of the film is not organic in composition. The ratio of organic to inorganic mass is fairly constant after the initial lag suggesting that film weight depends on the microbial layer, the inorganic chemistry and the particulate content of the seawater. The presence of microfouled surface upstream of a clean surface accelerates the initial fouling of that clean surface. The following parameters of the fouling layer correlate well with the increase in heat transfer resistance on all surfaces tested except Cu--Ni: organic carbon, nitrogen, protein/amine. Film weight did not correlate as well to R_f as did the other parameters.

A model for biofouling was proposed. Its predictive value is limited to early fouling and situations where frequent cleaning occurs. The model requires further testing with real-world data.

No single organism appears to initiate biofouling. The physical conditions of flow, the chemistry of the water and organic content appear to be variables which greatly affect the fouling picture. In the two last experiments, bacteria

appeared to be the major primary foulers. Not knowing the exact conditions of the first 3 experiments, it is difficult to explain the high numbers of phototrophic organisms observed in the pipes. Single individual rabbit-eared goose-necked whale barnacles were observed in pipe sections on 2 occasions. They may have become established during a pump stoppage.

5.8 Appendices

5.8.1 Project personnel in biofouling

Joyce A. Berger, MS	1977 to present
William F. McCoy, MS	1978-79
Renee Kosslak, BS	1978-79
Greg Win, MS	1979 to present

5.8.2 Subcontractors for biofouling

Oceanic Institute, Waimanalo, HI; water quality analyses

Pan Pacific Laboratories, Honolulu; biofouling on Noi'i and Buoy I and part of Buoy 2 experiments

5.8.3 Appendix: Chemical Analyses

1. Protein/primary amines: The fluorometric assays of Robrish et al. [2] is used for the "film" protein determinations. The test is based on the reaction between primary amines and o-phthalaldehyde to form a complex which fluorescence. We found that by using the acid hydrolysate of the film without doing a subsequent alkaline hydrolysis, more reproducible results could be obtained but at the expense of some sensitivity. Since the test is standardized against protein the assay is valid.
2. Inorganic iron: While the pipes in the UH CMU OTEC project do not have significant deposits of iron oxide in the fouling layer, those of the recent APL project did. We, therefore, modified one of the colorimetric assays for iron for use with the OTEC pipe studies. The test measures ferrous (iron-II); the iron is extracted from the film with mineral acid, reduced with hydroxylamine and reacted with the chromogen, o-phenanthroline. As used the sensitivity of the test is limited to samples containing about 100ng iron or more.
3. Carbon/Nitrogen Analyses; by CHN analyzer
4. Film dry weight, gravimetrically

5.8.4 Appendix: Buoy 3 data

Aluminum Data
UH

Day	Dry Weight µg cm^{-2}	Organic Carbon µg cm^{-2}	Nitrogen µg cm^{-2}	Protein µg cm^{-2}
1st Set Assays				
0	.0943	8.36	0.47	6.533
10	1.1213(?)	6.90	1.29	1.924
24	.741	5.38	1.02	4.518
36	.767	10.00	2.18	15.308
59BC	.7898	27.53	4.94	20.703
69	.6338	11.72	1.98	3.543
73	.7166	12.77	2.61	0.777
80	.5606	14.43	3.63	8.385
94BC	4.5094(?)	21.84	6.60	31.623
101	.4973	6.92	1.38	8.45
Repeat of Assays				
0	.0244	7.65	0	6.98
15	.5314	8.72	ND	4.14
51	.7703	15.06	3.01	15.67
59BC	.7166	23.83	4.45	7.98
59AC	.5411	9.33	2.32	--
69	.4923	10.33	1.45	1.10
73	.624	13.16	2.21	--
80	.5974	17.11	3.53	--
94BC	.9896	33.51	6.99	26.94
94AC	.6656	7.53	0.74	4.42
101	.7459	9.19	2.09	7.51

BC = before cleaning

AC = after cleaning

5.8.4 Appendix: Buoy 3 data

Copper-Nickel Data

Day	Dry Weight $\mu g\ cm^{-2}$	Organic Carbon $\mu g\ cm^{-2}$	Nitrogen $\mu g\ cm^{-2}$	Protein $\mu g\ cm^{-2}$
1st Set Assays				
0	.146	3.45	.614	4.23
10	1.157	5.56	3.071	0.55
24	1.128	5.21	0.819	0
36	2.142	13.93	1.775	2.72
59BC	4.592	20.51	2.662	3.61
69	2.569	16.69	2.516	--
73	2.233	17.43	2.340	13.49
80	2.657	22.90	3.676	5.92
94BC	3.500	33.54	4.579	15.57
101	3.349	35.02	4.481	--
2nd Set Assays				
0	0.068	2.80	0.406	1.50
15	3.266	10.83	1.284	10.69
51	5.060	23.62	2.832	12.90
59BC	3.439	18.12	2.155	8.35
59AC	.905	6.67	0.900	9.56
69	2.876	18.82	2.571	15.63
73	1.760	16.23	2.278	2.02
80	2.684	25.84	3.793	20.41
94BC	3.003	36.45	4.284	9.04
101	2.596	33.19	4.365	14.43

5.8.4 Appendix: Buoy 3 data

Titanium Data
UH

Day	Dry Weight µg cm^{-2}	Organic Carbon µg cm^{-2}	Nitrogen µg cm^{-2}	Protein µg cm^{-2}
1st Set Assays				
0	.127	2.39	1.09	0.163
10	.176	5.85	0.47	2.506
24	.241	5.85	2.18	4.583
36	.244	9.59	1.56	10.53
59	.351	24.89	5.14	57.46
69	.502	44.14	8.59	27.69
73	.619	45.17	10.41	103.90
80	.722	56.75	12.46	41.86
94BC	--	64.82	18.85	92.3
101	.151	9.33	1.62	4.453
2nd Set Assays				
0	.0439	1.58	0.22	5.85
15	.0462	2.98	0.84	4.42
51	.273	15.24	3.71	40.11
59	.395	28.14	6.17	29.09
69	.578	37.43	8.38	--
73	.580	41.05	9.57	52.07
80	.807	57.22	12.84	45.99
94BC	.907	72.29	16.55	34.06
94AC	.125	4.20	0.53	3.35
101	.203	5.90	1.43	5.82

5.8.4 Appendix: Buoy 3 data

Stainless Steel Data

Day	Dry Weight $\mu g\ cm^{-2}$	Organic Carbon $\mu g\ cm^{-2}$	Nitrogen $\mu g\ cm^{-2}$	Protein $\mu g\ cm^{-2}$
1st Set Assays				
0	.127	2.75	0.546	19.24
10	.26	2.75	0.546	3.41
24	.211	11.82	0.887	7.54
36	.309	12.46	2.798	6.53
59BC	.449	33.55	6.978	31.88
69	.195	11.41	2.776	12.48
73	.312	18.12	3.744	15.19
80	.327	21.10	4.319	29.40
94BC	.507	37.98	8.765	67.37
101	.224	8.41	1.823	6.70
Rerun of All Assays				
0	0.0561	4.31	1.157	1.59
15	.112	9.48	1.674	2.35
51	.297	21.83	4.261	19.96
59BC	.453	30.03	7.748	47.00
59AC	.127	6.42	0.800	1.82
69	.141	11.86	2.356	5.16
73	.254	14.81	3.097	7.73
80	.310	17.58	3.907	4.06
94BC	.629	40.31	8.684	40.96
94AC	.139	5.89	0.861	4.18
101	.236	10.31	2.187	7.41

BC = before cleaning; AC = after cleaning

5.8.4 Appendix: Buoy 3 data

Day	AL $R_f x 10^4$	Day	SS $R_f x 10^4$
2	.472	7	- .127
8	.212	11	.003
14	.415	18	.126
21	2.929	25	.156
28	.930	32	.784
35	1.325	38	1.251
43	1.764	115	1.565
50	2.141	51	2.266
57BC	2.984	59	2.987
57AC	.112	60	.238
63	.003	66	1.107
71	.633	74	2.960
77	1.286	82	3.582
85	2.241	88	4.502
91	2.907	94	4.591
95AC	.205	95AC	.754
99	.348	99	1.786
108	2.479		
121	4.447		

5.8.4 Appendix: Buoy 3 data

Day	Cu-Ni $R_f x 10^4$	Day	Ti $R_f x 10^4$	
2	.122	1	.049	
9	.412	8	.122	
14	.711	13	.101	
23	1.767	22	.153	
30	1.175	28	.307	
36	1.396	35	.534	
43	1.515	42	.693	
50	1.819	49	1.005	
57BC	1.823	57	1.114	
57AC	.049	63	1.583	
64	.165	71	2.465	
72	.426	77	3.031	
79	.547	85	4.251	
86	.788	91	4.808	
92	.555	94	- .400	0
94	.509	98	- .133	.267
122	.893	121	2.931	2.531

5.8.5 Appendix: 3" Pipeline Keahole Point Hawaii: Microfouling Data

Day of Flow	Dry Wt.	Carbon	Nitrogen	Protein	Iron	$R_f x 10^4$*	Coupon Days in Flow	
39	24.0	5.4	1.13	2.56	0.17	2.156	39	
53	73	7.14	1.81	4.08	0.21	2.011	53	
94	198	33.1	8.73	25.4	0.58	5.926	94	
112 (AB)	8.3	1.85	0.45	2.86	0.52	0.350	112 (AB)	
115	40.7	4.18	1.15	2.78	0	0.695	115	
122	40.2	6.99	1.93	7.24	0	1.434	122	
136	273	25.5	5.39	26.2	0.2	2.940	146	
143	166	32.7	8.04	35.5	0.28	3.757	143	
151	171	31.9	6.68	28.5	0.49	7.170	151	UNIT X
155	161	29.5	6.46	35.1	0.46	4.335	155	
163	354	33.1	7.8	40.9	0.41	5.868	163	
164 (BB)	289	15.3	4.26	19.8	0.57	6.040	164 (BB)	
164 (BB)	354	23.6	7.11	41.0	0.46	6.040	164 (BB)	
164 (AB)	208	5.73	0.77	1.53	0		164 (AB)	
114	18.6	1.53	0.46	0.79	0	0.501	2	
121	16.5	2.15	0.65	1.34	0.2	0.718	9	
135	112	5.78	1.56	4.46	0	1.993	23	
142**	73.0	10.8	2.69	14.1	0.1	2.548	30	
150**	48.8	3.8	1.84	4.90	0.1	8.065	38	
154	82.9	12.7	2.79	11.6	0.2	9.004	42	UNIT Y
162	6719 ***	14.9	3.43	14.5	0.18	8.049	50	
163	7192	15.6	2.4	10.1	0.39	7.153	51 (BB)	
163	8135	14.8	2.6	8.49	0.18	7.153	51 (BB)	
163	98.3	7.5	0.48	0.42	0		51 (AB)	

* R_f data extrapolated from nearest two dates of data taking

Unit Y biology sampling was introduced on 112th day of flow following acid cleaning of HIM

** Between days 142 and 150 flow in Unit Y was inadvertently left off

*** Sample filled with quantities of crystals (see also SEMs)

See elsewhere for list of short-time flow interruptions

5.9 References

1. Corpe, W.A., Microfouling: The role of primary film forming marine bacteria. Proc. Third Internat. Corrosion and Fouling Congr., 2-6 Oct. 1972, National Bureau of Standards, Gaithersburg, MD, pp. 598-609, 1972.

2. Robrish, S.A., Kemp, C. and Bowen, W.H. The use of the o-phthalaldehyde reaction as a sensitive assay for protein and to determine protein in bacterial cells and dental plaque. Analytical Biochemistry 84, 196-204, 1978.

2B. Berger, L.R. and Little, B. Effect of microfouling on heat transfer efficiency. Proceedings of the Fifth International Congress on Marine Corrosion and Fouling, Barcelona, pp. 139-154, 1980.

3. Siegel, A. Metal-organic interactions in the marine environment. In Faust, S.D. and J.V. Hunter (eds.), Organic compounds in aquatic environments, Dekker, N.Y., 1971

3B. LaQue, F.L. Qualifications of stainless steel for OTEC heat exchanger tubing. ANL/OTEC report prepared for the U.S. Department of Energy, Division of Central Solar Technology under contract W-31-109. January 1979.

4. Marszalek, D.S., Gerchakov, S.M. and Udey, L.R. Influence of substrate composition on marine microfouling. Applied and Environmental Microbiology, November 1979.

5. Little, B.J. and Lavoie, D.M. Gulf of Mexico ocean thermal energy conversion (OTEC) biofouling and corrosion experiment. Proceedings of the OTEC Biofouling, Corrosion, and Materials Workshop, Rosslyn, VA, January 8-10, 1979.

6. Bryers, J.D., Characklis, W.G., Zelver, N. and Nimmons, M.G. Microbial film development and associated energy losses. Proceedings of the Sixth Ocean Thermal Energy Conference, Washington, D.C., June 19-22, 1979.

6.0 Corrosion

One of the major goals of the OTEC program has been to qualify materials for use in OTEC heat exchangers. Because of the low thermal conductivity of nonmetallic materials, only metallic alloys were considered for these experiments. Included were titanium (grade 2), AL-6X stainless steel, CA-706 copper-nickel, and the aluminum alloys 5052 and Alclad 3003. Each of these alloys has advantages and disadvantages for OTEC applications.

Titanium should be essentially inert under OTEC conditions. It is sufficiently hard to resist any mechanical cleaning techniques likely to be used and can be fabricated into a wide variety of shapes. However, it is expensive and its availability in quantities required for the OTEC program is doubtful. But there is little doubt that titanium heat exchangers will provide a 30-year lifetime for OTEC heat exchangers.

The high-alloy stainless steels, typified by AL-6X, have shown excellent performance under simulated OTEC conditions, and they are readily available; nonetheless, their costs are comparable to titanium's and they are susceptible to crevice corrosion. Crevices could be formed on plate type heat exchangers using elastemeric gaskets. In spite of these problems, the high alloy stainless steels are generally agreed to be qualified for OTEC applications.

Copper-nickel alloys have been used extensively in marine heat exchangers. In the early stages of exposure a porous corrosion product of Cu_2O forms and is sufficiently toxic to prevent the colonization of biofouling films; however, sufficient water may be trapped in the porous structure to impede heat transfer. At later times a duplex layer forms consisting of an inner thin layer that controls further growth and a thicker outer layer consisting mainly of $Cu(OH)_3Cl$. After this duplex layer is established the material readily biofouls at rates similar to those of other alloys. Cleaning the copper-nickel alloy by brushing was found to accelerate corrosion weight loss and the corrosion becomes localized leading to the potential for early failure by pitting. On the basis of our results and the incompatibility of the copper alloys with the most widely accepted working fluid--ammonia, it is not expected that the copper-nickel alloys will be used for heat exchanger surfaces.

Only the aluminum alloys appear to have the potential for substantially reducing the overall costs of the heat exchangers, provided they can be qualified

for OTEC conditions. Aluminum's most serious drawback is its tendency to "pit" in the presence of heavy metal ions such as copper or iron, which could lead to premature failure of the thin walls of the heat exchanger.

Basically there are two classes of aluminum alloys -- clad and unclad. Unclad alloys, such as 5052, are used on the basis of their low overall corrosion rate and resistance to localized corrosion (pitting) and was the first Al alloy seriously examined in this program. The clad alloys, such as Alclad 3003 were the next to be selected based on their potential to resist pitting. They use an anodic outer layer metallurgically bonded to a more noble inner layer, analogous to galvanized steel. Presumably, if a pit forms in the outer layer it will not penetrate the inner layer until all of the cladding is exhausted. However, the corrosion rate of materials used for the outer layer is greater than that of the unclad alloys and may not provide the desired 30-year lifetime.

A number of studies have evaluated aluminum alloys for OTEC applications by monitoring the corrosive effects of mechanical cleaning as well as various concentrations of ammonia in seawater and chlorination. Susceptibility to and extent of pitting varies widely from study to study, but all studies generally agree that the aluminum alloys form protective layers that result in a steadily decreasing overall corrosion rate. If this protective film is not removed by cleaning techniques or dissolution, it has been estimated that aluminum alloys could easily provide a 30-year lifetime under OTEC conditions. Thus, at the present time the aluminum alloys can neither be qualified nor disqualified for OTEC heat exchangers. Future long-term testing, involving both warm and cold seawater at the Seacoast Test Facility will be required before aluminum can be used with confidence in OTEC heat exchangers.

6.1 Noi'i

Corrosion samples from the Noi'i experiment consisted of one-inch diameter schedule 40 Ti and Al 6061-T6 pipe. The Al alloy was selected more for its machining properties than its corrosion resistance. A cursory analysis was reported by Harvey [1] during his examination of the biota present on these materials.

Samples were exposed to flowing seawater for five weeks. The flow was interrupted on numerous occasions. No change in the surface features of the Ti pipes was found. However, the Al pipes, in some cases, were found to have "whitish

corrosion products" (presumed to be aluminum hydroxide) in pits beneath deposits of organic material. In addition, a "cracked and checked" appearance was found, characteristic of the dehydrated Al corrosion product layer.

No other corrosion results were reported.

6.2 Buoy 1

No corrosion analysis was performed for this deployment.

6.3 Buoy 2

The corrosion behavior of Ti and Al 5052 one-inch diameter split-ring coupons exposed to flowing seawater from times as short as a few hours to more than 8 months was investigated after all samples had been collected and cataloged [2]..

6.3.1 Experimental Methods

Aluminum samples were cleaned by a $NaOH/HNO_3$ treatment according to the method of Craig, et al. [3]. Titanium samples were cleaned with a 5% HNO_3-1% HF mixture. The coupons were placed downstream from the CMU heat transfer apparatus in the underwater buoy off Keahole Point and exposed to flowing seawater in the range of 1 to 2 m/s for times ranging from 3 hours to 8 months. None of the coupons were disturbed before removal.

In addition to the split ring coupons, brushed and unbrushed samples were obtained from the 8-1/2 ft long aluminum and titanium pipes used in the heat transfer instrument. These were brushed at the end of 13, 22, and 29 weeks' exposure to flowing seawater using 20 passes of a MAN brush after the fouling resistance reached predetermined values.

Coupons were removed periodically and immersed in seawater containing 2.5% glutaraldehyde to preserve the biofouling products. After biological examination the samples were scrubbed with a sponge under flowing tap water to remove the biofouling layer. After mounting on SEM holders the dried samples were transferred directly to the SEM without the application of a sputtered conducting film.

6.3.2 Experimental Results

Titanium Titanium samples removed from the buoy confirmed the excellent corrosion resistance of titanium in flowing seawater. No detectable change in the surface morphology of the titanium samples was found for either the brushed or unbrushed sections. The surface of an 8 month brushed titanium sample is shown in Fig. 6.1. The rough, grooved surface shown here is typical of the other

titanium samples and is undoubtably due to the manufacturing process used to produce the pipe sections. These surface irregularities are considerably larger than those found for the aluminum samples. The microscopically rough areas may present a rather attractive surface for the attachment of biofouling organisms.

Aluminum The surface of an aluminum sample immersed in seawater and then immediately preserved in the glutaraldehyde-seawater solution ("0-hour") is shown in Fig. 6.2. Extrusion lines, as well as numerous surface depressions, presumably due to the cleaning procedure, are evident, in addition to a number of particles randomly dispersed over the surface, which are assumed to be salt crystals.

After 8 months' exposure the surface had a cracked "dried mud" appearance over a large area, as shown in Fig. 6.3. This morphology is similar to that found by Craig, et al. [4] for 6061-T6 aluminum. They concluded that a continuous gelatinous film of aluminum oxide trihydrate was formed on exposure to seawater which fractured when dried. The dried corrosion product film of samples taken from the unbrushed region of the heat transfer section tended to flake off very easily, whereas the brushed samples had a much more tightly adhering film.

After examination of the long term exposures (8 months), a series of short-time samples were examined in an effort to determine the initial kinetics of film formation. The exposure times were 3 hours, 6 hours, 12 hours, 24 hours, 48 hours, 72 hours, 1 week, 2 weeks, and 3 weeks.

After only 6 hours, surface cracks were just visible at 800X, indicating the presence of a corrosion product film. This is in agreement with that found Craig, et al. [4] who found that polarization occurred after 45 to 75 minutes. It could not be determined by SEM techniques if the 3 hour coupon also had a passivating film present.

After 12 hours, the entire surface area was covered by a cracked, but continuous, film, as shown in Fig. 6.4. Higher magnification revealed occasional pieces missing from the continuous dried film. An estimate of the dried film thickness could be made in these areas. As the exposure time increased it was found that the thickness, as well as the average diameter of the cracked corrosion film platelets, steadily increased.

The 2 week sample is shown in Fig. 6.5. The hole in the film probably resulted from the drying process and is not believed to be a corrosion pit in the underlying aluminum surface. In fact, no evidence of pitting was found in any of the samples examined. This lack of pitting is presumably due to both the low copper concentration in the 5052 alloy as well as the caustic/acid cleaning procedure.

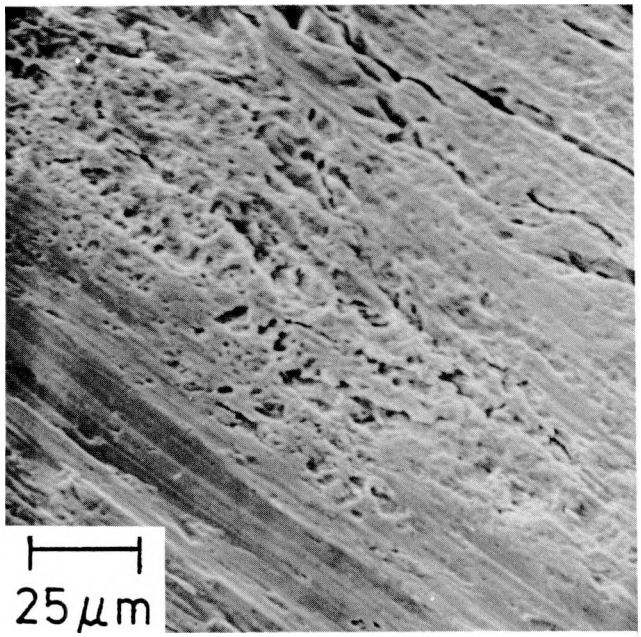

Fig. 6.1 SEM photograph of a periodically brushed titanium pipe after 8 months' exposure to flowing seawater.

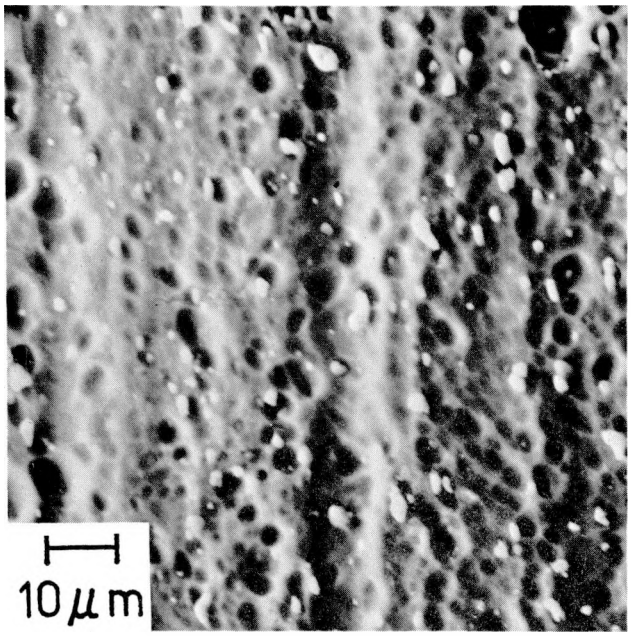

Fig. 6.2 SEM photograph of a "0-hour aluminum sample briefly exposed to seawater and then immersed in a 2.5% glutaraldehyde solution.

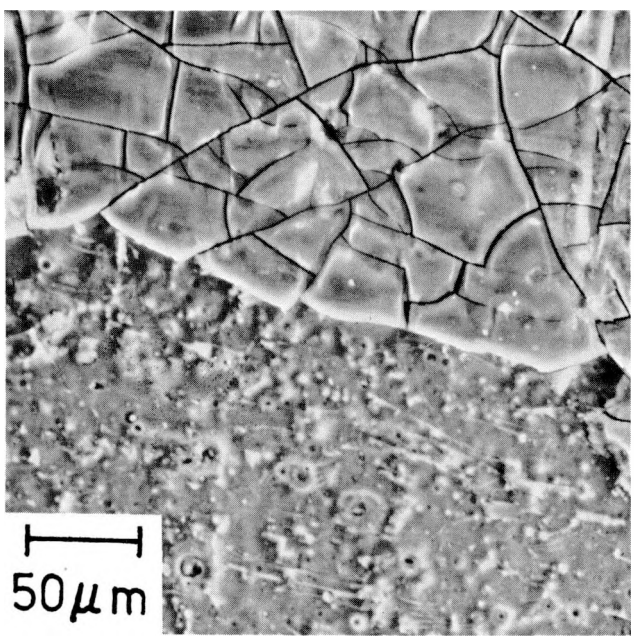

Fig. 6.3 SEM photograph of a brushed aluminum pipe after 8 months' exposure to flowing seawater.

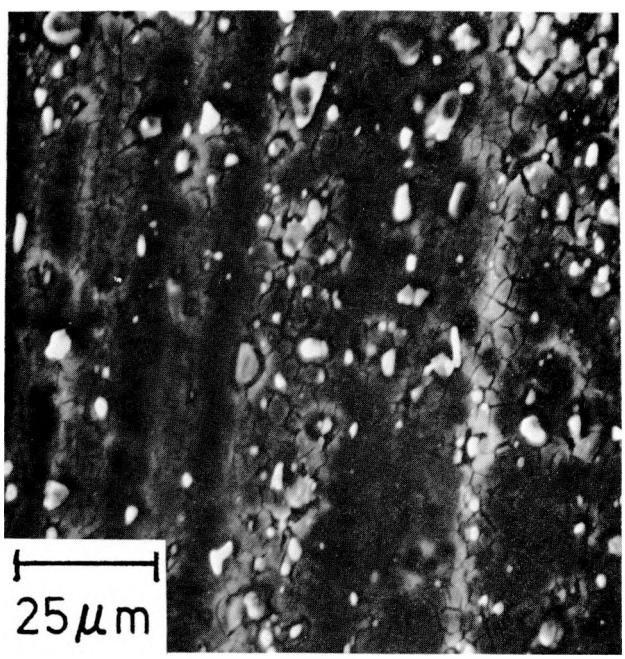

Fig. 6.4 SEM photograph of an umbrushed aluminum coupon after 12 hours' exposure to flowing seawater.

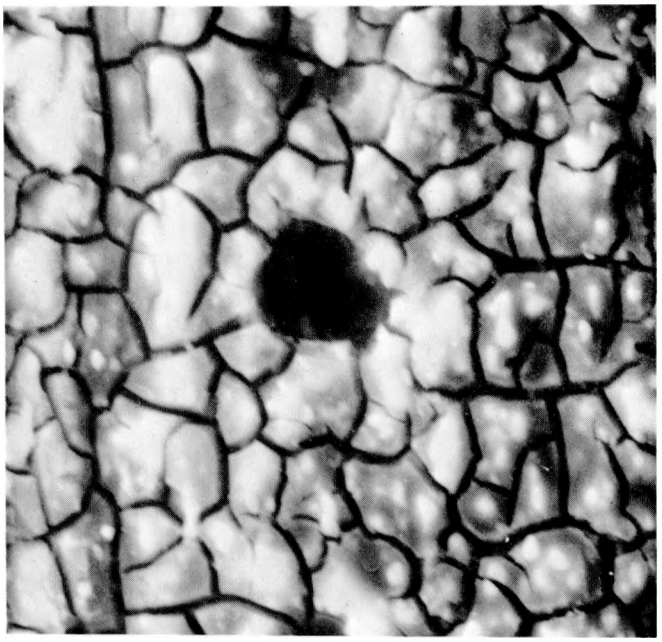

Fig. 6.5 SEM photograph of an unbrushed aluminum coupon after 2 weeks' exposure to flowing seawater. The hole in the corrosion product film is believed to have formed after drying of the film.

These results of increasing film thickness with time differ from those of Craig, et al. [4], who found that the corrosion product film of 6061-T6 aluminum showed no trend to be either heavier or lighter (per unit area) as exposure time increased. This constant film thickness was attributed to the steady-state dissolution of the hydrated aluminum oxide film. Their limiting film thickness was estimated to be of the order of 1.8 to 6.4 μm, which is an order of magnitude thinner than that estimated by Fetkovich from the heat transfer results [5].

6.3.3 Discussion

Although the corrosion resistance of titanium in flowing seawater was found to be excellent, its rough, irregular surface may result in increased rates of biofouling, compared to a "smooth" surface.

Little and Lavoie [6] measured the wet film thickness by light section microscopy as a function of exposure time. Their results indicated that the growth rate was initially much larger than at later times. Morse [7] determined the dry film thickness by measuring the residual sea salt values within the surface deposits. Again, the film thickness increased rapidly in the beginning, after which the growth was relatively slow and steady.

When aluminum is in contact with seawater under these conditions, a gelatinous corrosion product of aluminum oxide trihydrate forms at the metal/oxide interface [2]. If growth of the film is controlled by diffusion of some species through the film (e.g. water molecules), and the film is continuous, then the growth rate should follow the parabolic rate law in which the film thickness is proportional to the square root of time.

The aluminum oxide trihydrate film is expected to be continuous since the Pilling-Bedworth ratio (volume of the corrosion product to that of the metal) is about 3.22, which is greater than the critical value of unity required for a continuous film.

It has been estimated that nearly 90% of the initial film thickness is water of hydration [7]. Examination of corrosion products by SEM techniques, however, results in a nearly complete dehydration of the wet film. Therefore, correlation of actual film thickness under operating conditions with dry film thickness measured by other techniques, such as SEM, must be done with caution.

It was noticed that the platelets seen in the SEM steadily increased in size as the length of exposure time increased. It is expected that the platelet size, which is easy to measure in the SEM, is related to the wet film thickness for two reasons. First, as the film dehydrates, there are no restrictions as to how much it may shrink normal to the surface, but since it remains firmly attached to the substrate, a tensile stress large enough to produce the familiar "mud-cracked" pattern, observed in all samples, is induced in the dehydrated film. Second, since the film is constrained from shrinking laterally due to coherency with the substrate, the resulting platelet size should be proportional to that of the film thickness when hydrated. Therefore, assuming that the growth rate of the wet film is diffusion controlled, if the average platelet diameter, d, is plotted vs the square root of time, a linear relation should be obtained.

The average platelet diameter was determined by the line intersection method [8] and is given in Table 6.1 for the exposure times indicated. As shown in Fig. 6.6, d does, in fact, increase parabolically with time for exposure times at least less than three weeks. The relationship between d (μm) and time, t (hours), is given by:

$$d = 1.44\ \mu m + 0.66\ t^{1/2} \qquad (1)$$

The fact that d does not extrapolate to zero as time decreases can be explained if the minimum crack size is required to be about the same as the initial grain size of the underlying aluminum or if cleaning in NaOH results in an initial "zero-hour" film thickness of $\sim$ 1.5 μm. Craig, et al. [3] found that the crack network is of the same order of magnitude as the grain size.

The only measurements of wet film thickness available at the time were those of Little and Lavoie [6]. Their results, along with their estimates of error (±3μm), are shown in Fig. 6.7. The average platelet diameter, based on Eqn. 1, is shown to agree favorably with wet film thickness over the span indicated, lending further support to d being a good estimate to the wet film thickness. The deviation of the wet film thickness from that predicted at the early times of exposure may be due to a much less dense wet film initially [6], which would result in a larger film thickness than expected.

Assuming that the wet film thickness (d) is 3.22 times the reduction in aluminum thickness due to corrosion (based on an assumed wet film density of 2.423 g/cm^3 [4]), the corrosion loss, Δx(μm), can be predicted from Eqn. 1:

$$\Delta x = 0.20 t^{1/2} . \qquad (2)$$

Table 6.1

MEASURED PLATELET DIAMETER (d) AND PREDICTED CORROSION RATE (Δx) AT EARLY TIMES

t (hours)	$t^{1/2}$ $(hours)^{1/2}$	d (μm)	Δx (μm)
12	3.46	3.4	0.69
24	4.90	4.4	0.98
48	6.93	6.5	1.39
72	8.49	7.0	1.70
168	12.96	10.7	2.59
336	18.33	12.6	3.67
504	22.45	17.0	4.49
504	22.45	15.7	4.49

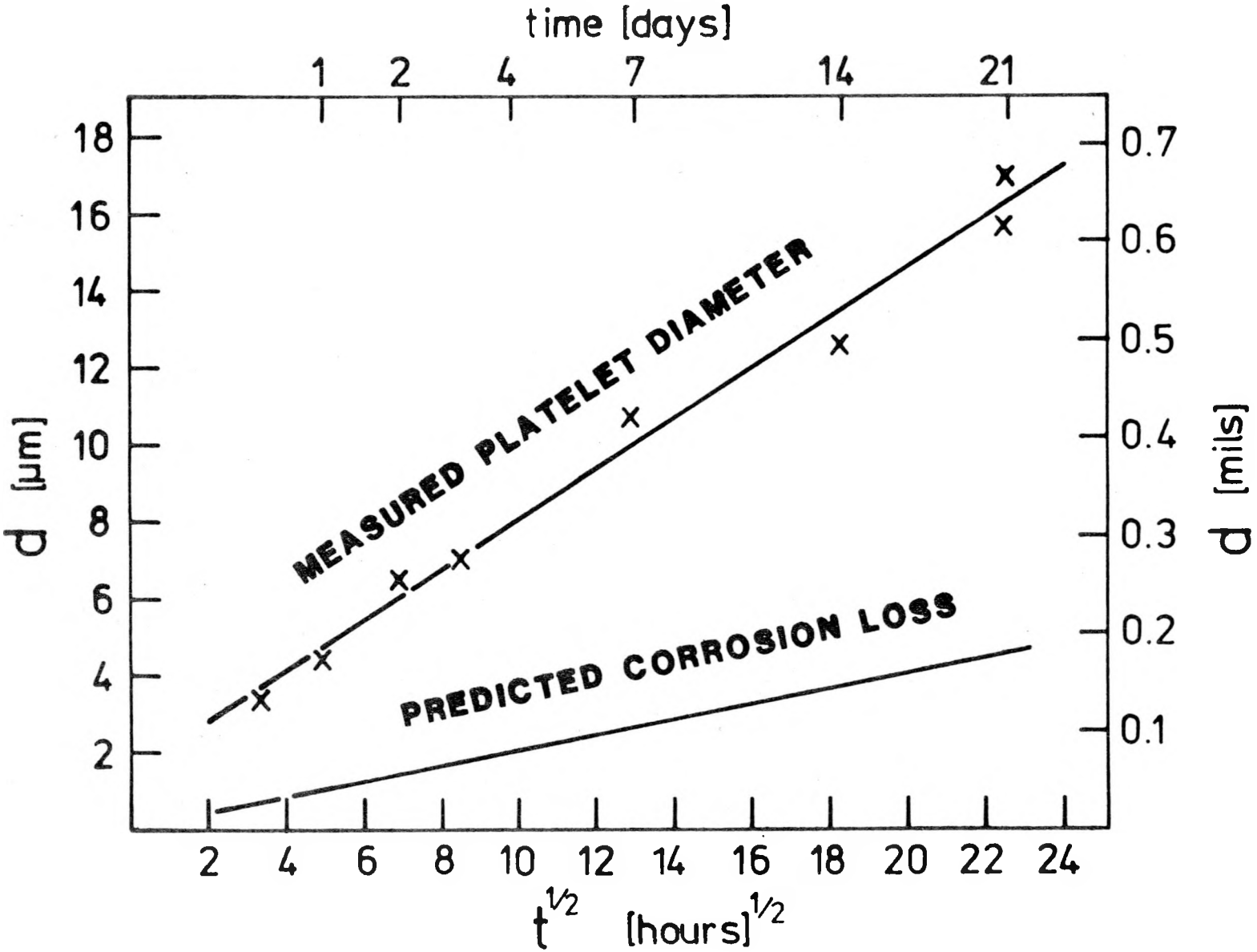

Fig. 6.6 Measured platelet diameter, d, as a function of the square root of time as well as the predicted corrosion loss, Δx, of 5052-H34 aluminum.

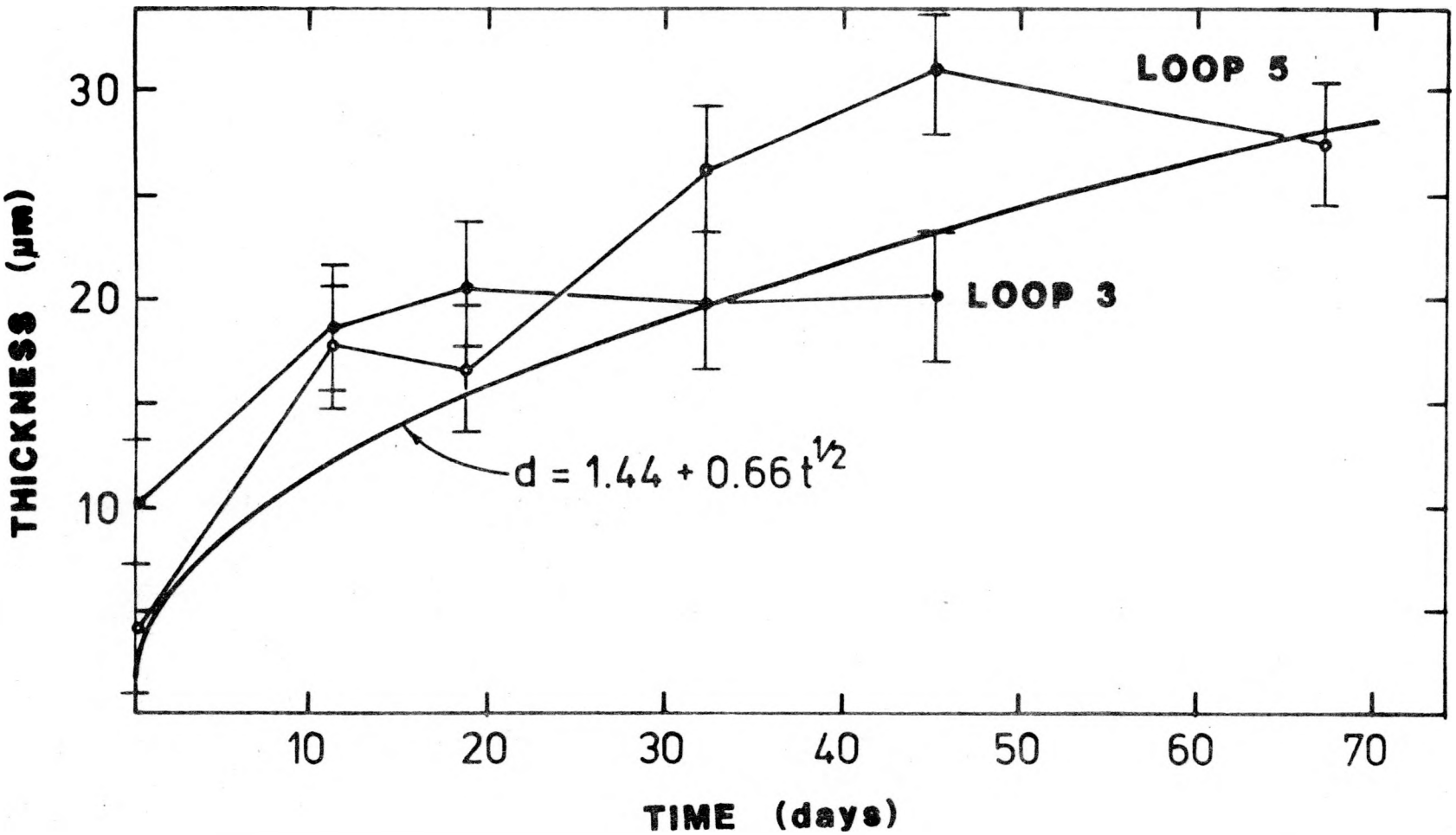

Fig. 6.7 Wet film thickness vs time as determined by light-section microscopy [6]. Predicted wet film thickness from the equation $d = 1.44 + 0.66\ t^{\frac{1}{2}}$.

(The time independent term, 0.45 μm, is neglected since Δx must approach zero as exposure time decreases.)

If the attack is uniform and the corrosion product film is not removed by brushing or dissolution, then the corrosion loss should only be 100 μm (4 mils) over a 30 year lifetime.

The instantaneous thickness growth rate, $\dot{G}$, as well as the corrosion rate, $\dot{C}$, (μm/yr) can be obtained by differentiating Eqn. 1 and 2 with respect to time:

$$\dot{G} = 2900\ t^{-1/2} \tag{3}$$

$$\dot{C} = 900\ t^{-1/2} \tag{4}$$

where time is, again, given in hours. These predicted rates are shown in Fig. 6.8 over a 12 month period.

At very early times, the rates are very large but decrease rapidly with time. There is no steady-state growth or corrosion rate predicted. If the corrosion product film is completely removed when the aluminum surface is brushed to reduce the fouling resistance (R_f), then the corrosion rate would again be very large. Assuming the aluminum heat exchangers were brushed once a month, and this resulted in complete removal of the corrosion product film, then the total corrosion loss over a period of 30 years is given by

$$\Delta x = 30 \times 12 \times 0.20(730)^{1/2} \simeq 75 \text{ mils},$$

a loss of metal thickness that could be tolerated.

In fact, the results from the 8 month exposure sample predict that the corrosion product film is not removed by the brushing procedure used in this experiment. The measured platelet diameter for the 8 month brushed sample was found to be 51 μm. If this is indeed the same as the wet film thickness before dehydration, and the film was removed by brushing, then a larger d would be predicted by Eqn. 1, because the film would reform after the three brushing operations. However, the predicted d is 54 μm, in good agreement with the measured d. Therefore, two conclusions can be made. First, the film continues to increase in thickness, and the aluminum continues to decrease in thickness, parabolically with time over at least an 8-month period. Second, the effect of brushing on film removal appears to be negligible.

The absence of pitting of 5052-H34 aluminum in flowing seawater over an 8-month period, as well as the low predicted corrosion rate recommended this alloy for further consideration for OTEC heat exchanger applications.

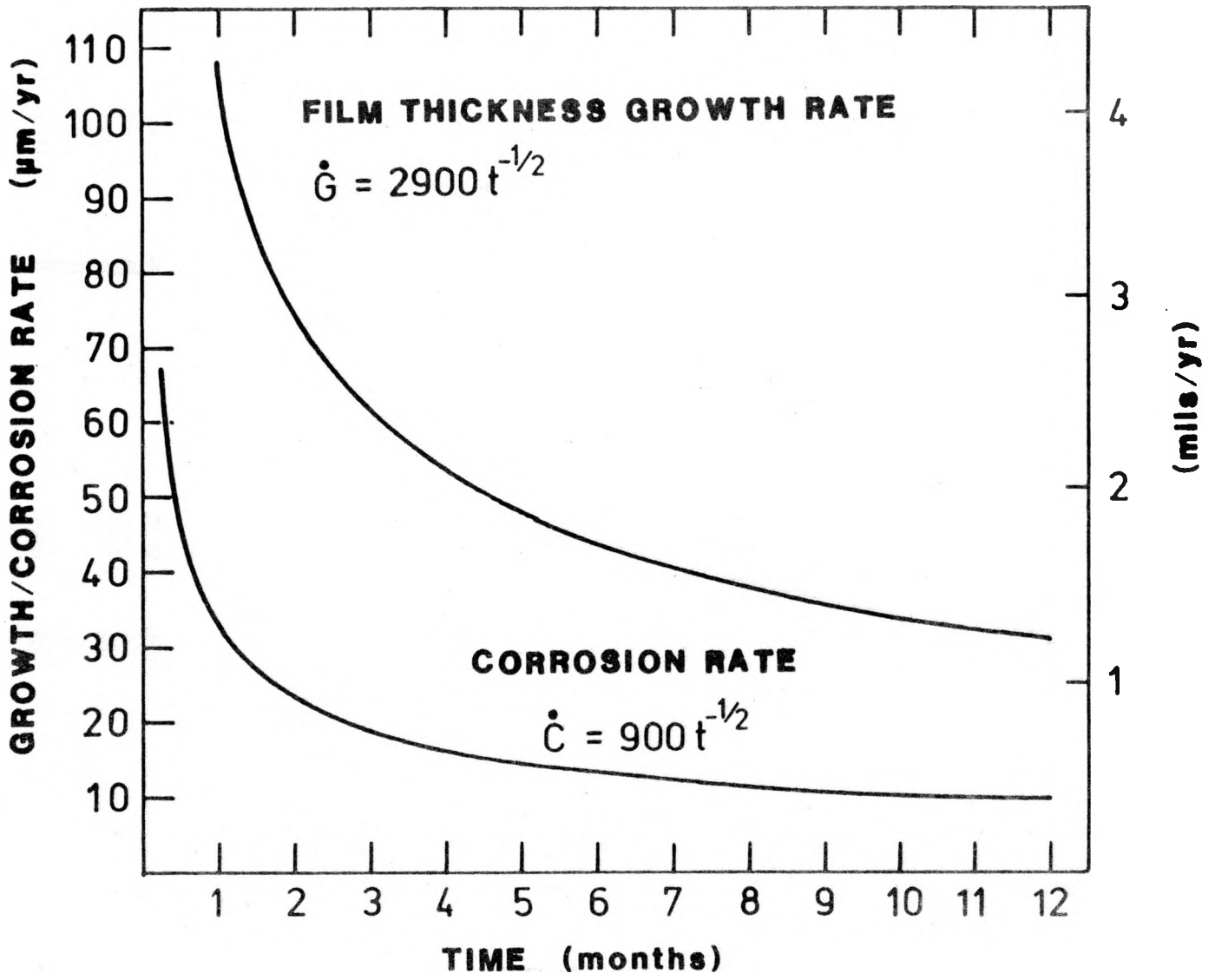

Fig. 6.8 Film thickness growth rate, $\dot{G}$, and corrosion rate, $\dot{C}$, (μm/year) predicted from the parabolic rate law.

6.4 Buoy 3

In the Buoy 3 experiment the corrosion behavior of four alloys, 5052 aluminum (Al), Grade 2 titanium (Ti), AL-6X stainless steel (SS), and CA-706 copper-nickel (CuNi), was studied under simulated OTEC conditions using warm, surface seawater in order to determine which would be viable materials for use in OTEC heat exchangers.*

6.4.1 Experimental Methods

The heat transfer pipe, along with most coupons, was periodically cleaned by several passes of a cylindrical bristle-brush in order to remove a majority of the fouling and maintain R_f close to initial values. Coupons were removed periodically by cutting off sections of the specimen pipe at the downstream end, preserved by either immediately immersing in seawater containing 2.5% glutaraldehyde or by draining and freezing. Short time samples were collected at the end of 3 hours, 6 hours, 12 hours, 24 hours, 48 hours, 72 hours, 1 week, 2 weeks and 3 weeks. Other samples were removed at times ranging from 36 days to 10 months.

Sample were cut longitudinally and lightly scrubbed with a sponge under flowing tap water to remove the biofouling layers for the Al, Ti and SS samples. The CuNi samples were examined "as is" due to the small amount of biological material present as well as the brittleness of the corrosion film. A stereo microscope (30X) was used to check for pitting, followed by a closer examination of areas of interest using either an optical microscope or a SEM, depending on the information to be obtained.

In most cases, Al samples did not require coating with a conducting film for SEM examination; however, the CuNi corrosion film was sufficiently electrically insulating to require a coating of a Au-Pd sputtered film (or a carbon evaporated film if EDAX was desired).

Small segments of the loose CuNi corrosion film were lifted off the interior surface and positioned perpendicular to the sample mount for thickness measurements using either a filar eyepiece in an optical microscope or SEM photographs.

The thickness of the dehydrated Al corrosion film was obtained by optical microscopy by selecting an area where a portion of the film was missing, focusing on the top of the layer and on the immediately adjacent substrate, and using the difference in readings of a graduated focusing knob. Repeatability to $\pm$ 1.5 μm was typical. The technique was useful for a film thickness above 5μm.

---

* Nominal compositions: 5052 Al - 2.5% Mg, 0.25% Cr, bal. Al; Ti - nominally pure; Al-6X SS - 7% Mo. 21% Cr, 24% Ni, 0.03% C, bal. Fe; CA 706 CuNi: 88.7% Cu. 10% Ni, 1.3% Fe.

The film thickness of a few samples was also determined using a newly adapted "spherical abrasion" technique.* This method, which can be used with the optically opaque films found on CuNi as well as with the transparent Al films, utilizes a rotating ball-bearing ball coated with 1 μm diamond paste to polish a circular taper section through the corrosion film, as shown in Fig. 6.9. It can be shown that the thickness of the film is closely represented by

$$h = \frac{XY}{D}$$

where X and Y are measured as shown in Fig. 6.9 and D is the diameter of the ball-bearing ball. The larger the ball the greater the accuracy; however, too large a diameter may produce a hole too large to be conveniently viewed in an optical microscope. A 19 mm diameter was found to be about the optimum size for this work.

A circular taper section will, of course, only be produced if the sample is flat. Since our sample coupons were in the form of cylinders, the resulting hole in the interior surface was oval. This does not introduce an error since the X and Y measurements were taken along the cylinder axis. In most cases the demarcation between the top of the film and the beginning of the oval hole was enhanced by coating the surface with an opaque plastic film.

For the Al samples an average platelet area was determined by counting the number of platelets in a known area using an optical microscope. The average platelet diameter was determined by the line intersection method [8].

6.4.2 Experimental Results

Titanium and Stainless Steel Examination of the Ti and SS samples again confirmed the excellent corrosion resistance of these alloys in flowing seawater. No detectable change in the surface morphology was found anywhere, including those areas containing deposits of inorganic material. Both of these alloys can be considered to be essentially inert under these conditions.

Aluminum A number of different techniques were used to obtain an estimate of the amount of corrosion loss of Al as a function of exposure time. Since the samples were fairly massive, the corrosion rate low, and the exposure times relatively short, weight-loss measurements were not practical. Weight measurements obtained for total removed film (organic plus inorganic) were apparently dominated by the presence of salts retained by the film [9], which resulted in an approximately constant removed film weight after the first 10 days of the experiment.

Optical measurements of the dehydrated film thickness using a graduated fine-focusing knob are listed in Table 6.2 for the different exposure times. The few

* This is an adaptation of a technique developed by the Laboratoire Suisse de Recherches Horlogères in Neuchâtel, Switzerland.

Table 6.2

DATA FOR ALUMINUM CORROSION FILM

[h = film thickness, A = platelet area, d = platelet diameter]

Time (days)	h(μm)	A (μm^2)	d (μm)
0.25	2.5*		
0.5	5.35**		3.4
1	5.95**		4.4
2	6.45**		6.5
3			7.0
7			10.7
14	7.0		12.6
21	7.5		15.7
21			17.0
42	8.7		
59***	9.5		
73	9.8	932	
80	9.9	972	
94***	10.2	1050	
243****	13.5****	1860****	
243	14.1	2030	51.0
297	15.1	2570	

*Estimated from SEM photo.

**Obtained from spherical taper sections.

***Indicates time of brushing.

****Indicates unbrushed sample.

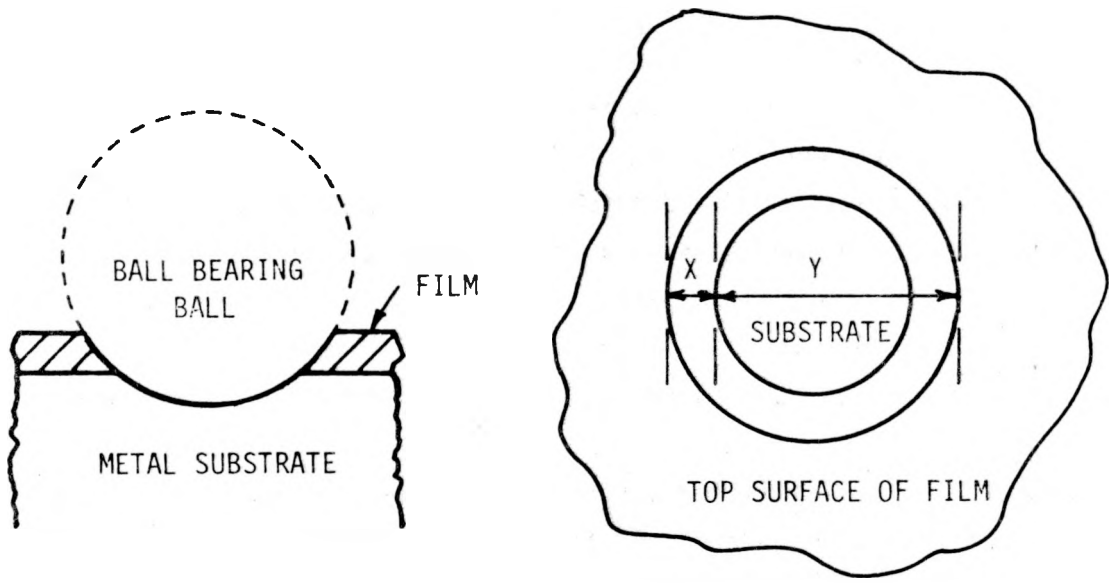

$$h = \frac{XY}{D}$$

Fig. 6.9 Illustration of the "spherical abrasion" technique. The thickness of the film may be determined from the values of X and Y knowing the diameter D of the ball-bearing ball.

data obtained to date with the "spherical abrasion" technique are in good agreement with these data. The film thickness was found to continuously increase with time. No pitting was found in any of the samples.

Copper-Nickel CuNi specimens were examined by optical microscopy as well as energy dispersive x-ray analysis (EDAX). The results are summarized below with the various corrosion products tentatively identified by color and comparison with the results of Krougman and Ijsseling [12].

The first sample was recovered after 10 days of exposure. The surface was found to be covered by a very thin film of red cuprite, Cu_2O. This film appears to be relatively tenacious, as compared with the other corrosion products described below, but does flake off in some places. In certain regions it appears that streaks of black tenorite, CuO, have developed from the top surface layer of the cuprite.

This inner film was partially covered by a loosely adhering layer that consisted of two different corrosion products in the form of crystals. One of these products was dark-green in color and was presumed to be the copper basic carbonate, malachite $CuCO_3 \cdot Cu(OH)_2$. The other was light-green and was presumed to be copper trihydroxy-chloride, atacamite or paratacamite $CuCl_2 \cdot 3Cu(OH)_3$. The crystals of both products appeared to nucleate individually on the Cu_2O surface. The next sample was recovered after 24 days of exposure. The inner cuprite film appeared to be somewhat thicker. It was covered by a layer of atacamite which, in turn, was covered by patches of the dark-green malachite and patches of a fine grained rust-colored layer. In some areas the malachite was covered by a blue film of a second basic carbonate, azurite, $2CuCO_3 \cdot Cu(OH)_2$.

For exposures greater than 24 days the azurite disappeared and the rust-colored film spread. After 36 days exposure this film completely covered the surface. Visual examination shows a pattern of lighter and darker regions generally aligned in the direction of flow. The darker regions are locations where the rust-colored film covered a substrate consisting of dark-green malachite regions.

As the rust-colored layer developed in thickness with time its adherence, in its dry state, to the underlying film of corrosion products decreased and the layer peeled spontaneously in numerous places. Measurements of the thickness of this layer are shown in Fig. 6.10 [9]. The layer grew linearly with time up to a thickness of approximately 18-20 μm after about 80 days of exposure. It was apparently not affected by a brushing on day 59.

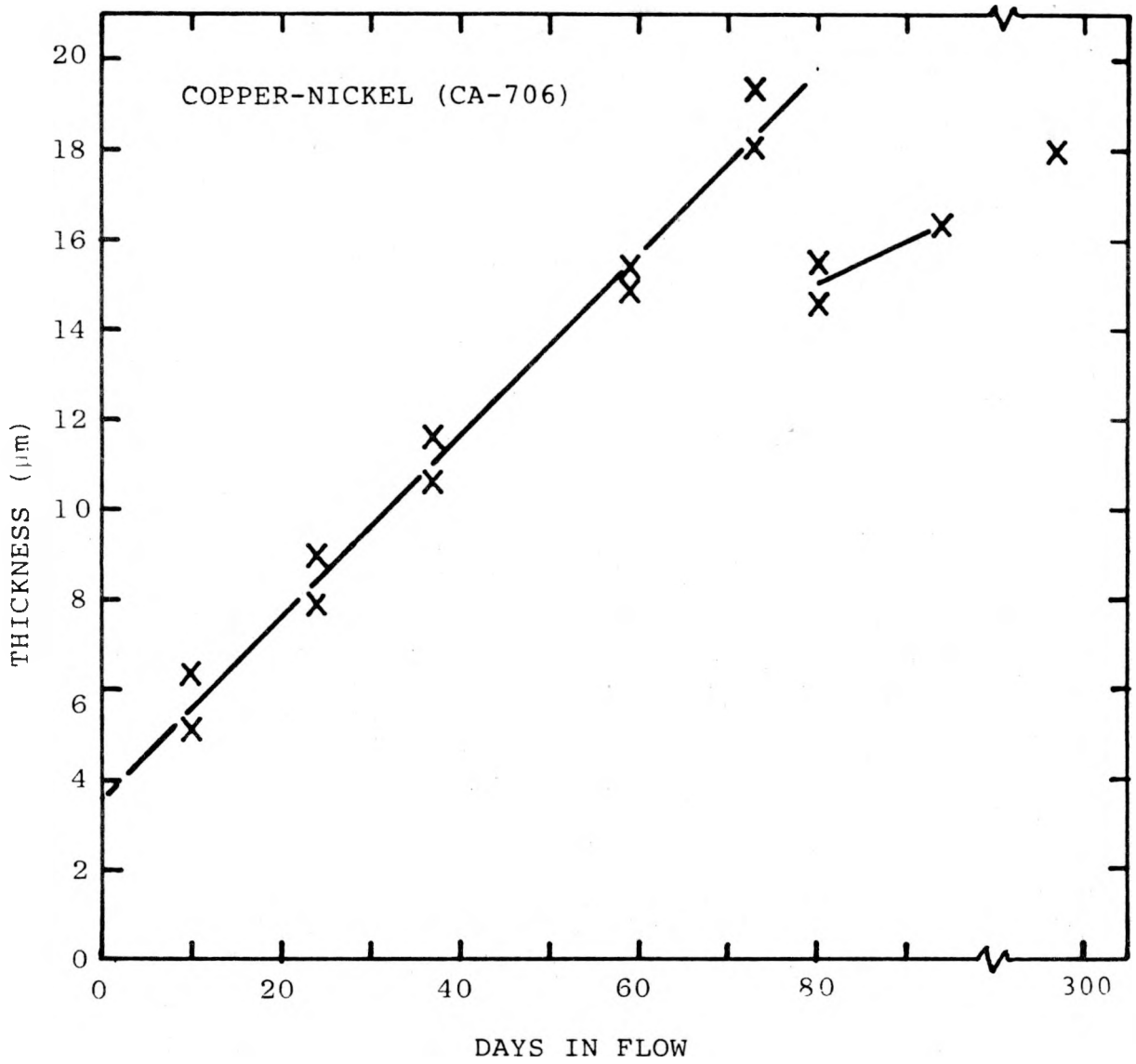

Fig. 6.10 Thickness of the Cu-Ni corrosion film measured in the SEM vs time in flowing seawater.

No data were obtained between 94 and 298 days of exposure. However, the 298 day film appeared to be very similar to the one at 94 days and has almost the same thickness, approximately 18 μm. It is not clear why the growth appeared to stop or reach a steady state at a layer thickness of 18-20 μm. The crystalline layers of malachite appeared to be redissolving after about 80 days, leaving behind a black material that forms streaks in, and often through, the film of rust-colord material.

A surprisingly different appearance was found for the 298 day sample recovered from the heat transfer test section. Close examination shows that the main difference between the two 298 day samples was due to precipitation of carbonate scale on top of the corrosion products, in case of the heat transfer test section specimen. This scale appeared in axial streaks of different morphology and thickness, overlying layers of corrosion products of different thickness. It appeared that different sets of these streaks on the metal surface corroded for different periods of time before having scale deposit to arrest the attack.

This scale was continuous and strongly adherent. Total film thickness varied between approximately 2 and 28 μm. The corrosion product layers initially appeared to be the same as described above for the corrosion samples; however, EDAX analyses show that the layers contain appreciable amounts of calcium.

6.4.3 Discussion

Sufficient experimental data were obtained in this study to permit an evaluation of the film growth rate for Al. It should be noted that a constantly growing film has not been found by all investigators. For example, Craig et al. [4] found that the corrosion product film of 6061-T6 Al showed no change in weight with time. This was attributed to a steady-state dissolution of the hydrated oxide film. Their estimate of the limiting film thickness was of the order of 1.8 to 6.4 μm, which is an order of magnitude smaller than that estimated by Fetkovich et al. [13] from the heat transfer results and considerably smaller than the results of the present study. Little et al. [10,11], who measured wet film thickness directly for 5052 Al, found results which are generally similar to those of the present study, and Poteat and Dale [14] who measured dry film thickness, found values which agree well with those presented here.

If the gelatinous film that forms on the surface of Al is continuous and is controlled by diffusion of some species through the film, then the growth rate of the film should follow the parabolic rate law, such that

$$h_w^2 = k_p t$$

where h_w is the wet film thickness k_p is a parabolic rate constant, and t is the time.

It is expected that the gelatinous aluminum oxide trihydrate film is continuous since the Pilling-Bedworth ratio (ratio of corrosion product volume to that of the metal consumed) is considerably above the dry-film value of about 3.22, which is greater than the critical value of unity required for a continuous film.

In order to undertake a definitive analysis of the growth rate of the film it is necessary to obtain actual thickness data for the film *in situ*. In the present experiments this was not possible; rather, measurements were made on a film which has been dehydrated due to exposure to air and, in many instances, to the vacuum of the SEM specimen chamber. The film is known to contain appreciable amounts of water which disappears during drying but a correlation between the *in situ* wet film thickness and the thickness of the dry film has not yet been obtained. Since, however, the two thicknesses are closely interrelated -- analysis can be made based on the data for dry film thickness and for dry film crazing platelet size which were obtained in the present study. This is outlined below.

As the exposure time increased it was readily apparent that the size of the platelets formed on drying of the Al film steadily increased. The platelet size was easy to measure in the SEM even at the very early times of exposure when the film is very thin.

The results from Fig. 6.11 are not surprising. As the film dehydrates, there are no restrictions as to how much it may shrink normal to the surface but, since it remains firmly attached to the substrate, a tensile stress large enough to produce the familiar craze cracking on "cracked mud" pattern observed in all samples is induced in the dehydrated film. In the Appendix a discussion is presented on why the platelet size should be directly related to the wet film thickness. The dry film data shown in Table 6.2 tend to support this prediction.

Therefore, assuming that the growth rate of the hydrated film is diffusion controlled and that the thickness of the wet film is proportional to the thickness of the dry film, if the average area of the platelets, A, or the square of the average platelet diameter, d^2, is plotted vs time, a linear relation should be obtained, i.e.

$$\bar{A} = k'_p t$$

$$\bar{d}^2 = k''_p t$$

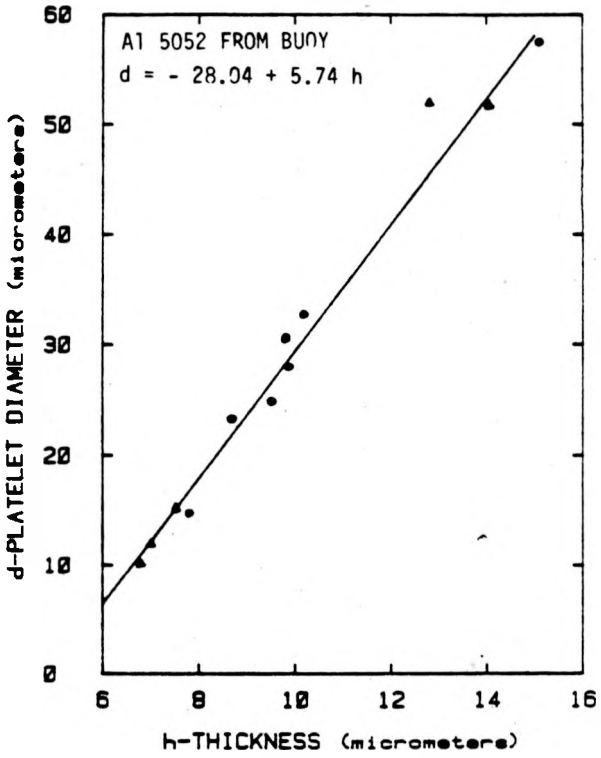

Fig. 6.11 Variation of platelet diameter with thickness for Al 5052 from the buoy experiment.

where k' and k" are parabolic rate constants. As shown in Fig. 6.12, the data do follow the parabolic rate law. Least-squares analysis give the following functional relationships:

$$\bar{A} = 413\ (\mu m)^2 + 6.73\ t$$

$$\bar{d}^2 = 12.3\ (\mu m)^2 + 12.0\ t$$

where time is given in days and the correlation coefficients are 0.974 and 0.977, respectively.

The fact that these do not extrapolate to zero as time decreases may be due to a number of reasons. First, the growth kinetics at the earliest time (less than one day) may not obey the parabolic rate law; rather, corrosion may follow a logarithmic rate law due to electrical space charges at the metal/oxide interface. Second, since the samples were cleaned either by a caustic/acid rinse or by an aqueous detergent, an initial film may have formed before deployment. Finally, there may be some minimum platelet size, possibly related to the underlying Al grain size, as suggested by Craig et al. [3].

The data indicate that d is 2-3 times the dry film thickness which, in turn, is 3.22 times the reduction in Al thickness due to corrosion (based on an assumed dry film density of 2.42 g/cm^3 [4]. Using a value of 2.5 the corrosion loss, Δx (μm), can be predicted from equation (6):

$$(\Delta x)^2 = 0.19 + 0.19\ t$$

or

$$\Delta x = 0.43\ t^{1/2}$$

if the time independent term can be neglected. If the attack is uniform and the corrosion product film is not removed by brushing or dissolution, then the corrosion loss should only be 45 μm (1.8 mils) over a 30 year lifetime. The few data obtained on the effect of cleaning by brushing show that the dry film thickness and the platelet size are not affected. However, a more detailed study will be necessary before any final conclusions can be drawn. If the cleaning method used were sufficiently vigorous to remove the film completely, if the film reformed at the same rate as found in this study, and if this cleaning were performed each month for 30 years, then the total metal loss would be about 850 μm, or 34 mils.

The results from the 8 month exposure sample predict that the protective corrosion product film was not removed by the brushing procedure used in this experiment.

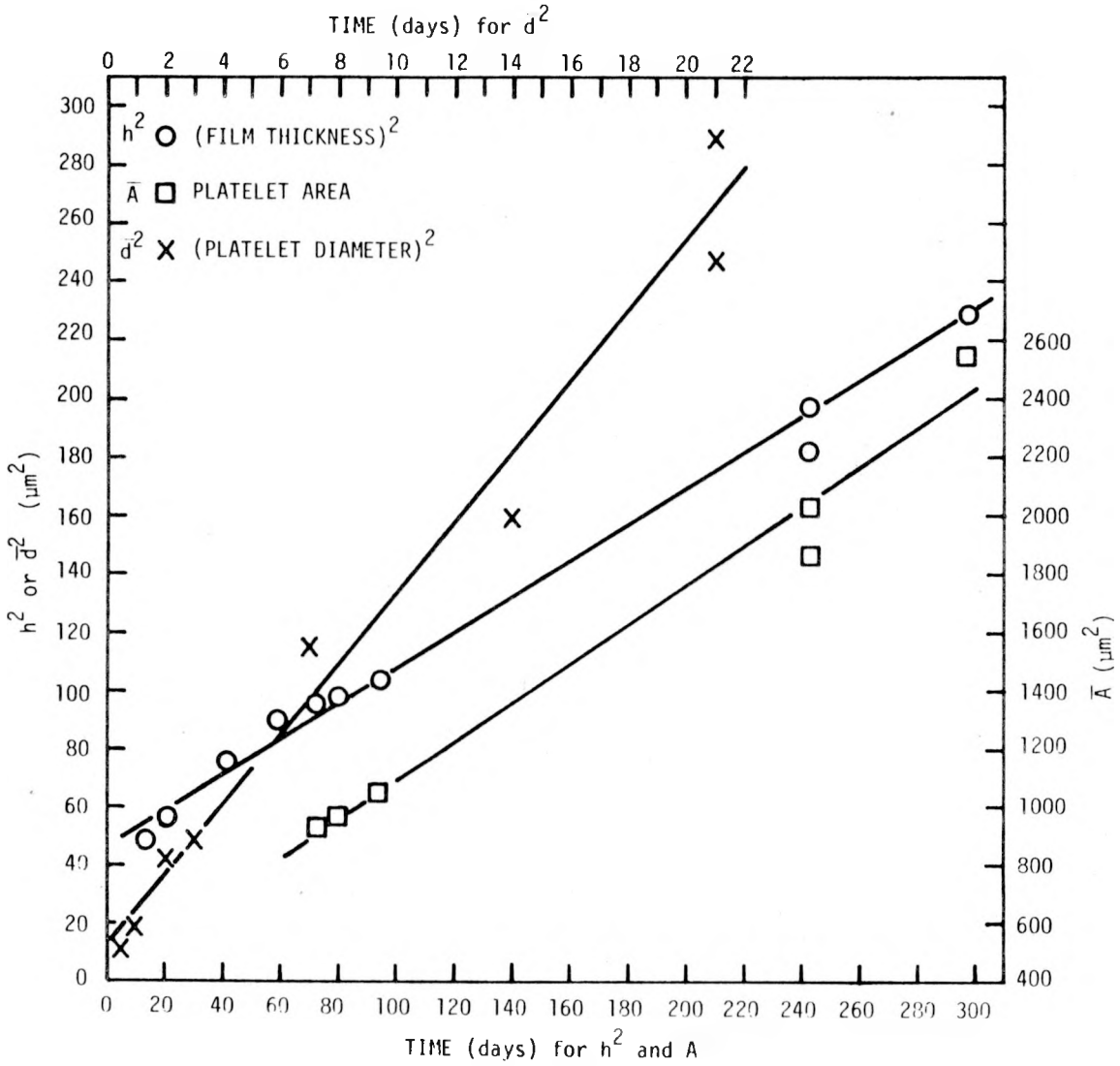

Fig. 6.12 Variation of film thickness and average platelet area and diameter as a function of time of exposure to flowing seawater. A parabolic corrosion rate is predicted from these results.

The measured platelet diameter for the 8 month brushed sample was found to be 51 μm. The values predicted from equation (6) are 54 μm for no interruption in film growth due to brushing and 42 μm for complete film removal at the 94 day brushing. Therefore, three conclusions can be made. First, the film continues to increase in thickness, and the Al continues to decrease parabolically with time over at least an 8 month period. Second, the effect of brushing on film removal appears to be negligible. Third, the metal loss due to corrosion is very small.

The directly measured dry film thickness data, h in Table 6.2 show similar parabolic behavior, as seen in Fig. 6.12 where h^2 is plotted vs t. The line fits the equation

$$h^2 = 48\ (\mu m^2) + 0.60\ t$$

with a correlation coefficient of 0.991. For a film of aluminum oxide trihydrate with a Pilling-Bedworth ratio of 3.22 the metal loss, Δx (μm), is given by

$$\Delta x^2 = 4.63 + 0.058\ t$$

The extrapolated metal loss for 30 years exposure is 25.3 μm or one mil. The metal loss for the same time period if monthly cleaning removes the film completely is 909 μm or 36 mils.

Support for the conclusion that 5052 Al corrodes at a parabolic rate in seawater can be found in published data for the time dependence of metal loss and corrosion rates reported in the literature.

In The Corrosion of Light Metals [15], Godard et al. report the weight loss of 5052 Al for 1, 2, 5 and 10 years' exposure at three different sites (note that the averaged data given in Table 12.5 in mg/dm^2 are incorrect). Good agreement to a parabolic rate is found for the Harbor Is., NC and Esquimalt, BC data.

A recent report by Schrieber et al. [16] on the corrosion rate of 5052 Al in flowing seawater indicates that the rate decreases proportional to $t^{-1/2}$.

Finally, Poteat and Dale [14] report a metal loss for 5052 Al vs time that is an almost perfect fit to a parabolic rate law for times from several days to 2 weeks.

In regards to the anomalous behavior of the CuNi sample from the heat transfer test section, it is not quite clear why carbonate scales formed to such an extent. Some stray current problems could possibly have occurred in this section of the test loop, while not in the section containing the corrosion test samples, and the

existence of a stray current can explain the phenomenon. It is obvious that once this tenacious carbonate scale has formed the CuNi alloy looses its resistance to biofouling and shows as rapid an increase in R_f as do the other materials tested. This probably means that only the R_f-values obtained during the first 100 days are valid for "normally" behaving CuNi, as exemplified by the specimens obtained from the corrosion test section. Further work will be necessary to determine the extent of biofouling and heat transfer deterioration for CuNi specimens exposed for longer periods of time.

6.5 3-Inch Pipeline

Corrosion samples were identical to those of the Buoy 3 experiment; however, the seawater entered the coupon after a 1200 ft. traverse through the 3" pipeline.

In the first series of tests, specimens of Alclad 3003 (7072 over 3003) were exposed in the water flow from the date of start-up until removed at different intervals. In the second series, both Alclad 3003 and alloy 5052 were used. The specimens were inserted in the flow on day 113 and removed at selected intervals. The purpose of this second series of samples was to obtain data for alloy 5052 for comparison with buoy data obtained for that alloy in earlier work and to determine if the virgin pipeline would give results different from results obtained after the pipeline had been used for a few months.

6.5.1 Experimental Methods

Coupons were removed periodically by cutting off sections of the specimen pipe at the downstream end.

Since the materials to be evaluated for corrosion studies were in the form of continuous lengths of pipe from which coupons were cut, weight-loss measurements were not possible. However, it was possible to measure the air-dried thickness of corrosion films present on the inside of the pipe.

Estimates of corrosion rates were determined using the techniques described for Buoy 3.

6.5.2 Experimental Results

When exposed to flowing seawater, the Al 5052 formed a continuous, gelatinous corrosion product over the entire surface within hours; however, the scale on Alclad 3003 grew in patches that appeared to start developing at different times. In either case, when Al is removed from seawater and allowed to air dry, water of

hydration was readily lost resulting in shrinkage of the film and subsequent crazing of the entire surface, forming platelets, as before.

In addition to the Al 5052, visual confirmation of the relationship between platelet size and film thickness for Alclad 3003 is clearly seen in Fig. 6.13. The central region has dissolved forming a slight depression in the cladding. Both the film thickness and platelet diameter increase in size radially away from the center.

Data obtained for the 3-inch pipeline Alclad specimens exposed from start-up are shown Fig. 6.14. As shown previously in Fig. 6.13, there is either extensive local dissolution of the film over the entire surface or the film grows in patches which appeared to develop at different times. This is responsible for the grouping of the results around several different curves. A rather substantial film thickness does develop for this alloy - 35 μm in 150 days.

Similar groupings were found for the second series of Alclad specimens, though at higher values, while the data for the Al 5052 fell around one single curve. A summary and comparison of the data is shown in Fig. 6.15, where buoy data for Al 5052 have been included. For the Alclad alloy, the highest-valued curves have been used.

6.5.3 Discussion

Several conclusions can be drawn from the results in Fig. 6.15. First, there is a distinct effect of pipeline start-up. Film build-up is considerably slower during the early life of the pipeline and follows an almost linear or paralinear rate, while a parabolic or near-parabolic growth curve was found for the later experiments, similar in shape to the growth curves found in the buoy experiments for Al 5052. Second, for Al 5052 and growth curves were almost identical for shore-based and buoy experiments. The growth rate may be slightly higher for the waters which have passed through the pipeline, but the difference is small. Third, the film thickness on Alclad was 2-3 times greater than on Al 5052.

A rough estimate of the corrosion rate of Al 5052 exposed for two months with the 3-inch pipeline can be made from the change in depth of the abrasion groves that resulted from abrasion of the surface with 600X SiC paper. At the end of two months, the grooves decreased in depth only 1-2 μm from an initial depth of 3-5 μm. This would give a corrosion rate of 1-2 μm in two months and for the worst case - linear corrosion (which we do not have) - this amounts to about 10 μm/yr or 100 μm in 10 years at the very most.

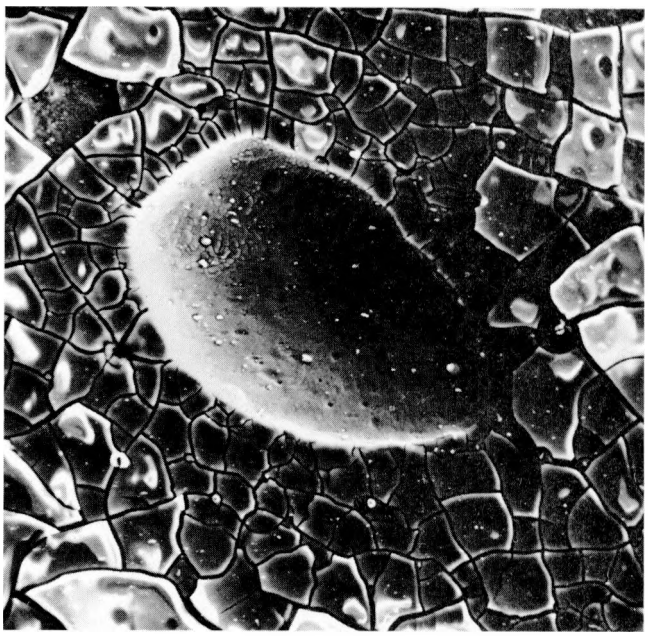

Fig. 6.13 Alclad 3003 after 24 days' exposure, 95X. Note the platelet size variation with thickness of the film. Three-inch pipeline experiment.

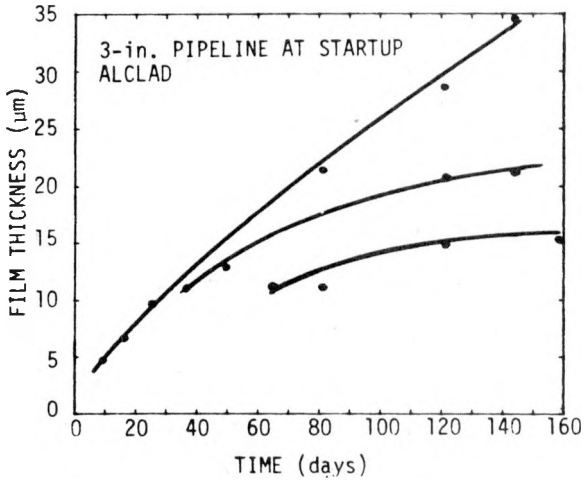

Fig. 6.14 The grouping of film thickness for Alclad 3003 vs time.

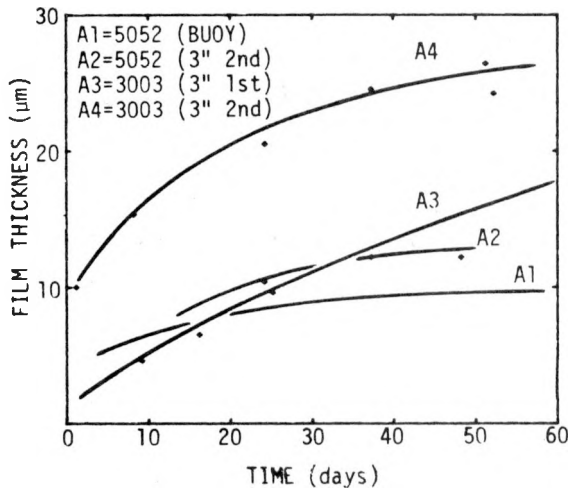

Fig. 6.15 Film thickness of the A1 5052 from the buoy and the three-inch pipeline as well as the Alclad at start-up (A3) and after the pipeline had been in operation for 113 days (A4).

6.6 Summary and Conclusions

The titanium and the high alloy stainless steel do not corrode under the experimental conditions used in this study.

The copper-10% nickel alloy showed a very complex pattern of film formation which has been only tentatively identified. The film is brittle when dry and grows linearly with time, suggesting that an interface reaction controls growth. At 20 μm thickness, film growth stops or reaches a steady state.

The corrosion film on Cu-Ni has an effective thermal conductivity about that of water, and is responsible for the increase in R_f with time.

The 5052 aluminum corrodes at a rapid rate during the first 15-17 days of exposure. After this period the film grows according to a parabolic equation, showing that diffusion through the film is rate controlling. The aluminum showed no pitting, and extrapolation of the 10 months of data give total corrosion losses of 1-2 mils for a 30-year period. The film is not affected by brushing by a bristle brush which removes most or all of the biofouling.

The film that forms on Al 5052 and Alclad 3003 is protective, which results in a continuously decreasing overall corrosion rate with time. Alclad corrosion rates tend to be larger than those of Al 5052.

Film thickness and platelet dimensions are correlated with one another to a large degree allowing the corrosion rate to be estimated from a simple microscopic observation of platelet size under conditions of no film dissolution.

Our results strongly suggest that, in waters representative of OTEC conditions, the inexpensive aluminum alloys will be able to last at least 10 to 30 years in OTEC heat exchangers and may prove to be the single most effective solution to reducing the overall cost of an OTEC plant.

6.7 References

1. George W. Harvey, "Biofouling Experiments at Keahole Point, Hawaii, 1976. Biological Studies Progress Report." Unpublished (1976).

2. Bruce E. Liebert, "Corrosion of Aluminum and Titanium at Keahole Point over an Eight Month Period," Proc. OTEC Biofouling, Corrosion, and Materials Workshop, Rosslyn, VA, 1979 .

3. H.L. Craig, J. Nelson, and R.S.C. Munier, "Cleaning Procedures for Aluminum Pipe and Tubing for Biofouling and Corrosion Experiments," Proceedings of the Ocean Thermal Energy Conversion (OTEC) Biofouling and Corrosion Symposium, Seattle, WA, Oct. 10-12, 1977.

4. H.L. Craig, R.S.C. Munier, and J. Morse, "Corrosion Results from a 72-day Field Test of Simulated OTEC Aluminum Heat Exchanger Surface at St. Croix, U.S.V.I., "Proceedings of the Fifth Ocean Thermal Energy Conversion Conference, Miami Beach, FL, Feb. 20-22, 1978.

5. Fetkovich, J.G., G.N. Grannemann, L.M. Mahalingam, and D.L. Meier, "Measurements of Biofouling in OTEC Heat Exchangers," Proceedings of the Fifth Ocean Thermal Energy Conversion Conference, Miami Beach, FL, Feb. 20-22, 1978.

6. B. Little and D. Lavoie, "Gulf of Mexico Ocean Thermal Energy Conversion (OTEC) Biofouling and Corrosion Experiment," Proceedings of the OTEC Biofouling, Corrosion, and Materials Workshop, Rosslyn, VA, Jan. 8-10, 1979.

7. J.W. Morse, "Nonbiogenic Desposits at the OTEC Heat Exchanger-Seawater Interface," Proceedings of the OTEC Biofouling, Corrosion, and Materials Workshop, Rosslyn, VA, Jan. 8-10, 1979.

8. E.E. Underwood, "Applications of Quantitative Metallography," Metals Handbook, Vol. 8, Eighth Ed., p. 42, 1973.

9. B.E. Liebert, L.R. Berger, H.J. White, J. Moore, Wm. McCoy, J.A. Berger, and J. Larsen-Basse, "The Effects of Biofouling and Corrosion on Heat Transfer Measurements," Proceedings of the 6th Ocean Thermal Energy Conversion Conference, Ocean Thermal Energy for the 80's, Washington, D.C., June 19-22, 1979.

10. Bruce E. Liebert, K. Sethuramalingam, and Jorn Larsen-Basse, "Corrosion Effects in OTEC Heat Exchanger Materials," Proceedings of the 5th International Congress on Marine Corrosion and Fouling, Barcelona, Spain, May 19-23, 1980.

11. Handbook of Chemistry and Physics, 48th ed.

12. J.M. Krougman, and F.J. Ijsseling, "The Corrosion Behaviour of CuNi10Fe in Seawater," Proceedings of the 4th International Congress of Marine Corrosion and Fouling, June 14-18, 1976

13. J.G. Fetkovich, G.N. Grannemann, L.M. Mahalingam, D.L. Meier, and F.C. Munchmeyer, "Degradation of Heat Transfer Rates Due to Biofouling and Corrosion at Keahole Point, Hawaii," Proceedings of the Fifth Ocean Thermal Energy Conversion Conference, Miami Beach, FL., Feb. 20-22, 1978.

14. L.E. Poteat, and W.G. Dale, "Corrosion of Aluminum and Titanium During the First Gulf of Mexico Buoy Deployment," Proceedings of the OTEC Biofouling, Corrosion and Materials Workshop, Rosslyn, VA, Jan. 8-10, 1979.

15. H.P. Godard, W.B. Jepson, M.R. Bothwell, and R.L. Kane, "The Corrosion of Light Metals," Wiley, New York, 1967.

16. C.F. Schrieber, W.D. Grimes, and W.F. McIlhenny, "A Study of the Corrosive Effect on Aluminum and CP Titanium of Mixtures of Ammonia and Seawater That May be Encountered in OTEC Heat Exchangers," Dow Chemical USA, Texas Division, Freeport, TX, Argonne National Laboratory, ANL/OTEC-BCM-004, 1979.

6.8 Appendix: The Relationship Between Film Thickness and Platelet Size of the Aluminum Corrosion Product

Consider a hydrated film of thickness t' before drying, as shown in Fig. A-1. If the film were not attached to the substrate, it would shrink on drying as shown in Fig. A-2. Let us suppose that the average linear shrinkage strain is

$$\varepsilon_s = \frac{\Delta L}{L}$$

Now, suppose that the film is bonded perfectly to the substrate and that the film, once dried, has infinite strength. In that case an average tensile stress

$$\sigma_f = E\varepsilon_s$$

would develop in the film on drying, as shown in Fig. A-3. Now, suppose that fracture occurs by crack initiation at the *outside* surface of the film. We suppose that cracking will occur if σ_f exceeds some critical fracture stress σ^*. Obviously, if cracking is ever to occur σ_f must be greater than σ^*.

Now let us consider what happens when a single crack forms as shown in Fig. A-4. The central question is: Does the formation of a single crack cause σ_f to drop below σ^*? At a point such as A in Fig. 4, the answer is obviously "Yes". But what about point B? If the thickness t is much less than L/2 then the stress at B will *not* be relieved by the formation of the first crack. This is because the loading on the film is tangential, as shown in Fig. 4. This is very much like the problem of loading of fibers in fiber composites.

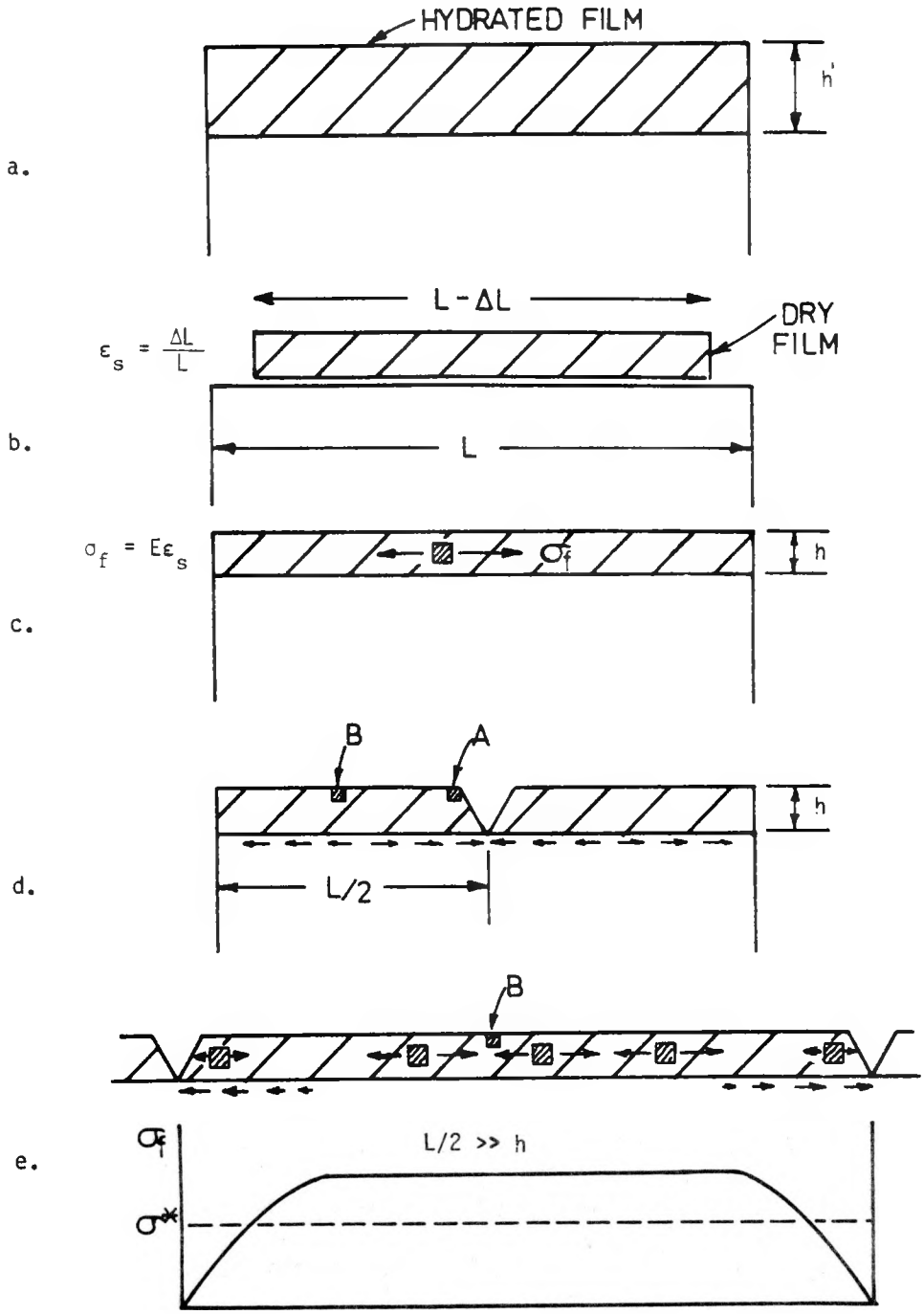

Fig. A-1 a. Hydrated aluminum oxide film when exposed to flowing seawater. b. Appearance of film after dehydration if attachment to the substrate did not occur. c. Fracture stress induced in the film due to dehydration and attachment to the substrate. d. Formation of a crack at the midpoint of the film due to the stress exceeding a critical fracture stress. e. Variation of the film stress along the platelet.

Distribution for ANL/OTEC-BCM-026

Internal:

J. B. Darby, Jr. (15)
J. D. Ditmars
B. R. T. Frost
L. E. Genens
A. B. Krisciunas
J. J. Lorenz
C. B. Panchal
J. J. Roberts
N. F. Sather
H. C. Stevens
A. Thomas
ANL Contract File
ANL Patent Dept.
ANL Libraries (2)
TIS Files (6)

External:

DOE-TIC, for distribution per UC-64 (261)
Manager, Chicago Operations Office, DOE
Chief, Office of Patent Counsel, DOE-CH
President, Argonne Universities Association
J. H. Anderson, Sea Solar Power, Inc., York, Pa.
W. H. Avery, Applied Physics Lab., Johns Hopkins U.
P. J. Bakstad, TRW Systems and Energy, Redondo Beach
E. J. Barsness, Westinghouse Electric Corp., Lester, Pa.
K. J. Bell, Oklahoma State U.
L. R. Berger, U. Hawaii (5)
E. Burcher, Div. of Ocean Energy Systems, USDOE
R. Cohen, Div. of Ocean Energy Systems, USDOE
W. A. Corpe, Columbia U.
R. S. Dalrymple, Reynolds Metals Co., Richmond, Va.
S. Dexter, U. Delaware
J. G. Fetkovich, Carnegie-Mellon U.
H. D. Foust, The Trane Co., La Crosse
S. Gronich, Div. of Ocean Energy Systems, USDOE
L. W. Hallanger, Research Corp., U. Hawaii
W. Hartt, Florida Atlantic U.
W. E. Heronemus, U. Massachusetts
J. F. Jenkins, Civil Engineering Lab., Naval Construction Battalion Center, Port Hueneme
E. H. Kinelski, U. S. Naval Academy
F. L. LaQue, Kingston, Ont., Canada
A. Lavi, Pittsburgh, Pa.
T. S. Lee, LaQue Center for Corrosion Technology, Wrightsville Beach, N. C.
L. F. Lewis, Div. of Ocean Energy Systems, USDOE
R. O. Lewis, LaQue Center for Corrosion Technology, Wrightsville Beach, N. C.
B. E. Liebert, U. Hawaii (5)
B. Little, National Space Technology Lab., NSTL Station, Miss.
R. N. Lyon, Oak Ridge National Lab.
J. H. Michel, Oak Ridge National Lab.
R. Mitchell, Harvard U.
J. Morse, Rosensthiel School of Marine and Atmospheric Science, Miami
R. S. C. Munier, Tracor Marine, Port Everglades, Fla.
J. Nicol, Arthur D. Little, Inc., Cambridge, Mass.
M. Olmsted, General Electric Co., Schenectady
F. W. Poucher, Energy Technology Engineering Center, Canoga Park
D. Price, National Oceanic and Atmospheric Administration, Rockville
W. E. Richards, Div. of Ocean Energy Systems, USDOE
W. W. Rogalski, Jr., Gibbs & Cox, New York City
J. F. Rynewicz, Lockheed Missiles and Space Co., Inc., Sunnyvale

D. S. Sasscer, U. Puerto Rico
C. F. Schrieber, Dow Chemical Co., U.S.A., Freeport, Tex.
B. Shelpuk, Solar Energy Research Inst.
T. J. Summerson, Kaiser Aluminum and Chemical Corp., Pleasanton, Calif.
R. B. Teel, Chatham, N. J.
F. Vukovich, Research Triangle Inst.
J. P. Walsh, VSE Corp., Alexandria, Va.
E. T. Wanderer, Aluminum Company of America, Alcoa Center, Pa.
R. L. Webb, Pennsylvania State U.
D. C. White, Florida State U.
P. Wilde, Lawrence Berkeley National Lab.
R. Williams, PRC Energy Analysis Co., McLean, Va.